

General Disclaimer

One or more of the Following Statements may affect this Document

- This document has been reproduced from the best copy furnished by the organizational source. It is being released in the interest of making available as much information as possible.
- This document may contain data, which exceeds the sheet parameters. It was furnished in this condition by the organizational source and is the best copy available.
- This document may contain tone-on-tone or color graphs, charts and/or pictures, which have been reproduced in black and white.
- This document is paginated as submitted by the original source.
- Portions of this document are not fully legible due to the historical nature of some of the material. However, it is the best reproduction available from the original submission.



IMPROVED HIGH PRESSURE TURBINE SHROUD

Final Report

by

I. I. Bessen, D. V. Rigney, R. C. Schwab

GENERAL ELECTRIC COMPANY
AIRCRAFT ENGINE GROUP
CINCINNATI, OHIO 45215

Prepared For

National Aeronautics and Space Administration

(NASA-CR-135181) IMPROVED HIGH PRESSURE
TURBINE SHROUD Final Report, 26 Jun. 1974 -
24 Jan. 1977 (General Electric Co.) 82 p
HC A05/MF A01 CSCL 21E

N77-29150

Unclas
40845



February 1977
NASA Lewis Research Center
CONTRACT: NAS 3-18905

1. Report No. CR-135181		2. Government Accession No.		3. Recipient's Catalog No.	
4. Title and Subtitle IMPROVED HIGH PRESSURE TURBINE SHROUD				5. Report Date FEB 1977	
				6. Performing Organization Code R77AEG481	
7. Author(s) II BESSON, DV RIGNEY, RC SCHWAB				8. Performing Organization Report No.	
				10. Work Unit No.	
9. Performing Organization Name and Address GENERAL ELECTRIC COMPANY AIRCRAFT ENGINE GROUP 1 Jimsom Road Cincinnati, Ohio 45215				11. Contract or Grant No. NAS 3-18905	
				13. Type of Report and Period Covered FINAL JUNE 26, 1974 JANUARY 24, 1977	
12. Sponsoring Agency Name and Address NASA LEWIS RESEARCH CENTER 21000 BROOKPARK RD. CLEVELAND, OHIO 44135				14. Sponsoring Agency Code	
15. Supplementary Notes PROJECT MANAGER, S.G. YOUNG NASA - LEWIS RESEARCH CENTER CLEVELAND, OHIO 44135					
16. Abstract					
17. Key Words (Suggested by Author(s))			18. Distribution Statement		
19. Security Classif. (of this report) UNCLASSIFIED		20. Security Classif. (of this page) UNCLASSIFIED		21. No. of Pages 74	
				22. Price*	

* For sale by the National Technical Information Service, Springfield, Virginia 22161

FOREWORD

This Final Technical Report covers the work performed by the Aircraft Engine Group, General Electric Company under NASA Contract NAS3-18905. The NASA Project Manager was Mr. S.G. Young, Materials and Structures Laboratory, Lewis Research Center.

The authors would like to acknowledge the efforts of the following personnel whose technical contributions were invaluable to the success of the program: Mr. C.H. Gay, AETPD, General Electric, who performed shroud design analysis as part of this program; Mr. J.Z. Hoyer, CF6 Design Engineering, whose valuable support permitted successful engine test of the Genaseal shrouds; Mr. M.J. Lucas and Mr. H.J. Heckler whose technical leadership assured success of the hot press scale-up phase of this program; and, finally Mr. G.G. Wyatt, M&PTL, General Electric who performed the many laboratory evaluations which were required as part of this program.

Finally, the authors would like to thank the members of the Materials and Structures Laboratory, NASA, whose advice and counsel was always timely and helpful.

ABSTRACT

A new high pressure turbine shroud material has been developed from the consolidation of prealloyed powders of Ni, Cr, Al and Y. The new material, a filler for cast turbine shroud body segments, is called Genaseal (GE-NASA-seal). The development followed the identification of oxidation resistance as the primary cause of prior shroud deterioration, since conversion to oxides reduces erosion resistance and increases spalling under thermal cycled engine conditions. The NiCrAlY composition (22Cr, 10Al, 1Y) was selected in preference to NiAl and FeCrAlY alloys, and was formulated to a prescribed density range that offers suitable erosion resistance, thermal conductivity and elastic modulus for improved behavior as a shroud.

TABLE OF CONTENTS

	<u>Page</u>
List of Tables	vi
List of Figures	vii
Summary	1
Introduction	6
Technical Plan	7
Materials and Laboratory Screening Procedures	9
Results	11
Screening Tests	11
Oxidation Mechanisms	23
Rub Behavior and Erosion Resistance of Oxidized Filler Material	23
Material Selection	27
NiCrAlY Compositional Variations	28
Properties of Ni-22Cr-10Al-1Y	28
Design Analysis	39
Shroud Component Rig Test	48
Fabrication	48
Fabrication Scale-Up	50
Cost Factors	61
Engine Tests	64
Conclusions	75

LIST OF TABLES

<u>Table</u>		<u>Page</u>
I	Initial Rub and Erosion Test Results	13
II	1204C (2200F) Oxidation Test Weight Gain Data	15
III	Static Oxidation Weight Gains	29
IV	Metallographic Examination of Oxidized NiCrAlY Powders	30
V	Deleted	
VI	Deleted	
VII	Erosion Test Weight Loss Data	62
VIII	Labor Costs for NiCrAlY Shrouds	65

LIST OF FIGURES

<u>Figure</u>		<u>Page</u>
A	Effect of Density on Cold Particle Erosion Resistance	2
B	Genaseal and Bradelloy Shrouds after 1000 Engine Test Cycles	4
C	Microstructures of Bradelloy and Genaseal Engine Test Shrouds . . .	5
1	Program Flow Diagram	8
2	Surfaces of Erosion Tested Compacts	12
3	Surfaces of Rub Tested Compacts	14
4	Structure of Oxidation Tested Compacts	16
5	NiCrAlY and FeCrAlY Compacts after 1316C (2400F)/100 Hr. Dynamic Oxidation	18
6	Low Velocity Oxidation Tests	19
7	Low Velocity Oxidation Tests	20
8	NiCrAlY and FeCrAlY Compacts after 1204C (2200F)/150 Hr. Dynamic Oxidation	21
9	Oxide Formation on NiCrAlY and FeCrAlY Particles	22
10	FeCrAlY Oxidation Mechanism	24
11	Fe ₂ O ₃ -Al ₂ O ₃ and NiO-Al ₂ O ₃ Phase Diagrams	25
12	Cold Erosion Resistance Data	26
13	Thermal Diffusivity Data	31
14	Thermal Conductivity Data	33
15	Thermal Expansion Data	34
16	Modulus of Elasticity Data	35
17	Melting Point Determination of NiCrAlY	36
18	1316C (2400F) Low Velocity Oxidation Test Data	37
19	Microstructures of NiCrAlY and Bradelloy after 1316C (2400F)/ Mach 0.8 Oxidation Tests	38
20	Hot Particle Erosion Tests	40
21	HPT Shroud Cooling Study: As-Processed Bradelloy	41
22	HPT Shroud Cooling Study: Oxidized Bradelloy	42
23	HPT Shroud Cooling Study: As-Processed NiCrAlY	43
24	HPT Shroud Cooling Study: Oxidized NiCrAlY	44
25	Temperature and Stress Summary	47
26	NiCrAlY and Bradelloy Shroud Surfaces after Thermal Shock Tests .	49
27	Microstructural Comparison of NiCrAlY Filler Densities	51
28	Erosion Tested NiCrAlY Shrouds	52
29	Bonding of NiCrAlY Particles	53
30	Two Segment Argon Press Box	55
31	Microstructures of Vacuum and Argon Hot Pressed NiCrAlY	56
32	Four Segment Argon Press Box	57
33	Six Segment Argon Press Box	58
34	Filling Sequence for NiCrAlY Shrouds	59
35	Schematic Drawing of Argon Press Box Configuration	60

LIST OF FIGURES (Cont.)

<u>Figure</u>		<u>Page</u>
36	Deleted	
37	Deleted	
38	Deleted	
39	Microstructure of NiCrAlY-Braze Bonding	63
40	Microstructure of Bradelloy and Genaseal Engine Test Shrouds	67
41	Microstructure of Blade Rub Areas on Bradelloy and Genaseal Engine Test Shrouds	68
42	Engine Test Cycle	69
43	Genaseal and Bradelloy Shrouds after 1000 Test Cycles	70
44	Genaseal and Film-Cooled Bradelloy Shrouds after 1000 Test Cycles	71
45	Microstructures of Bradelloy and Genaseal Engine Test Shrouds . . .	72
46	Blade Rub on Genaseal Shroud	73

EXECUTIVE SUMMARY

A new high pressure turbine shroud material has been developed from the consolidation of prealloyed powders of Ni, Cr, Al and Y. The new material, a filler for cast turbine shroud body segments, is called Genaseal (GE-NASA-seal). The development followed the identification of oxidation resistance as the primary cause of existing shroud deterioration, since conversion to oxides reduce erosion resistance and increases spalling under thermally cycled engine conditions. NiCrAlY was selected in preference to NiAl and FeCrAlY alloys, and the selected composition (22Cr, 10Al, 1Y) was formulated to a prescribed density range that affords suitable erosion resistance, thermal conductivity and elastic modulus for improved behavior as a shroud.

The program was launched in 1975 in an effort to provide improved clearance control between high pressure turbine blade tips and the shroud, a static member that defines the outer diameter of the turbine gas path over the blades. Existing shrouds are constructed of cast superalloy segments which contain a porous metallic filler in contact with the gas path so as to provide a thermal barrier and overheating protection for outer support rings. Bradelloy is the name of a NiAl filler in commercial use for such segments. It has excellent thermal barrier properties, but it oxidizes too quickly, resulting first in filler swelling (that wears down blade tips) and segment distortion, and later in erosion or spalling of the oxide (that opens clearances further). It was expected that the use of a more oxidation resistant filler would not only provide longer life for the shroud, but would favorably influence performance and fuel consumption.

Three types of alloy compositions (FeCrAlY, NiCrAlY, and NiAl) and a vacuum hot press processing method for an improved shroud filler were identified by General Electric prior to the NASA-funded development. The vacuum hot pressing technique was based toward obtaining porous, sintered fillers that stay in the segment casting. Most materials shrink upon sintering (Bradelloy is an exception - it expands and bonds well to the casting), and the process must be carried out under compressive forces to achieve bonding of filler to the segment cavity walls. These basic procedures were used in the NASA development, first on a small vacuum press with single shroud segment capacity, and later in a larger air press with special tooling for up to six segments and argon flushing.

The program was executed in four tasks: (1) preliminary evaluation and selection of processing methods, composition and properties, (2) laboratory rig testing of shrouds, (3) engine tests, and (4) a first scale-up attempt to reduce process costs. The first task made a selection of the NiCrAlY composition and the density of filler. The selection was made on the basis of laboratory oxidation, erosion and rub tests. The effect of density for three candidate materials on particle erosion testing is shown in Figure A compared to Bradelloy. The curve illustrates why a 70% minimum density level was selected as one of the material requirements. The first task also analyzed by finite element analysis the effect on CF6 shroud temperatures that would result from a filler substitution of NiCrAlY for Bradelloy.

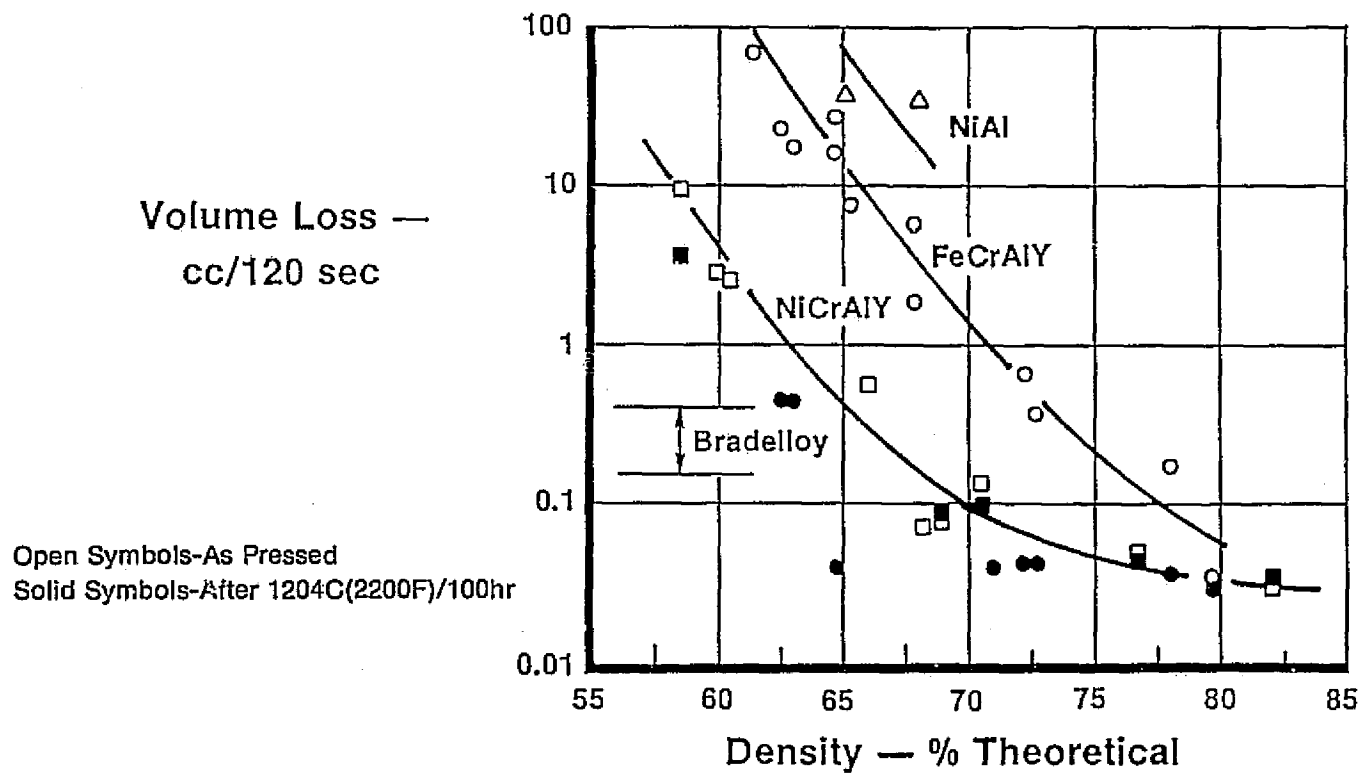


Figure A Effect of Density on Cold Particle Erosion Resistance of Three Candidate Filler Materials

Task II evaluated NiCrAlY shroud segments in high velocity oxidation and thermal shock rigs prior to engine evaluation in Task III. In the third task CF6-50 factory engine tests showed that NiCrAlY (Genaseal) shrouds constituted an improvement. The improvement can be seen visually in Figure B where every other shroud is Genaseal, and alternate shrouds are Bradelloy. This was a result of 1000 engine cycles under particularly severe conditions, a technique used to accelerate field service effects. Note that the filler cavity contains pegs as part of the superalloy casting. These are part of the Bradelloy design used on the CF6 engines to promote retention of the filler. Figure C shows microstructures alongside pegs in a Bradelloy shroud and a Genaseal shroud. Using the peg height as a mark of the original machined filler surface, it is apparent that the Bradelloy filler has swelled considerably during the test, a feature that tends to wear blade tips and open clearances. Genaseal seems to be an improvement in this regard.

The scale-up attempt in Task IV succeeded in reducing the initial high cost of one-at-a-time shroud fabrication in the laboratory vacuum hot press by demonstrating a six per batch method in an argon retort-hot press technique; additional cost reductions and flight service evaluations are planned under GE and USAF support to assess the cost effectiveness and life improvement in aircraft engines.

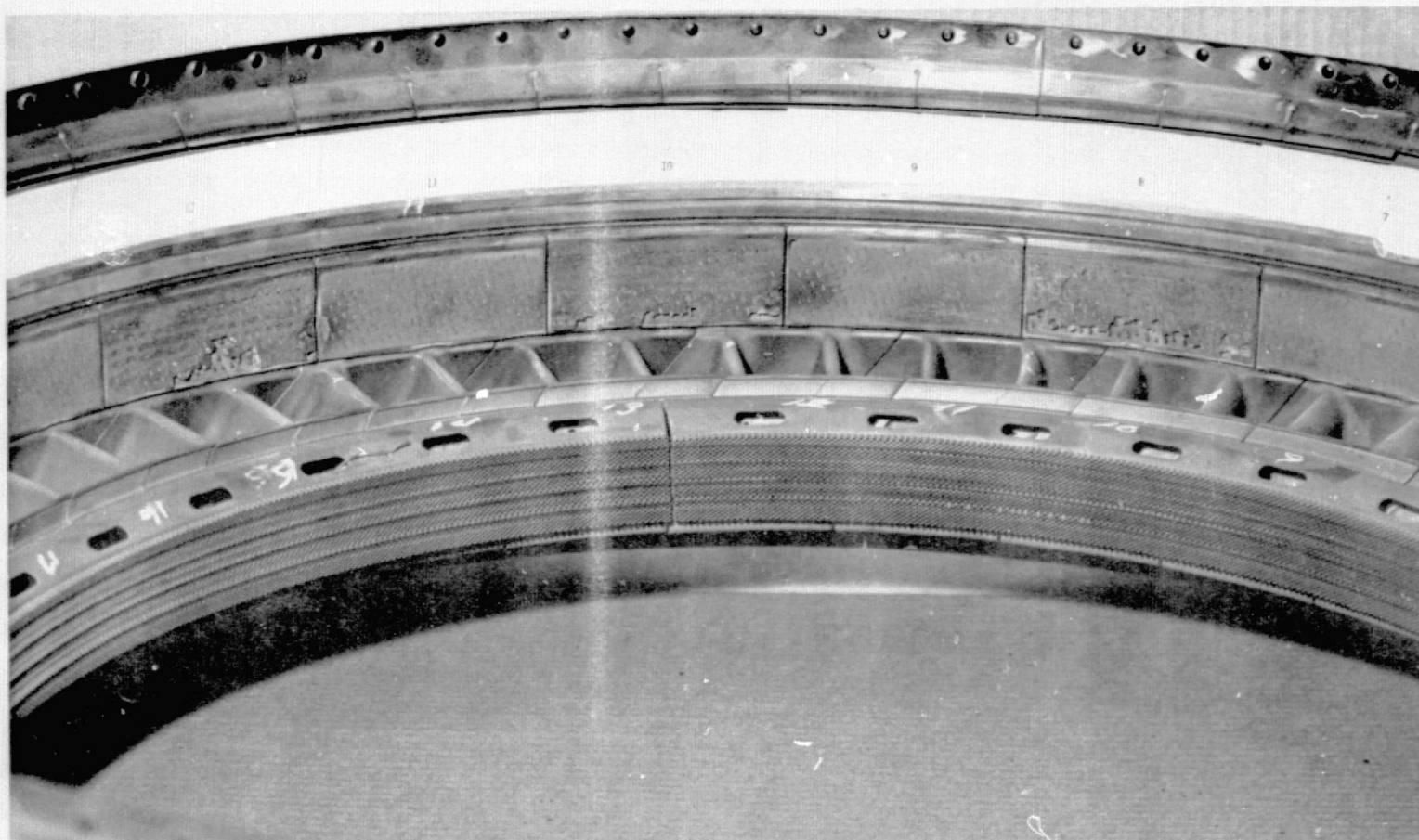


Figure B Genaseal and Film-Cooled Bradelloy Shrouds After 1000 "C" Cycles
CF6-50L Conditions. Genaseal Numbers 1, 3 and 5, Film-Cooled;
Bradelloy Numbers 2, 4 and 6

Filler Oxidation in Engine Test

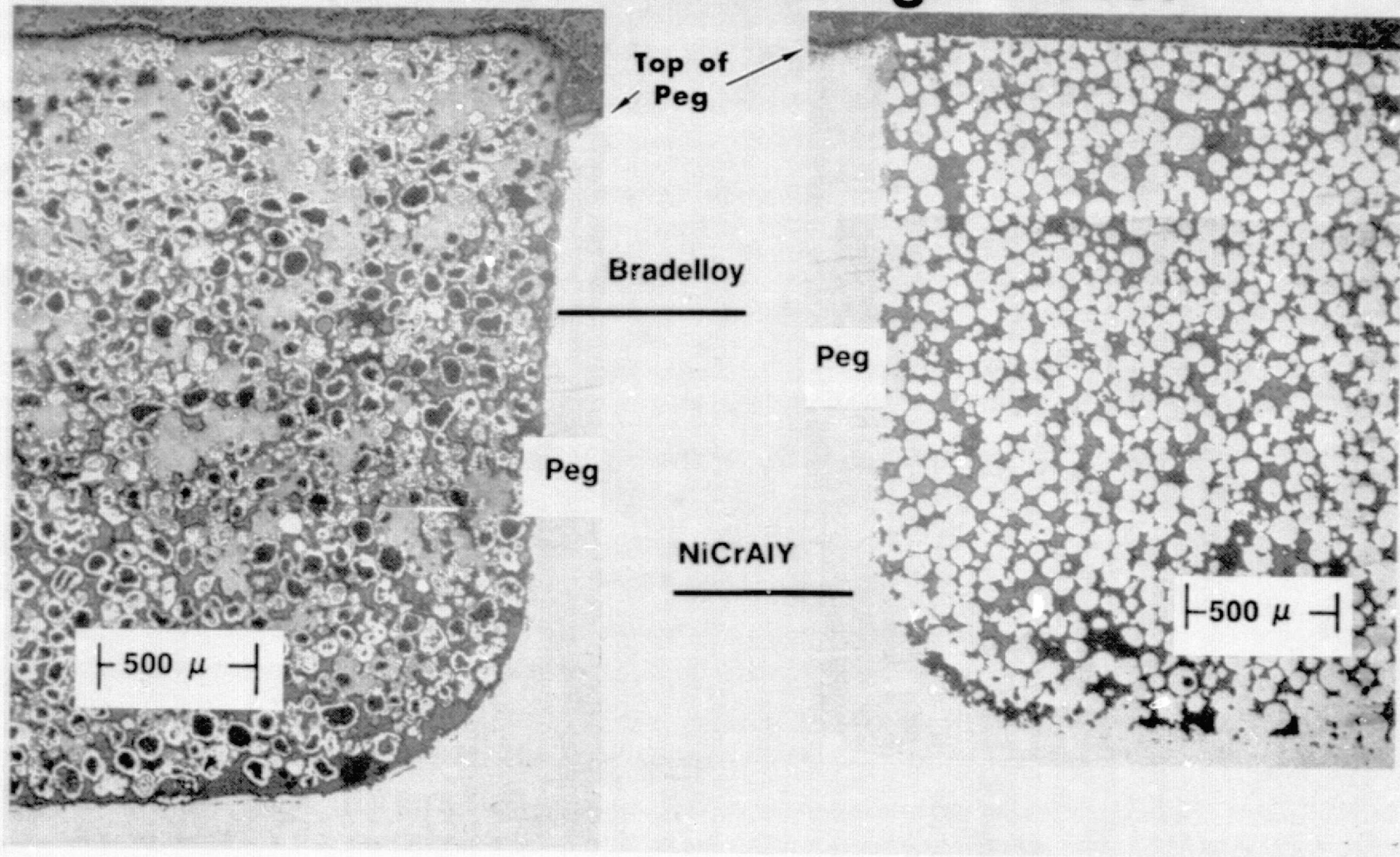


Figure C Typical Microstructure of Bradelloy (Left) and Genaseal (Right) Engine Test Shrouds (50x)

INTRODUCTION

Advancement in turbine materials technology has been fundamental to the evolution of the jet engine for its entire history. The desire for increased turbine inlet temperatures has been continuous, and just as turbine bucket and vane materials are developed to meet these needs, so are improvements in turbine shrouds required. In addition, the need for improved efficiencies and lower specific fuel consumption (SFC) has placed further requirements on the materials and processing technology for turbine shroud development. This development has ranged from the early forms of shrouds, which were simply metal rings that defined the outer gas envelope, to open face honeycomb, transpiration cooled materials such as Porolloy and to both honeycomb and, more recently, peg-style shrouds filled with an abradable material, Bradelloy.

Bradelloy is a low density sintered material made from nickel coated aluminum powder blended with nickel powder (Bradelloy 500) or Coast Metal 50 (Bradelloy 502). Bradelloy filled shrouds are currently operating in all CF6 engine high pressure turbines, and improvements, both in materials and design, over recent years have resulted in a reliable structure for current operating temperatures. However, it is realized that the upper temperature capability for Bradelloy filled shrouds is being approached, and more oxidation resistant materials are desirable for growth versions of current engines and for longer life under current operating conditions.

In order to extend shroud life or increase the temperature capability, an improved seal material must be more resistant to high temperature oxidation and have greater dimensional stability.

Oxidation resistance in metallic materials is dependent upon the formation of an adherent, protective scale on exposure to air at elevated temperatures. As the prevailing conditions in practical applications have become more severe, it has become increasingly necessary to rely on alloys forming α - Al_2O_3 as the protective film. In addition, the alloy should contain a sufficient concentration of aluminum to allow reformation of the protective Al_2O_3 film, since spallation of the initial film will occur in the high velocity, cyclic oxidizing environment of high pressure turbine (HPT) service. A series of materials has been developed to withstand this environment for extended periods of time (several thousands of hours at temperatures in excess of 1100C).

For a shroud material, however, the alloy must possess not only high temperature oxidation resistance, but also the ability to inhibit metal transfer and severe wear of the turbine bucket alloy throughout its service life. For this reason, a porous structure was examined which is compliant and which compresses and flows when taking a bucket tip rub. At the same time, however, a resistance to erosion, both by hot gas and particle impingement, must be maintained.

In-house work at General Electric demonstrated methods for achieving the required improvements in both material and processing factors. These methods were refined in the program to be described.

TECHNICAL PLAN

The technical plan for the development of an improved turbine shroud material was originally divided into three major tasks. Task I consisted of initial material selection, laboratory evaluation, design analysis and fabrication development leading to the most suitable shroud component material and design. Task II consisted of shroud fabrication and component rig testing, simulative of engine conditions, to determine whether material or design modifications were necessary. Task III consisted of factory engine testing.

Material selection and initial fabrication in Task I progressed more rapidly than expected and prompted interest in accelerated engine testing from CF6 and advanced engine groups. As a result, the work plan was revised to provide for concurrent work on the remainder of Task I, Task II and Task III. In addition, Task IV, scale up of the selected fabrication process to achieve some cost reduction was added to the program. A flow diagram showing the sequence of events in the revised program is shown in Figure 1.

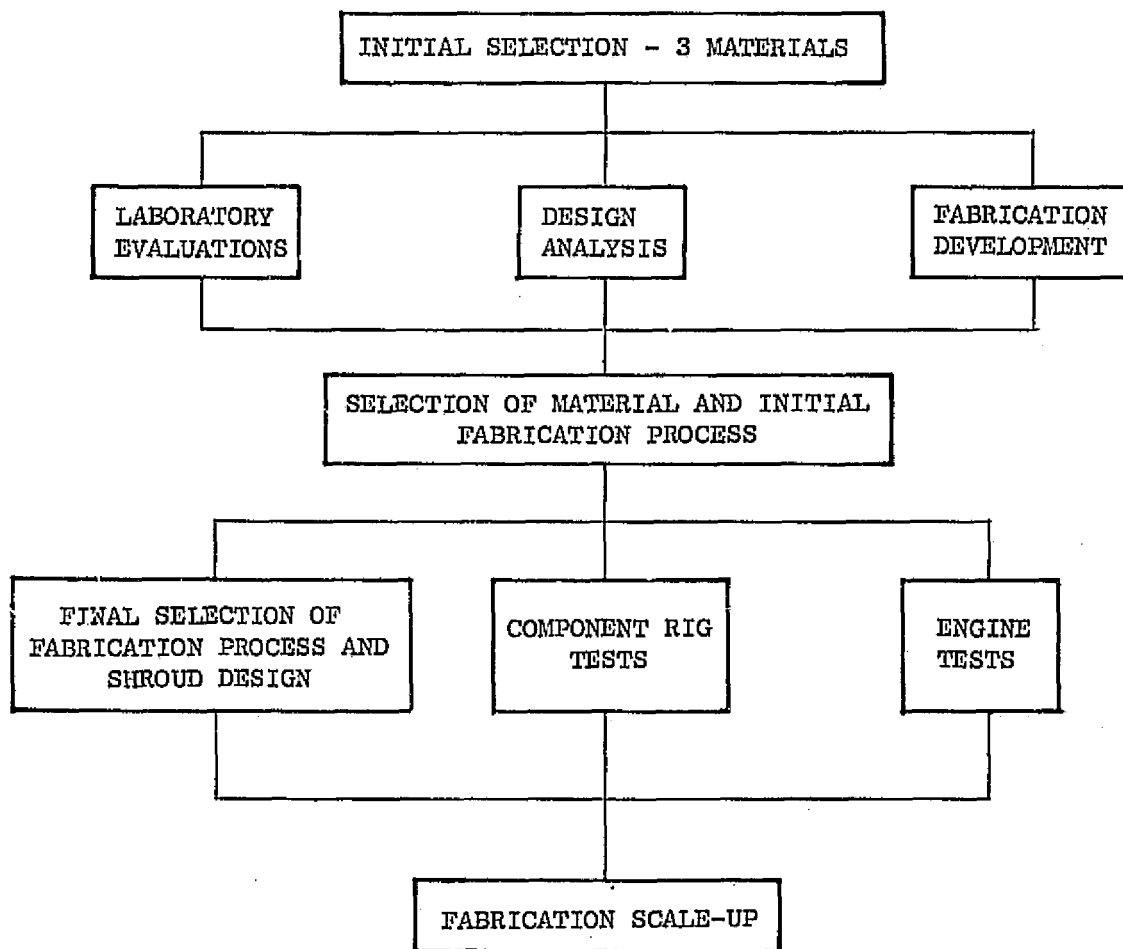


Figure 1 Program Flow Diagram

MATERIALS AND LABORATORY SCREENING PROCEDURES

The selection of NiCrAlY, FeCrAlY and NiAl alloys as candidates for high temperature shroud filler materials was based on the ability of these alloys to form a stable, protective α -Al₂O₃ layer, which could be reformed if the original layer were lost in the course of engine operation. An analysis of compositional variations of these alloy types constituted prior work on in-house programs. From this, three nominal compositions were chosen for the initial screening phase of Task I*:

- 1) Fe-25Cr-10Al-1Y
- 2) Ni-20Cr-10Al-1Y
- 3) Stoichiometric NiAl (β)

Conventional vacuum hot pressing was used to compact -150/+270 mesh alloy powders to a controlled density between 55 and 70% of theoretical. Hot pressing was carried out at 1038C (1900F) with pressures ranging from 100 to 1000 psi depending on the density desired. Test samples were cut from the "master" compact using a saw or wet cut-off wheel. After sectioning the samples were cleaned and dried in an oven at 121C (250F) prior to testing.

Three test criteria used in the initial screening phase of the candidate materials were rub behavior, erosion resistance and high temperature (1204C (2200F)) oxidation resistance. These tests, together with metallographic, scanning electron microscope (SEM) and chemical analysis of the powders and test specimens formed the basis for further selection of materials and for more detailed evaluation. In all tests Bradelloy 502 specimens were simultaneously evaluated as a basis for comparison.

For rub testing, the material to be tested was supported on a platform beneath the blades (15) of a 10 inch diameter wheel rotating at ~700 surface feet per second. During the test, after the rotational speed of the wheel had been attained, the platform was slowly raised to allow incursion of the blades into the rub material. In all tests in this program, the rate of incursion and the duration of the test were controlled at 1 mil/sec and 15 seconds, respectively. All tests were conducted at ambient temperature with fully heat treated, cast Rene' 80 blades.

*Composition in weight percent.

The purpose of the rub test was to rank the material compacts as to their rub behavior and to obtain an assessment of scabbing* tendency and blade wear. Scabbing should be avoided because it promotes rapid, non-uniform blade wear resulting in loss of turbine clearances.

The erosion test used in the screening work was the standard test used at General Electric as a quality control check on all Bradelloy filled shrouds. In this test, a sample was held normal to, and at a distance of six inches from the nozzle of a spray gun from which 750 grams of 50 μ m alumina powder were sprayed, using a line pressure of 414kPa (60 psi). The weight loss of the sample was measured, and this value was used as a relative measure of the erosion resistance of the material being tested.

For Bradelloy 502 filled shrouds, a weight loss of 0.5 to 1.25 g is considered acceptable for a test of two minutes duration. It should be emphasized that this test was used only as an aid in ranking the new materials with respect to Bradelloy 502, and the absolute weight loss measured was not used as an acceptance or rejection criterion in the early parts of the program.

Dynamic oxidation flame tunnels were used for the first 500 hour/1204C (2200F) test of the candidate materials, and were also used for additional testing at both 1204C (2200F) and 1316C (2400F) as the program continued. These facilities were available for oxidation testing of selected materials under low velocity (0.05 Mach) gas flow conditions and at temperatures to 1371C (2500F). Heating was provided by the combustion of natural gas (10:1 air to gas ratio), and the heating range was programmed to cycle from the test temperature to below 371C (700F) by automatically lowering the specimen fixture into a cold air blast six times per hour. Temperature was monitored by thermocouple control and checked optically. A test specimen fixture rotating at 5 rpm assured an equivalent exposure for all samples. For this program, a specimen holding fixture was designed to allow testing of up to 30 specimens simultaneously and to facilitate removal for weight change and dimensional measurements as a function of time on test. For the 500 hour, 1204C(2200F) test specimens were removed for measurement following 112, 250 and 500 hour exposures. Small pieces of selected samples were cut at each of these intervals for metallographic examination and possible additional microprobe or S. E. M. analyses.

*Scabbing is the buildup of transferred blade tip metal on the shroud.

RESULTS

SCREENING TESTS

The Cr, Al and Y levels of the FeCrAlY and NiCrAlY powders used for initial screening specimens were within one-half percent of the nominal Fe-25Cr-10Al-1Y and Ni-20Cr-10Al-1Y compositions. The 29% Al content of the NiAl powder was below the nominal stoichiometric NiAl composition. However, the powder was still β -NiAl and the properties were not expected to be significantly affected so specimens were made from the Ni-29Al powder.

The erosion resistances of the hot pressed compacts were ranked as poor, fair or good with the ranking defined as:

Poor - erosion through the specimen during test

Fair - specimen did not erode through, but was less resistant than Bradelloy 502

Good - equivalent or greater erosion resistance than Bradelloy 502

Table I shows the results of initial erosion testing. All compacts except NiCrAlY eroded quite readily and were classified as poor. NiCrAlY was fair to good and exhibited an expected trend, indicating greater erosion resistance with increased density. Typical erosion test specimens are shown in Figure 2.

Also included in Table I are the rub test results for the three alloys. Only the most dense NiCrAlY specimen exhibited any scabbing or blade wear. As might be expected, this specimen also had the best erosion resistance indicating the need to "trade-off" between rub tolerance and erosion resistance. Typical rub surfaces are shown in Figure 3.

The 1204C (2200F) oxidation test data (Table II) confirmed the predicted superior oxidation resistance of all three candidate materials. In addition, the data indicated oxidation resistance to be independent of density for the density ranges of the candidate materials evaluated. Based on percent weight gain, the FeCrAlY and NiCrAlY appeared superior to NiAl. Also during the oxidation testing, the lowest density compacts of the candidate materials (<64% theoretical density for FeCrAlY and <61% for NiAl and NiCrAlY) developed many cracks, an indication that a lower density limit must be exceeded for resistance to thermal cracking.

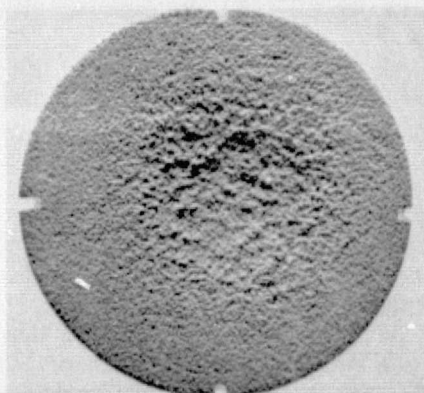
Typical structures of oxidation specimens are shown in Figure 4. As shown in Figure 4, sporadic, complete oxidation of some FeCrAlY particles occurred, and an investigation of this phenomenon was begun.



(A) NiCrAlY
60.5% DENSE



(B) NiCrAlY
68.1% DENSE



1.3X

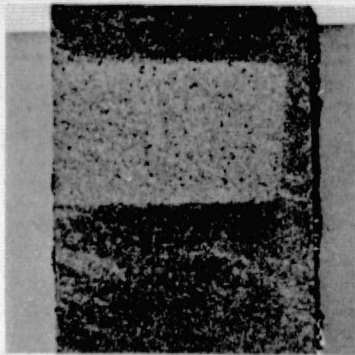
(C) BRADELLOY

Figure 2 Typical Surfaces of Erosion Tested Compacts

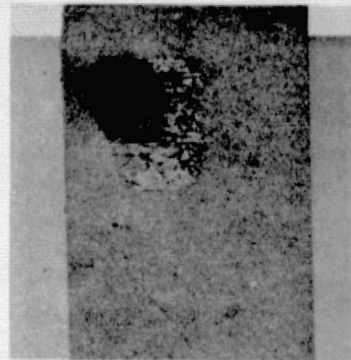
TABLE I

INITIAL RUB AND EROSION TEST RESULTS

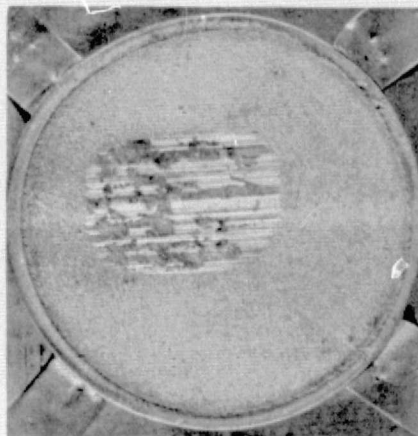
<u>MATERIAL</u>	<u>SPECIMEN</u>	<u>DENSITY g/cc</u>	<u>% THEO.</u>	<u>BLADE WEAR</u>	<u>SCAB.</u>	<u>EROSION</u>
FeCrAlY (lot 4915)	74-67-6	4.08	61.4	No	No	Poor
	74-72-6	4.30	64.7	No	No	Poor
	74-66-6	4.33	65.2	No	No	Poor
	74-68-6	4.51	67.9	No	No	Poor
	74-69-6	4.51	67.9	No	No	Poor
NiCrAlY (lot 4928)	74-79-6	4.67	59.9	No	No	Fair
	74-78-6	4.72	60.5	No	No	Fair
	74-71-6	5.12	66.0	No	No	Fair
	74-77-6	5.31	68.1	Yes	Yes	Good
NiAl (lot A476)	74-82	3.90	65.0	No	No	Poor
	74-80	4.08	68.0	No	No	Poor



(A) NiCrAlY - GOOD RUB
59.9% DENSE



(B) NiCrAlY - POOR RUB, SCABBING
68.1% DENSE



1.3X

(C) BRADELLOY - POOR RUB, SCABBING

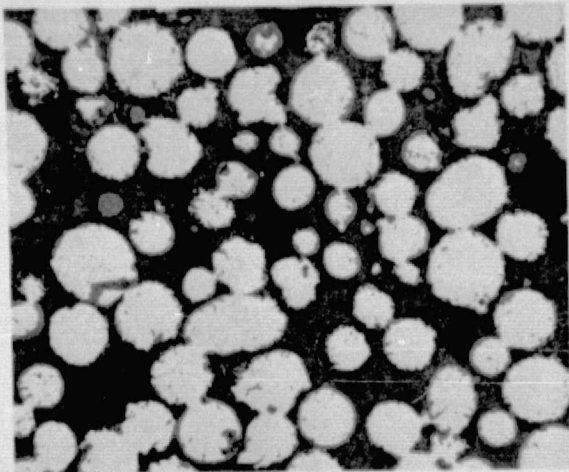
Figure 3 Typical Surfaces of Rub Tested Compacts

TABLE II

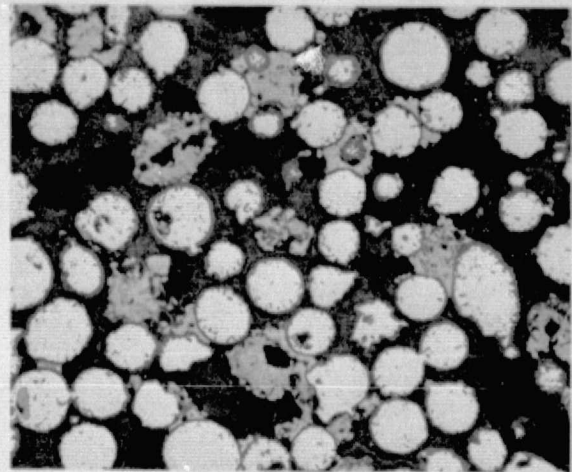
1204C (2200F) OXIDATION TEST WEIGHT GAIN DATA
FOR FeCrAlY, NiCrAlY, NiAl AND BRADDELLOY 502

<u>MATERIAL</u>	<u>SPECIMEN NUMBER</u>	<u>% THEO. DENSITY</u>	<u>% WEIGHT GAIN</u>		
			<u>112 Hr.</u>	<u>200 Hr.</u>	<u>500 Hr.</u>
FeCrAlY	74-69-7a	56.9	7.9	9.7	10.5
	74-69-7b	59.3	7.9	9.2	10.2
	74-66-7 ₃	60.0	7.0	8.35	9.21
	74-67-7b	60.5	6.5	7.93	-
	74-68-5c	63.8	6.3	8.4	9.42
	74-66-7 ₂	62.8	7.4	9.3	11.5
	74-68-5d	67.7	6.3	8.4	9.4
	74-68-5b	68.0	7.7	9.4	10.0
	74-69-5-1b	67.2	6.2	8.4	-
	Average		7.0	8.8	10.0
NiCrAlY	74-78-7b	60.0	7.7	8.1	9.1
	74-78-7a	60.3	7.7	8.1	9.3
	74-78-5a	59.6	7.8	8.1	10.9
	74-77-7a	69.7	7.8	8.4	9.4
	74-77-5a	68.2	7.8	8.3	8.9
	74-77-5b	69.3	7.6	8.1	10.2
	Average		7.7	8.2	9.6
NiAl	74-82-1	60.5	7.4	15.1	20.4
	74-82-2	60.0	6.9	11.2	21.7
	74-82-3	57.7	9.7	17.7	30.2
	74-80-1	63.2	6.4	10.0	18.9
	74-80-2	61.7	9.6	17.9	28.9
	74-80-3	63.0	6.6	11.1	21.1
	Average		7.8	13.8	23.5
Bradelloy	502-1	—*	30.5	34.5	34.5
	502-2	—*	34.4	33.8	33.4
	502-3	—*	29.8	34.2	33.8
	Average		31.57	34.7	33.9

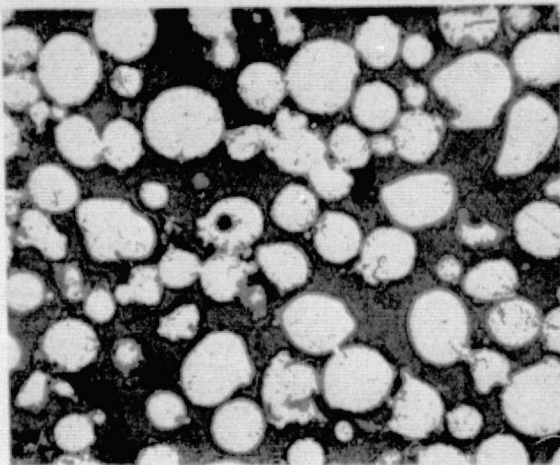
* Density of Bradelloy 3.5 g/cc



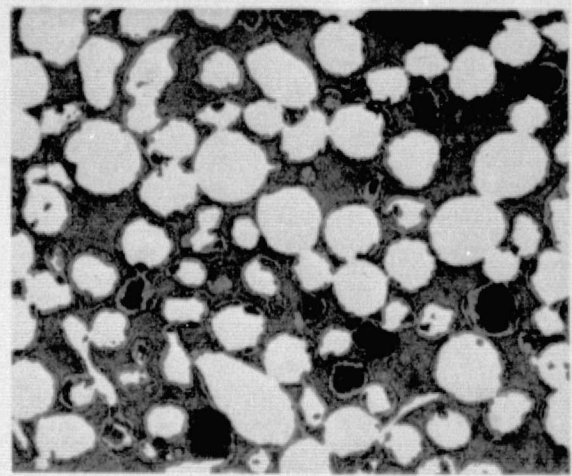
(A) FeCrAlY



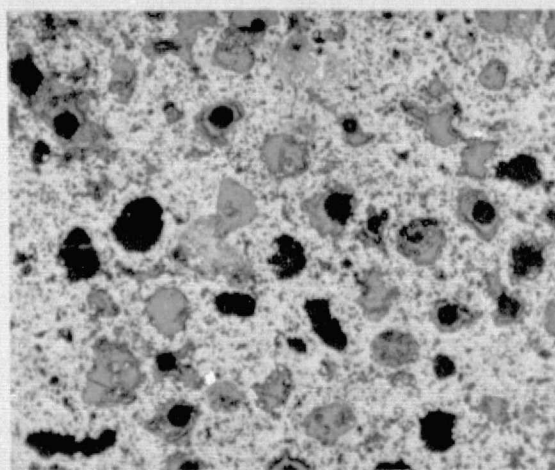
(B) FeCrAlY



(C) NiCrAlY



(D) NiAl



(E) BRADDELLOY

Magnification 100X

Figure 4 Typical Structure of Oxidation Tested Compacts - 1204C (2200F)/250 Hrs.

On the basis of the superiority of NiCrAlY and FeCrAlY in the 500 hour/1204C (2200F) oxidation tests, NiAl was eliminated from further consideration and not included in subsequent tests.

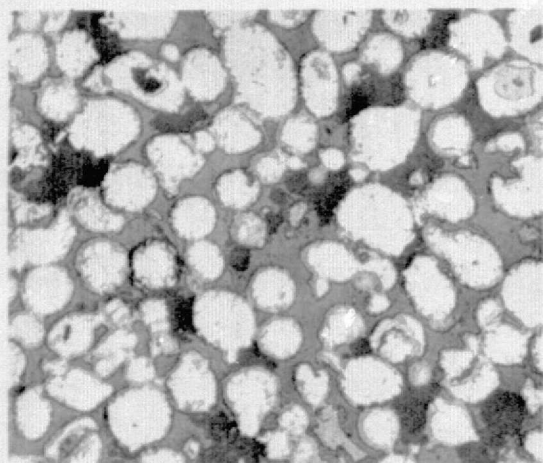
Further low velocity oxidation tests were conducted with NiCrAlY, FeCrAlY and Bradelloy for 100 hours at 1316C (2400F). Again, NiCrAlY and FeCrAlY proved superior to Bradelloy, and gain, FeCrAlY exhibited a wide variation in oxidation behavior within a given sample (Figure 5).

In both oxidation tests, the rate of weight gain for FeCrAlY and NiCrAlY, Figures 6 and 7 top, were nearly identical and independent of density. NiCrAlY, however, exhibited greater volume change than FeCrAlY (but less than Bradelloy) at both temperatures. The oxidation behavior of NiCrAlY and FeCrAlY after 250 hours at 1204C (2200F) is depicted metallographically in Figure 8 at 100X. Virtually all of the NiCrAlY particles have a uniform oxide film and some intergranular oxidation, and only the worst areas show an occasional particle that has been completely converted to oxide. With the FeCrAlY compact there was a wide variation in behavior. The best areas showed particles with the same uniform oxide film as the NiCrAlY particles, but, more typically, there were scattered, completely oxidized particles as presented in the lower center photomicrograph. Also observed were areas where breakaway oxidation had occurred, lower right.

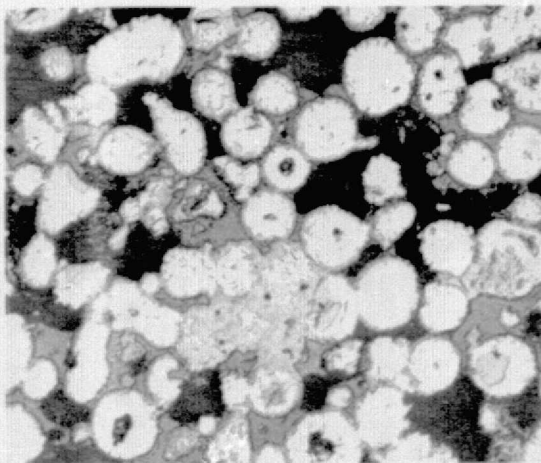
After 500 hours exposure at 1204C (2200F), the best areas of the FeCrAlY remained virtually unchanged, and the typical areas showed considerable attack on many particles and more extensive breakaway oxidation. After the same exposure, the NiCrAlY showed little change in the best areas and moderate intergranular oxidation in the typical areas. The worst areas were at the surface where individual particles had completely oxidized, but there was no evidence of breakaway oxidation.

The greater volume expansion of the NiCrAlY compacts versus the FeCrAlY (Figures 6 and 7) may be explained by examination of the oxide film formation on the intact particles after exposure for 112 and 500 hours at 1000X. Figure 9 shows that a heavier film was formed on the NiCrAlY particle after 112 hours than on the FeCrAlY, and after 500 hours, the NiCrAlY showed the presence of a second phase, probably a spinel, in the oxide where the oxide film on the FeCrAlY was still single phase and somewhat thinner. The volume expansion may therefore have been due, in part, to the expansion caused by spinel formation.

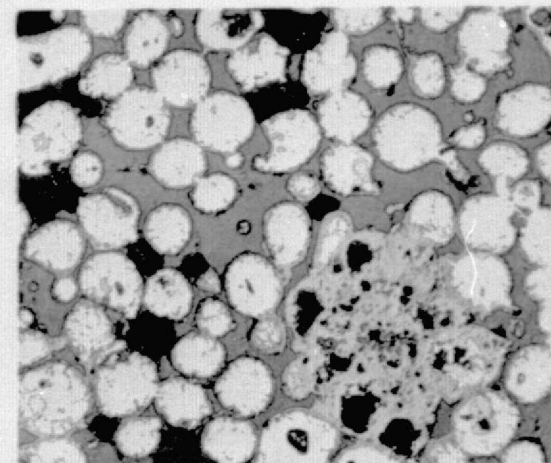
One would assume that the breakaway oxidation of FeCrAlY would execute a greater influence in volume change than the secondary phase formation with NiCrAlY. However, the breakaway oxidation observed was localized and represented only a small percentage of the total mass of particles. It should also be noted that when localized breakaway oxidation occurred the oxidation products filled in the void areas between the particles and did not necessarily contribute to appreciable expansion.



BEST AREA

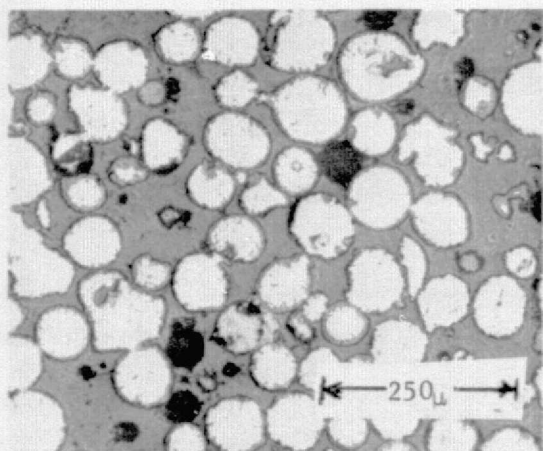


TYPICAL AREA

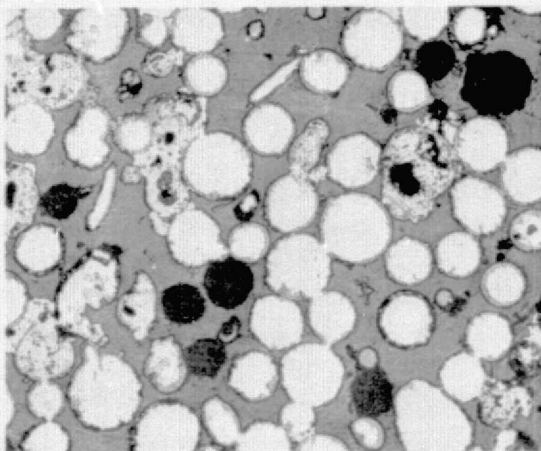


WORST AREA

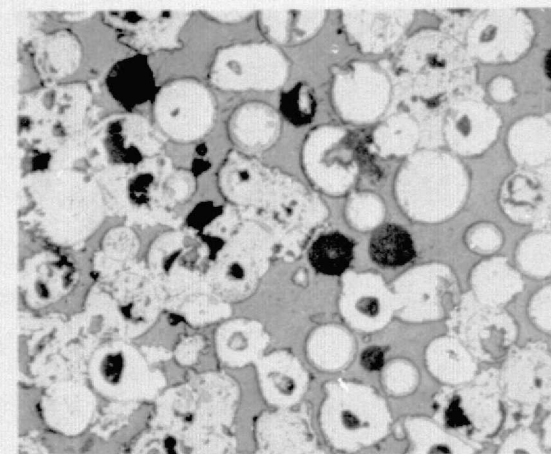
NiCrAlY



BEST AREA



TYPICAL AREA



WORST AREA

100X

FeCrAlY

Figure 5 NiCrAlY and FeCrAlY Compacts After Cyclic Dynamic Oxidation, Low Velocity, At 1316C (2400F) for 100 Hours

65 - 70 Percent Theoretical Density

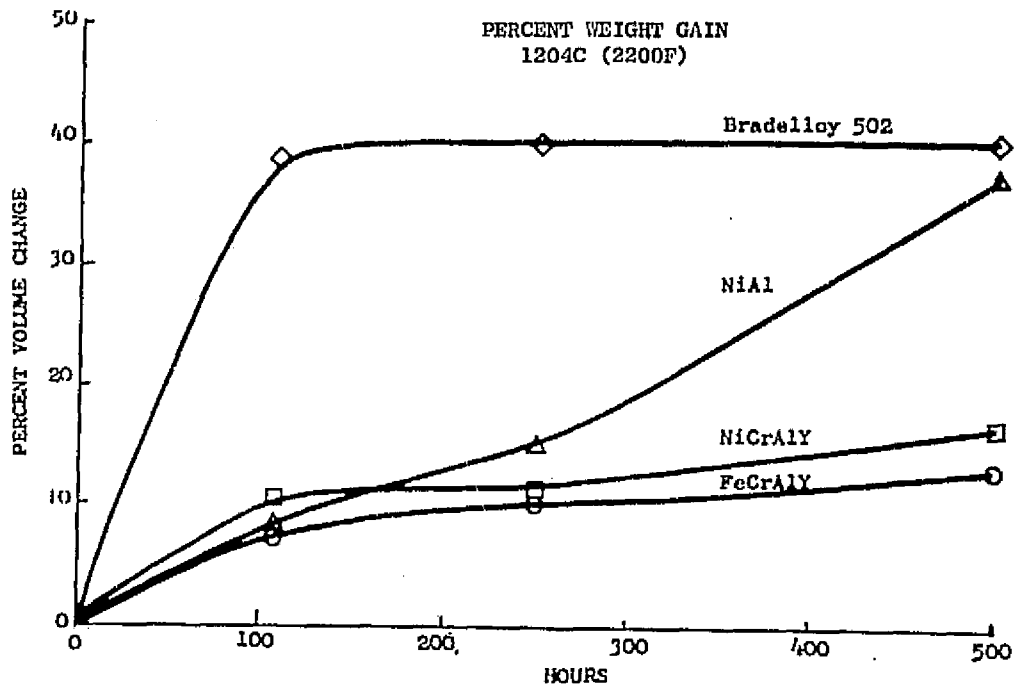
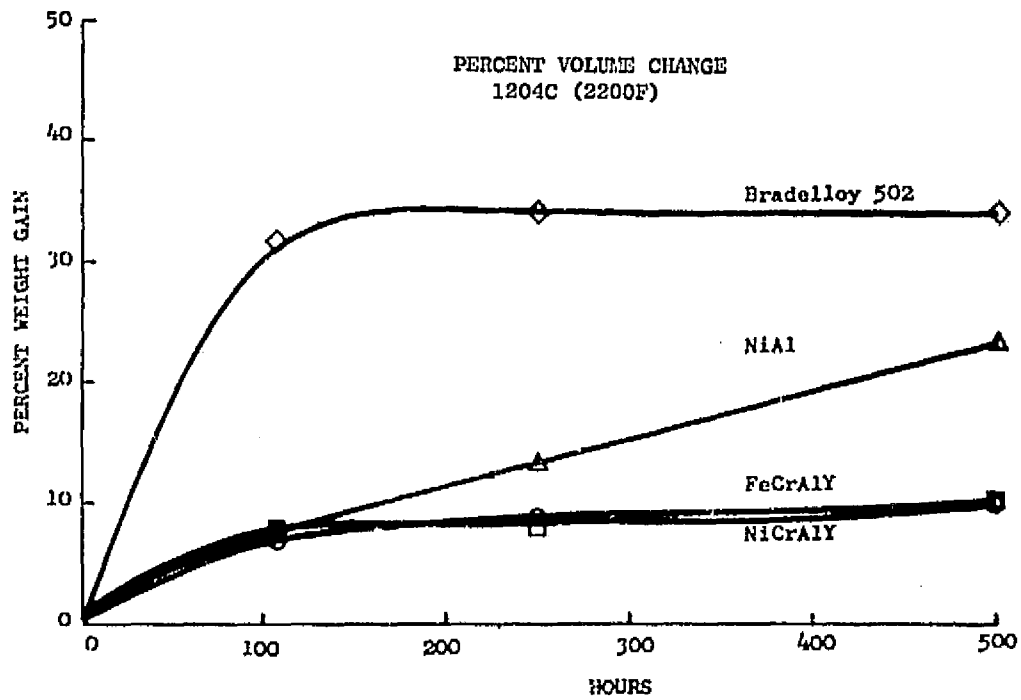


Figure 6 Low Velocity Oxidation Tests

65 - 70 Percent Theoretical Density

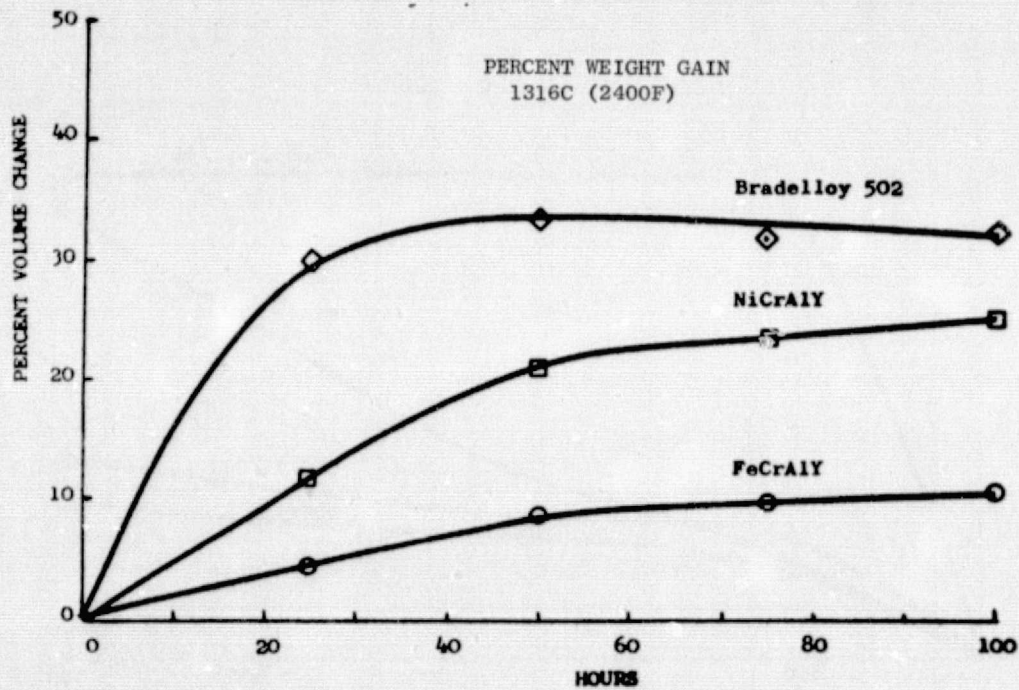
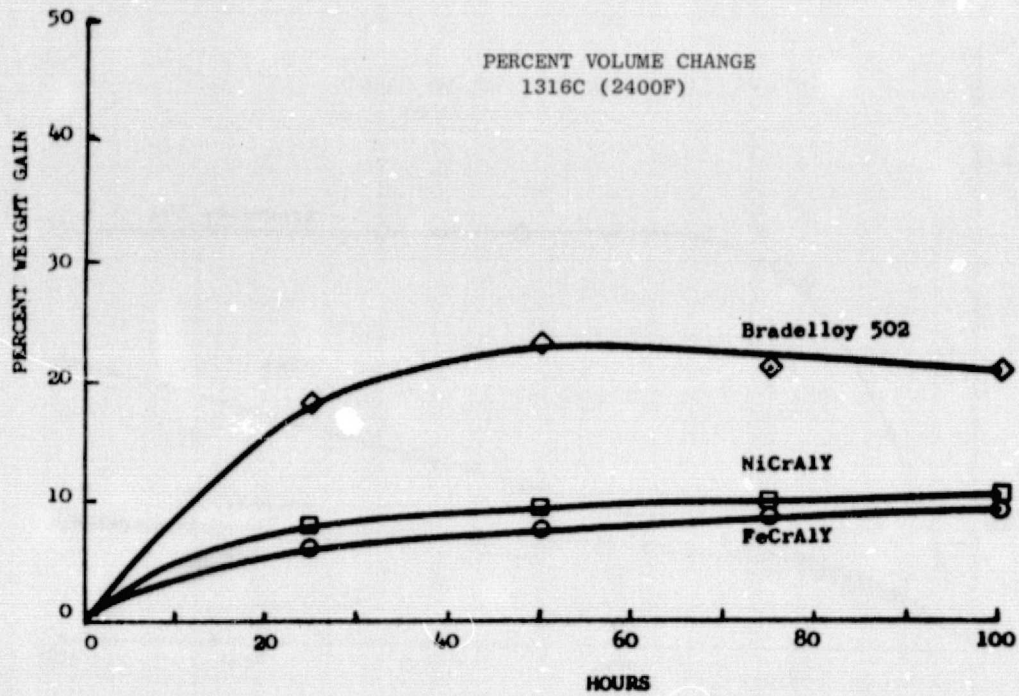
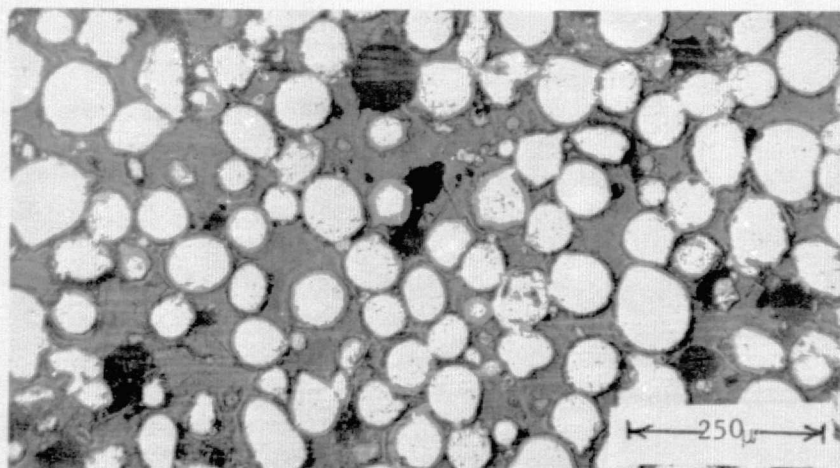
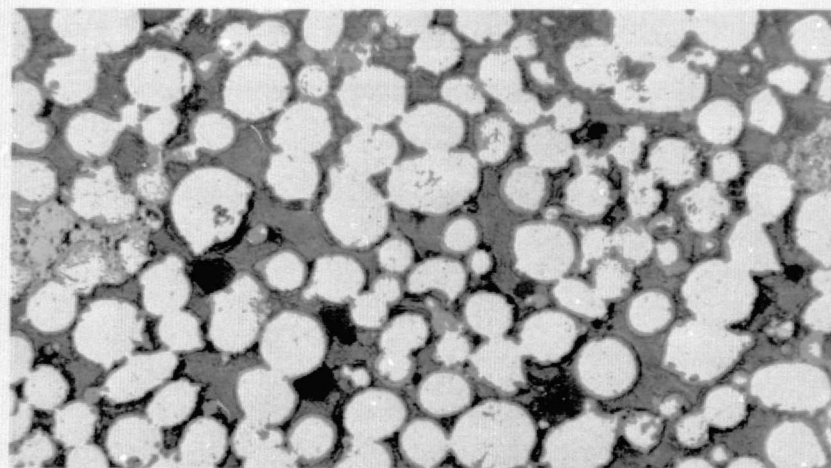


Figure 7 Low Velocity Oxidation Tests

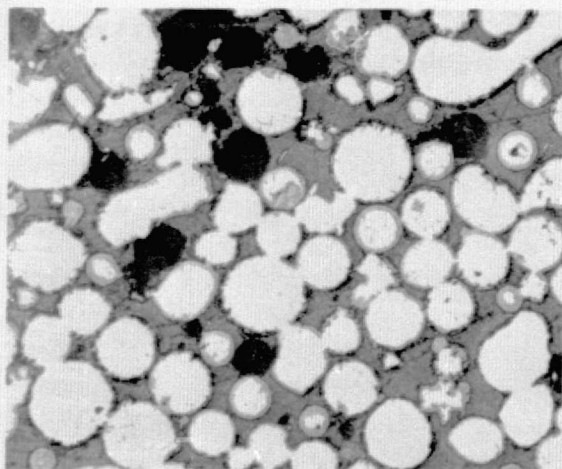


TYPICAL AREA

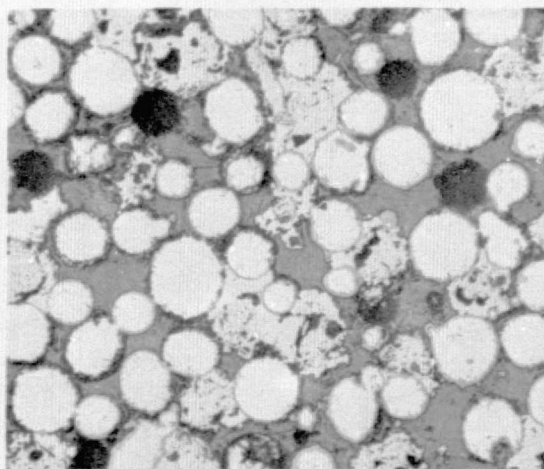


WORST AREA

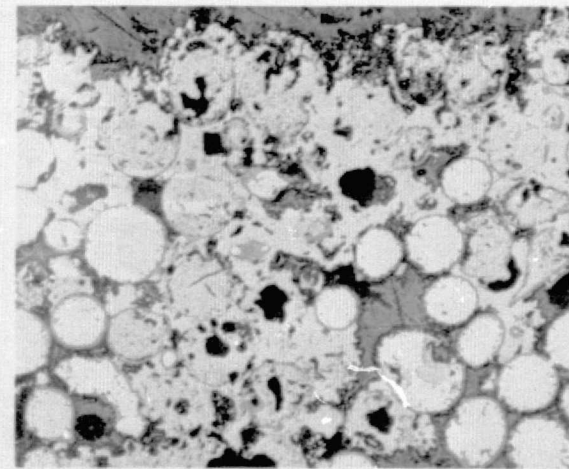
NiCrAlY



BEST AREA



TYPICAL AREA

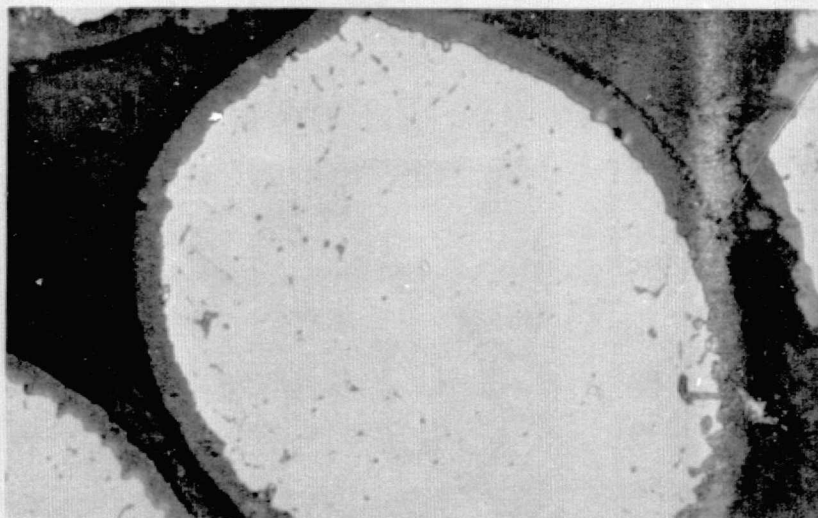


WORST AREA

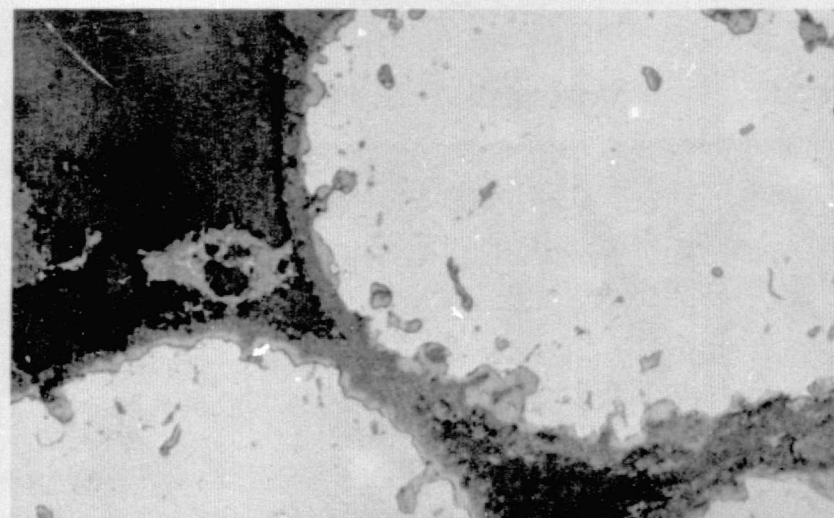
100X

FeCrAlY

Figure 8 NiCrAlY and FeCrAlY Compacts After Cyclic Dynamic Oxidation, Low Velocity, At 1204C (2200F) for 250 Hours

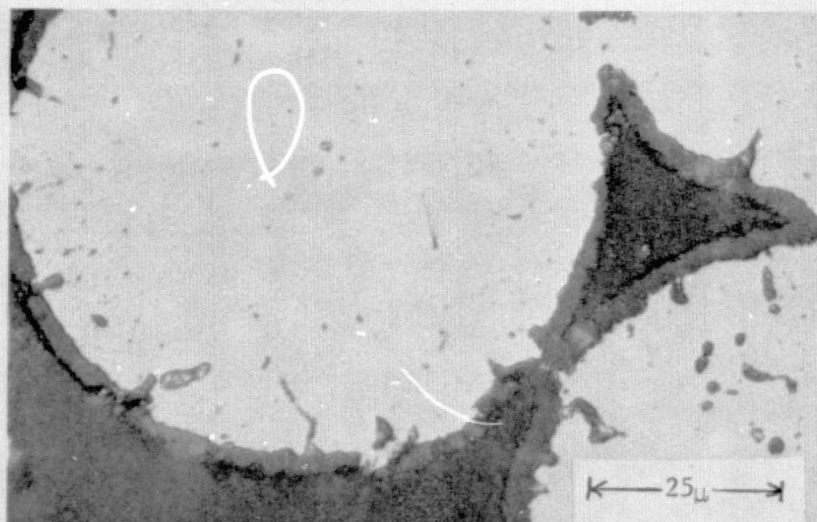


112 HOURS

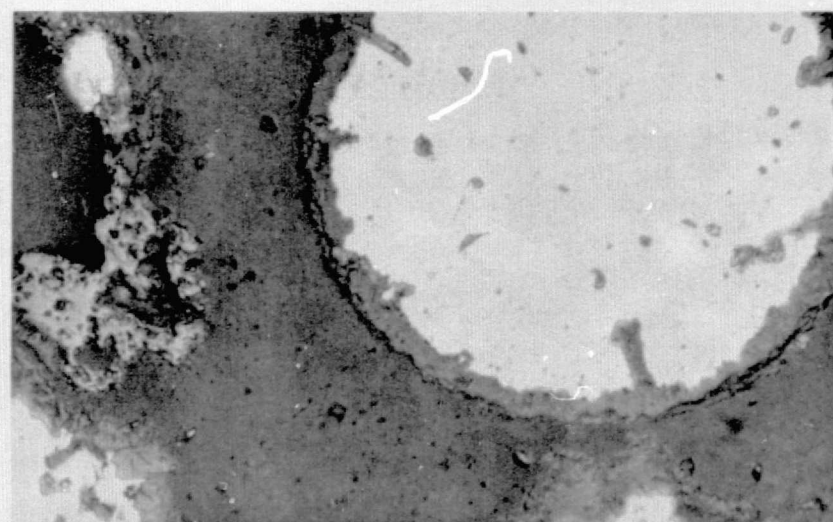


500 HOURS

NiCrAlY



112 HOURS



500 HOURS

FeCrAlY

1000X

Figure 9 Oxide Formation on NiCrAlY and FeCrAlY Particles After 112 and 500 Hours Cyclic Dynamic Oxidation, Low Velocity, at 1204C (2200F)

OXIDATION MECHANISMS

a) Normal Oxidation

SEM EDAX* analyses of FeCrAlY and NiCrAlY powder particles after 1204 (2200F) and 1316C (2400F) exposures indicated that, after as little as 24 hours at 1316C (2400F), the aluminum level at the center of the original powder particles dropped to a point equivalent to background, i. e., less than 1%, leaving basically a FeCr or NiCr core surrounded by an Al-containing rim and scale. Loss of the protective scale due to spalling, rubbing or erosion would be expected to result in more rapid oxidation of the remaining particle and formation of Cr_2O_3 , FeO, Fe_2O_3 or NiO. Formation of FeO and Fe_2O_3 in the case of FeCrAlY could then lead to breakaway oxidation of adjacent particles.

b) Breakaway Oxidation

SEM EDAX analysis of alloy powders and oxidized FeCrAlY samples, and examination of appropriate binary ceramic phase diagrams helped to explain why breakaway oxidation was sometimes observed in FeCrAlY and why NiCrAlY was much less susceptible to this phenomenon.

SEM EDAX analysis of a normal oxide is shown at the top of Figure 10 and indicates a high concentration of Al in the scale with lesser amounts of yttrium, chromium and iron. Analysis of the oxide in the center, a product of breakaway oxidation, shows high concentrations of chromium and iron. Analysis of as-received FeCrAlY powders revealed that about 20% of the particles were lower in aluminum than the other particles. The smaller particles of this lower aluminum level could be readily oxidized at 2200F, thereby forming some iron oxides. Once formed, the iron oxides tend to destroy the effectiveness of the protective Al_2O_3 film of adjacent particles by forming non-protective $\text{Fe}_2\text{O}_3 \cdot \text{Al}_2\text{O}_3$. This is shown in Figure 11, left, where Fe_2O_3 and Al_2O_3 have a limited solubility in each other of about six percent, beginning at 1000C (1840F) and increasing with temperature. This condition would not occur to the same degree with NiCrAlY with any NiO that may have formed at Al-lean particles. The solubility of Al_2O_3 in NiO is very low at 1400C (2552F), Figure 11, right. Thus, the oxidation of a NiCrAlY particle will proceed in situ rather than spreading to affect adjacent particles.

Rub Behavior and Erosion Resistance of Oxidized Filler Material

FeCrAlY and NiCrAlY hot pressed compacts varying in density from 58 to 86% of theoretical were tested for rub behavior and erosion resistance as-processed, and again after 100 hours cyclic exposure at 1204 (2200F). The volume of material eroded in 120 seconds as a function of percent theoretical density is shown in Figure 12. Also included are the initial data for as-processed NiAl compacts. As-processed, NiCrAlY exhibited erosion resistance equivalent to the upper limit for Bradelloy at a lower density than FeCrAlY (65 versus 73% theoretical). After high temperature exposure both materials exhibited nearly the same erosion resistance. The increased erosion resistance of FeCrAlY after exposure indicated possible additional sintering during the exposure or an effect of oxides.

*Energy Dispersive Analysis by X-rays.

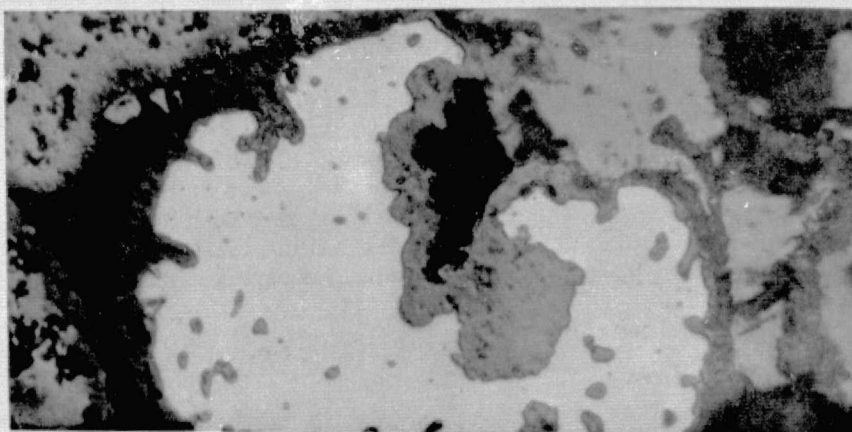
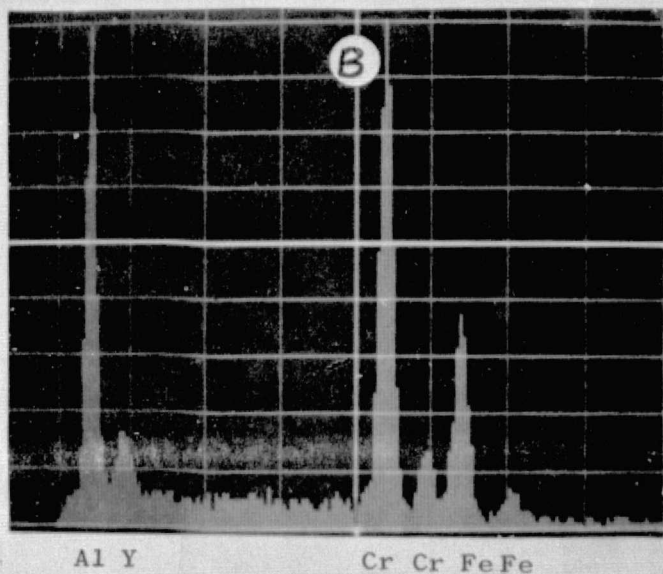
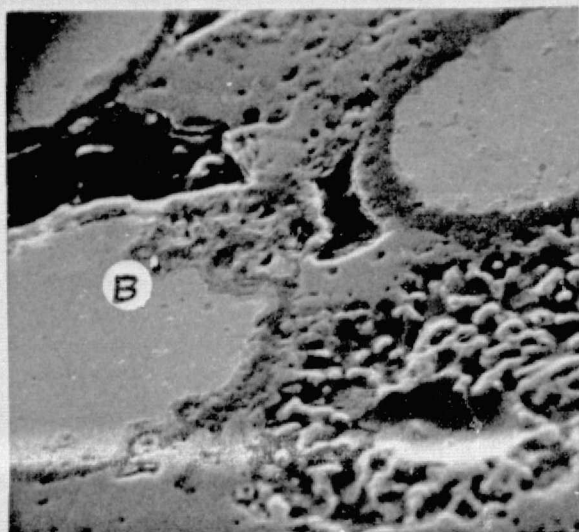
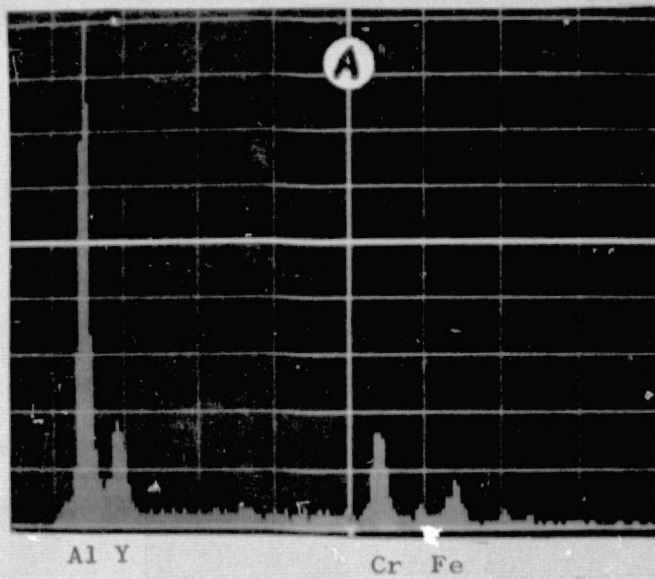


Figure 10 FeCrAlY Oxidation Mechanism-Breakaway Oxidation

Top: Normal Oxide - SEM-1450X
 Center: Breakaway Oxidation - SEM-725X
 Bottom: Breakaway Oxidation - 500X

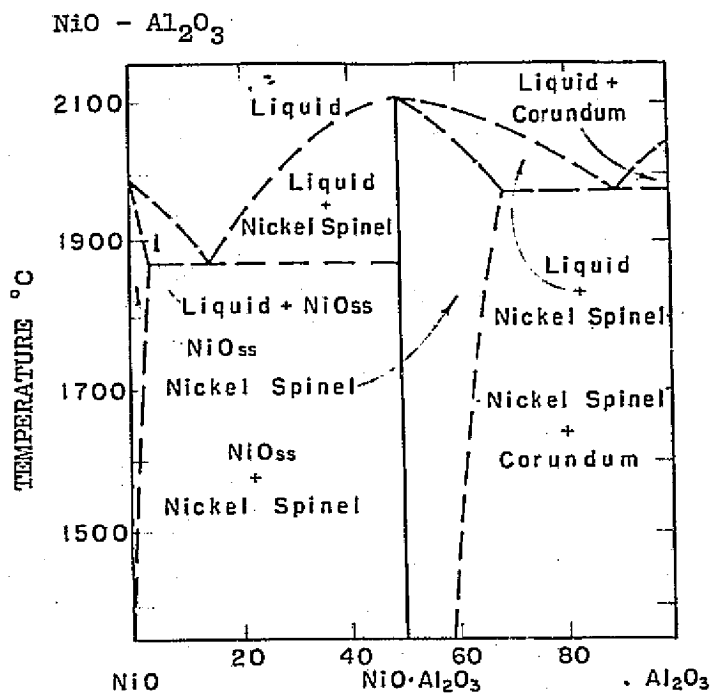
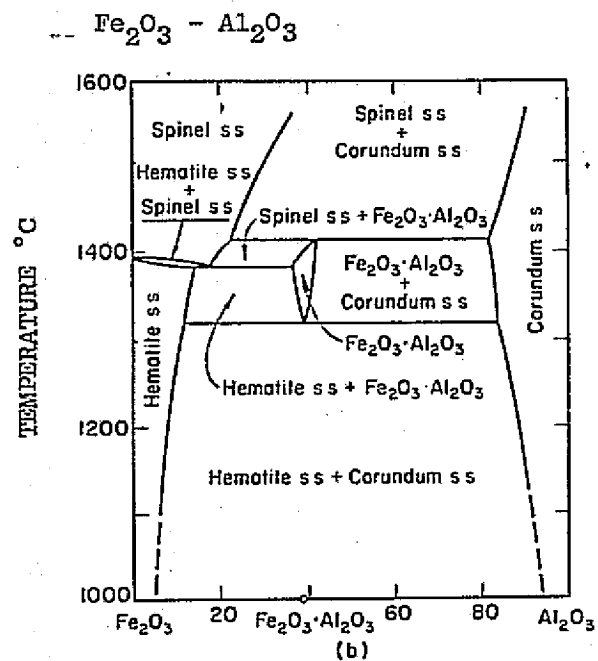


Figure 11 $\text{Fe}_2\text{O}_3 - \text{Al}_2\text{O}_3$ and $\text{NiO} - \text{Al}_2\text{O}_3$ Phase Diagrams - Ref. Phase Diagrams for Ceramists, 1964

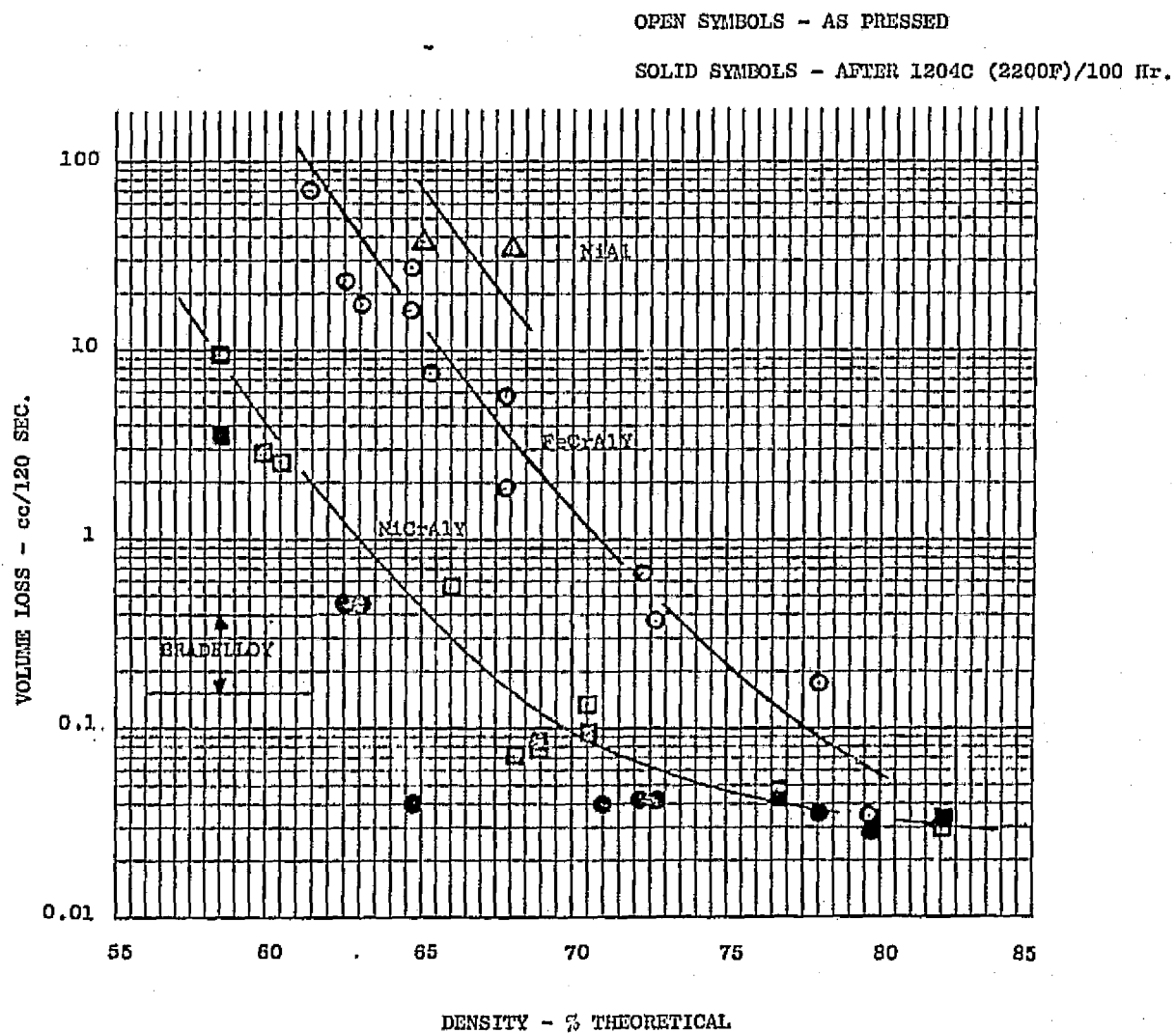


Figure 12 Cold Erosion Resistance

As-processed FeCrAlY exhibited good rub behavior (no blade wear or scabbing) in the laboratory test (700 fps) for compacts less than 71% of theoretical density. However, after the 1204C (2200F)/100 hour exposure, compacts at 61% of theoretical density exhibited 1 mil of blade wear with 4 mils wear at 63%. Densities greater than 71% caused severe blade wear and scabbing both as-processed and exposed. In the case of NiCrAlY, as-processed compacts exhibited good rubs at densities less than 68% of theoretical. After exposure slight blade wear (1 mil) was indicated at 63%. At 68% and above NiCrAlY exhibited severe blade wear both as-processed and exposed.

Results of a General Electric in-house program involving MCrAlY-filled turbine shrouds indicated that scabbing of high density FeCrAlY and NiCrAlY filler material by the rubbing of turbine blades might be less of a problem than indicated by the laboratory tests. In two separate cold (CF6-6) rotor rub tests (1440 fps tip speed) incorporating a full set of turbine blades, no blade wear was experienced during rapid incursions (1 mil/sec and 20 mil/sec) of 20 mils. In contrast, testing in the laboratory facility (700 fps tip speed) produced blade wear and scabbing on the denser compacts. These cold rotor rub tests of both hot pressed FeCrAlY and NiCrAlY filled shroud showed unexpectedly good rubs of both filler materials at the higher densities under more simulative test conditions (engine hardware, blade tip speed and incursion rate). It should be noted that during the rotor tests the rub surfaces were observed to be white hot, i.e., the test was made at room temperature with the rub surfaces increasing in temperature substantially.

MATERIAL SELECTION

The Work Plan called for selection of one or two materials for continued development. The requirements for an advanced shroud filler fell into two categories, necessary and desired, as follows:

<u>Necessary Requirements</u>	<u>Desired Characteristics</u>
Oxidation resistance > 3X Bradelloy	Low volume expansion on prolonged exposure
Erosion resistance ≥ Bradelloy	No scabbing

All three candidate materials met the necessary oxidation requirements; however, NiAl failed to meet the erosion goal (NiAl also was the poorest candidate in oxidation tests). In the case of necessary and desired properties, the FeCrAlY and NiCrAlY are compared to Bradelloy 502 below:

<u>DESIRED PROPERTIES</u>			
<u>Property</u>	<u>FeCrAlY</u>	<u>NiCrAlY</u>	<u>Bradelloy</u>
Oxidation resistance (0.05 Mach)	Good, but exhibits breakaway oxidation	Very good	Limited
Erosion resistance			
As-processed	Good	Best	Good
After 1204C (2200F)/100 hrs	Good	Good	Poor

DESIRED PROPERTIES (Cont.)

<u>Property</u>	<u>FeCrAlY</u>	<u>NiCrAlY</u>	<u>Bradelloy</u>
Volume expansion			
1316C (2400F)	Best	Good	Poor
1204C (2200F)	Good	Good	Poor
Scabbing			
700 fps (lab tester)	Good	Best	Scabs and wears blades
1400 fps (cold CF6 rotor)	Good	Good	Wears blades

As noted, FeCrAlY and NiCrAlY were comparable except for the occurrence of breakaway oxidation with FeCrAlY, a significant factor. NiCrAlY, therefore, was the material selected for continued development as an advanced shroud filler material.

NiCrAlY COMPOSITIONAL VARIATIONS

Evaluations were made of NiCrAlY compositions adjusted to optimize oxidation resistance. Compositions included 20Cr-8Al-1Y, 20Cr-10Al-1.4Y, 22Cr-10Al-1.0Y, and 23Cr-13Al-1.0Y. Testing consisted of placing the alloy in powder form in ceramic boats and exposing to static air at 1204C (2200F) and 1316C (2400F). In the 1316C (2200F) tests on the basis of weight gain (Table III) and metallographic examination (Table IV), the 23Cr-13Al-1Y composition was the most oxidation resistant with the 20Cr-10Al-1.4Y close behind. The 22Cr-10Al-1Y was slightly inferior, and the 20Cr-8Al-1Y was definitely inferior. At 1316C (2400F) there was a drastic shift in performance with the best performer being the 22Cr-10-1Y followed closely by the 20Cr-10Al-1.4Y. Both the 23Cr-13Al-1Y and the 20Cr-8Al-1.0Y were inferior in performance.

PROPERTIES OF Ni-22Cr-10Al-1Y

Ni-22Cr-10Al-1Y was chosen as the most promising candidate for further development as a shroud filler material on the basis of the oxidation test results for various NiCrAlY compositions.

Physical properties were determined for nominally 75% dense* Ni-22Cr-10Al-1Y compacts. Thermal diffusivity was measured over the temperature range 300 to 1100C (575 - 2012F) for NiCrAlY and Bradelloy 502, both as-compacted and after a 100 hour, 2200F oxidation exposure. As shown in Figure 13, NiCrAlY exhibited greater thermal diffusivity than Bradelloy 502 over the entire temperature range. In addition, NiCrAlY exhibited less of a change in thermal diffusivity due to the oxidation exposure.

*A 75% density was selected as the approximate mean density of acceptable material based on Figure 12.

NOTE: Tables V and VI to be forwarded under separate cover.

TABLE III

STATIC OXIDATION WEIGHT GAINS OF SEVERAL NiCrAlY POWDERS

<u>NiCrAlY Powder</u>	<u>Composition (Wt%)</u>			<u>Percent Weight Gain</u>			
	<u>Cr</u>	<u>Al</u>	<u>Y</u>	<u>1204 (2200F)</u>		<u>1316 (2400F)</u>	
				<u>24 Hrs</u>	<u>90 Hrs</u>	<u>24 Hrs</u>	<u>80 Hrs</u>
Lot # 3574	22.2	10.1	0.95	14.6	27.4	17.1	32.0
Lot # 4928	19.4	8.0	0.90	13.4	36.0	19.3	31.1
Lot # 6091A	23.0	12.7	0.64	15.1	27.3	33.5	37.4
Lot # 6091B	23.0	12.7	0.64	14.6	26.4	33.3	39.4
Lot # 6179	19.6	10.0	1.45	14.3	28.4	15.8	32.4

TABLE IV

METALLOGRAPHIC EXAMINATION OF OXIDIZED NiCrAlY POWDERS

<u>LOT NO.</u>	<u>TEST TEMP.</u>	<u>TIME, HRS</u>	<u>OBSERVATIONS - NOS. OF PARTICLES IN SPECIMEN CROSS-SECTION -45 mm² (0.07 in²)</u>	
3574	1204C (2200F)	24	Totally oxidized particles	- ~ 65
4928	"	"	" " "	- ~ 225
6091A	"	"	" " "	- ~ 55 - mostly slivers
6091B	"	"	" " "	- ~ 45 - mostly slivers
6179	"	"	" " "	- ~ 30 - partially slivers
3574	"	90	Intact particles	- ~ 135
4928	"	"	" " "	- ~ 65
6091A	"	"	" " "	- ~ 230
6091B	"	"	" " "	- ~ 225
6179	"	"	" " "	- ~ 195
3574	1316C (2400F)	24	Totally oxidized particles	- ~ 210 - intermittent localized - breakaway oxid. - 3-6 particles
4928	"	"	" " "	- >500 - numerous breakaway oxid. areas
6091A	"	"	Gross oxidation	- > 75% - converted to oxide
6091B	"	"	" " "	- > 75% - " " " "
6179	"	"	Totally oxidized particles	- ~260 - intermittent localized - breakaway oxid. - 3-8 particles
3574	1316C (2400F)	80	Intact particles	> 650
4928	"	"	" " "	~ 550
6091A	"	"	" " "	20; 99% converted to oxide
6091B	"	"	" " "	14; 99% converted to oxide
6179	"	"	" " "	> 800

NOTE: Total number of particles in cross-section \approx 2000 - 2500

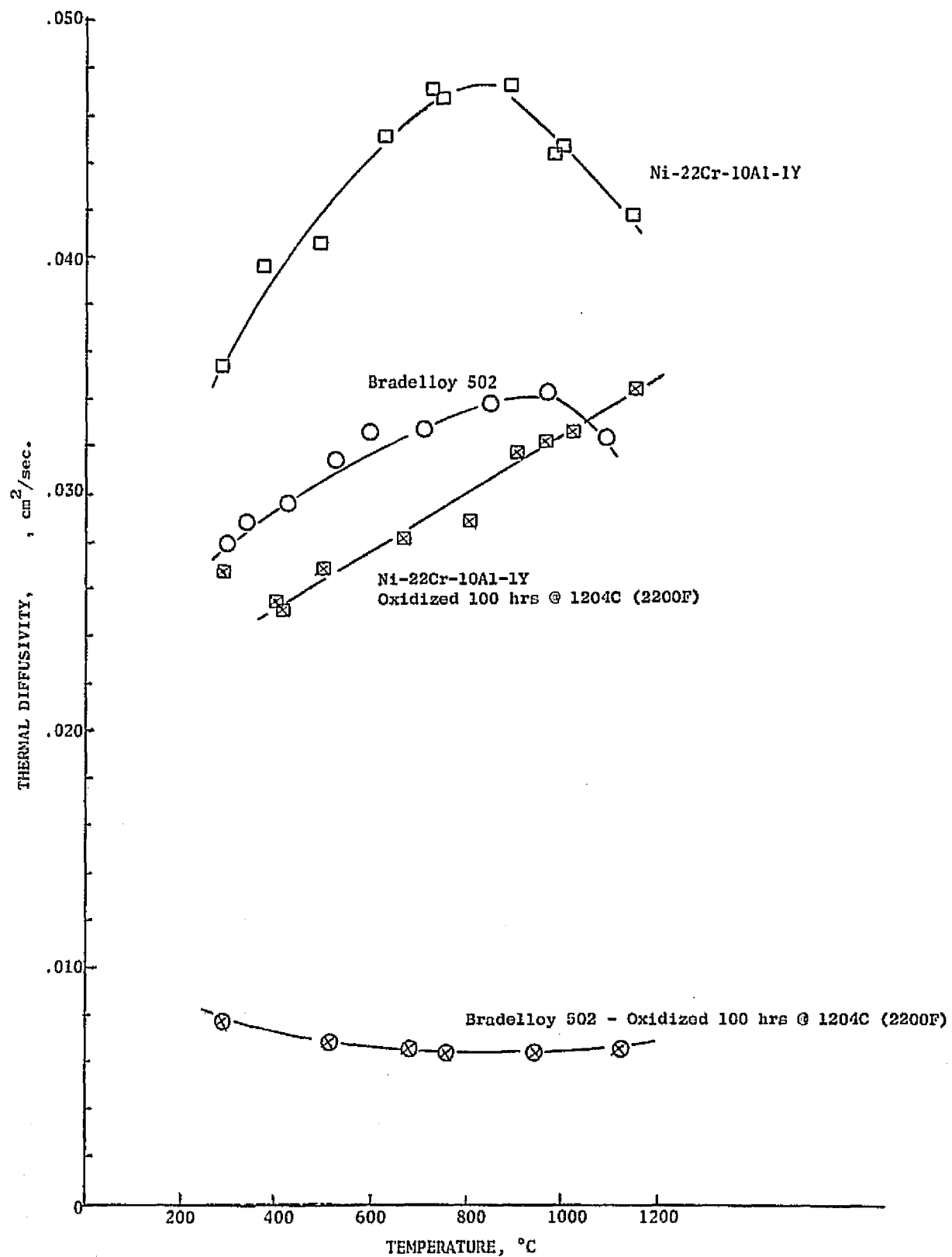


Figure 13 Thermal Diffusivity

Specific heat (C_p) data for NiCrAlY and Bradelloy 502 were used in conjunction with the thermal diffusivity to calculate thermal conductivity (K), shown in Figure 14. The C_p data were determined from the enthalpy-temperature relationship of the materials as measured in a modified Parr adiabatic water calorimeter (drop technique). Thermal diffusivity data were determined by a laser-pulse, transient heat flow technique.

Total linear thermal expansion of NiCrAlY was measured from 100 to 1000C (212 - 1832F) in a Chevenard Model 50 dilatometer, and the results are shown in Figure 15 along with data for Bradelloy 502.

Modulus of elasticity data, shown in Figure 16, were measured by the floating beam dynamic resonance method employing a Magnetest FM-500 Elastomat*.

The melting point of NiCrAlY was measured by exposing as-processed compacts for 15 minutes at various temperatures (1288-1371C) in a hydrogen atmosphere. Subsequent metallographic examination, Figure 17, indicated incipient melting at 1288C and definite melting at 1316C.

Low velocity cyclic oxidation tests, described earlier, were conducted for hot pressed compacts of the selected Ni-22Cr-10Al-1Y material. A 100 hour, 1316 (2400F) test was run for compacts in the range of 74 to 78% theoretical densities and Bradelloy 502 specimens. Test results, weight gain versus time, are presented in Figure 18. Again NiCrAlY proved to be superior to the Bradelloy types, having unoxidized material remaining after 100 hours, whereas the Bradelloy types were almost completely oxidized after one and five hour exposures.

Mach 0.8 high velocity cyclic oxidation tests were conducted with NiCrAlY and Bradelloy 500 specimens. Specimens, wedge shaped sections of filled CF6 shroud bodies, were placed in an eight station rotating specimen holder such that the hot gas stream impinged on the specimen surfaces at a 30 degree angle. The specimens were rotated at 450 rpm and cycled to about 204C (400F) once per hour in this test.

Two tests were conducted, one at 1204C (2200F) for 80 hours and another at 1149C (2100F) for 200 hours. Results of both tests confirmed that NiCrAlY had better oxidation resistance than Bradelloy. In the 1204C (2200F) test, Bradelloy was virtually all converted to oxide after only 22 hours, whereas NiCrAlY exhibited only a thin oxide film around the particles after 80 hours (see Figure 19). In the 1149C (2100F) test, Bradelloy was nearly completely converted to oxides in 90 hours, while NiCrAlY particles exhibited only thin oxide films after 200 hours. In addition, NiCrAlY exhibited superior resistance to erosion by the hot gas stream, with Bradelloy eroding when converted to oxide.

Hot particle erosion testing of NiCrAlY, Bradelloy 500, and Bradelloy 502 was conducted in a test facility comprised of a low velocity oxidation flame tunnel and a rotating specimen fixture (rotational speed up to 300 rpm) with axis set at a 45° angle to the hot gas stream.

*Magnaflux Corporation, Chicago, Illinois.

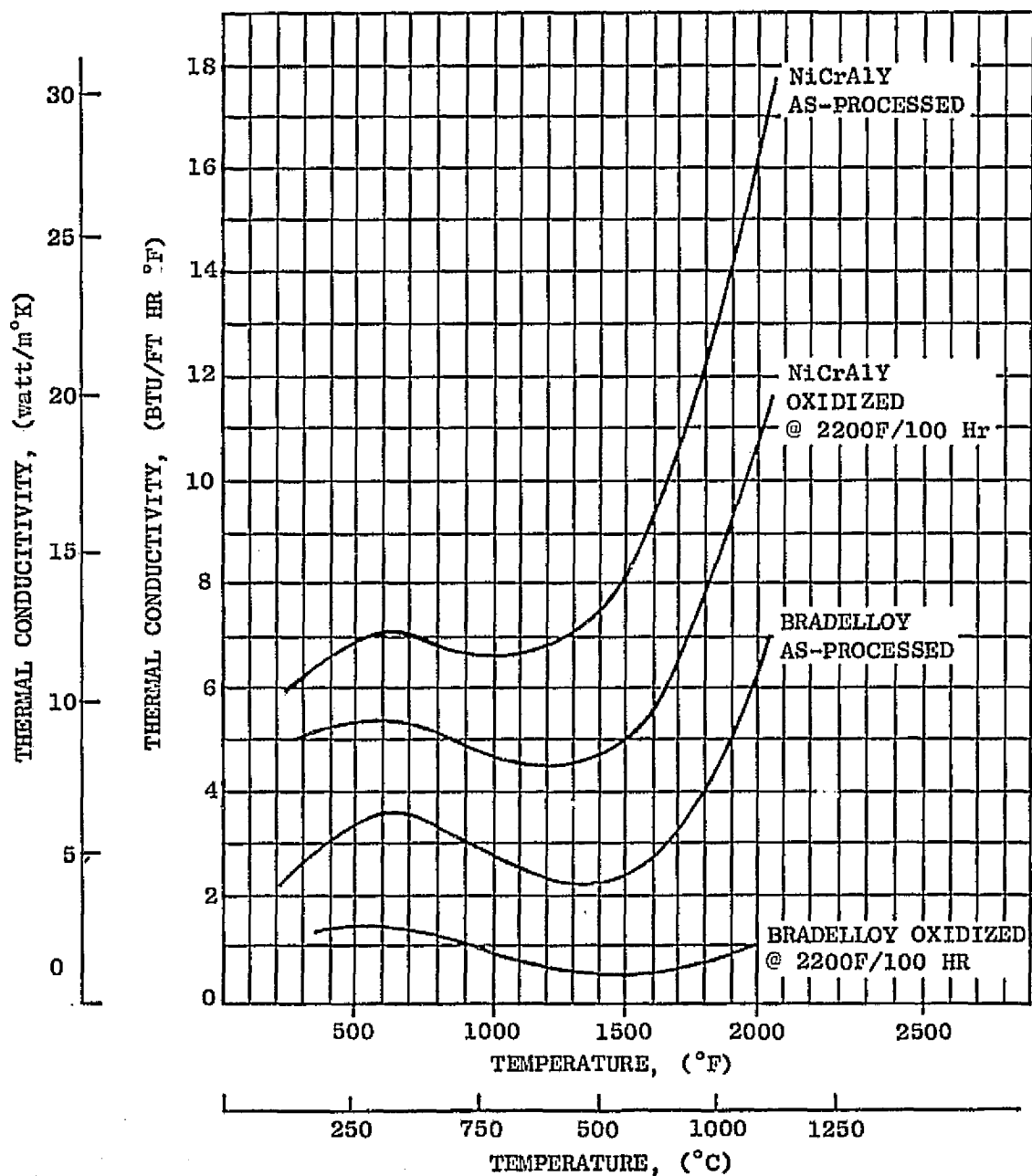


Figure 14 Thermal Conductivity of NiCrAlY vs Bradelloy

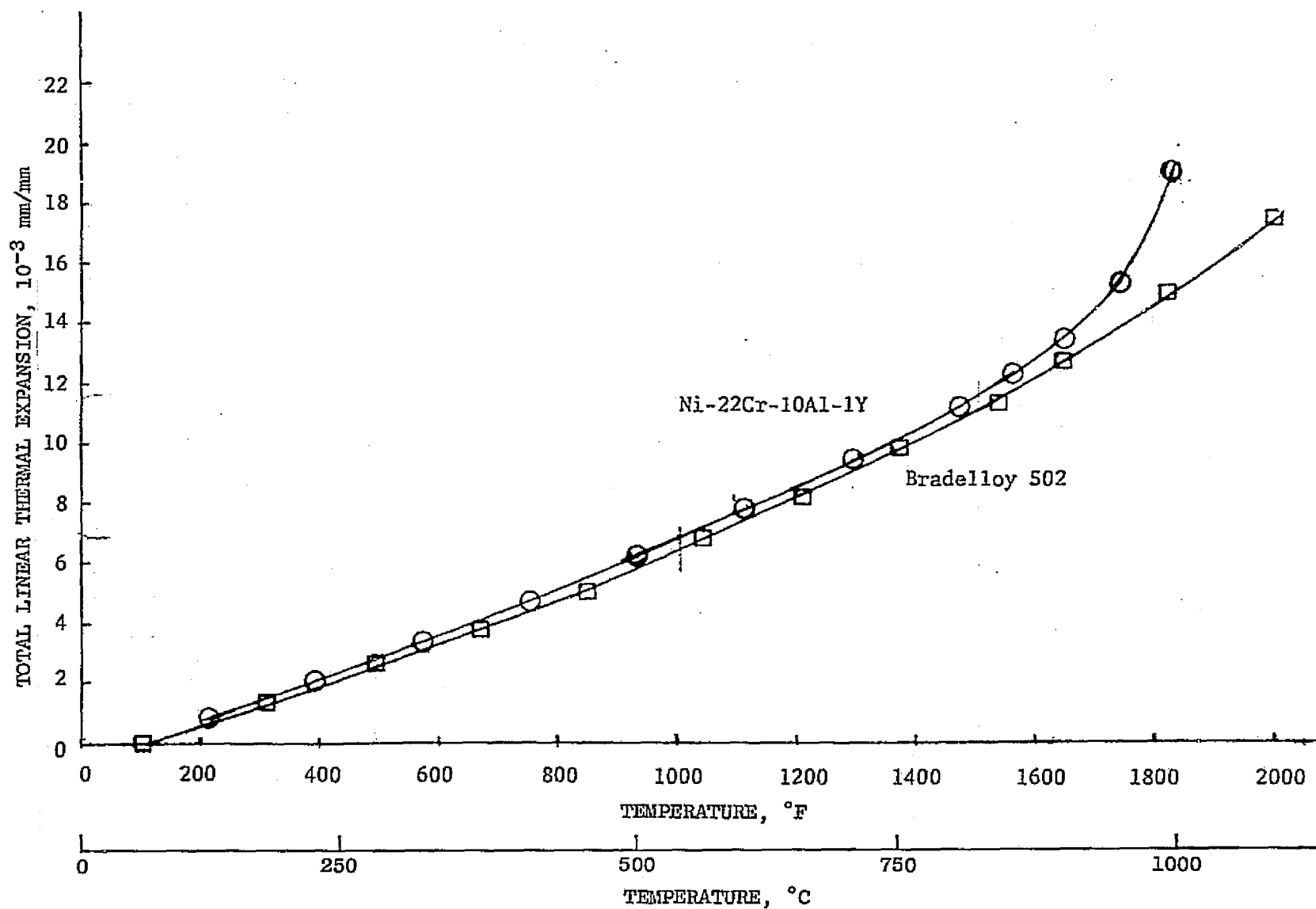


Figure 15 Total Linear Thermal Expansion

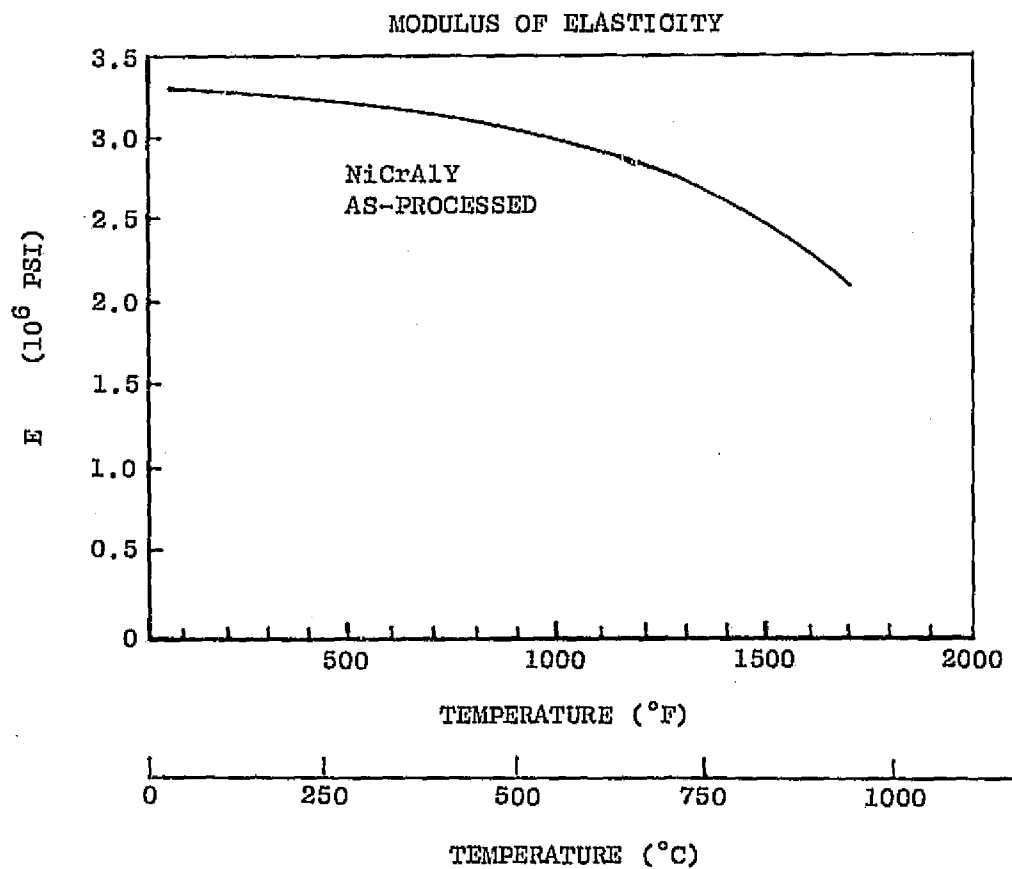
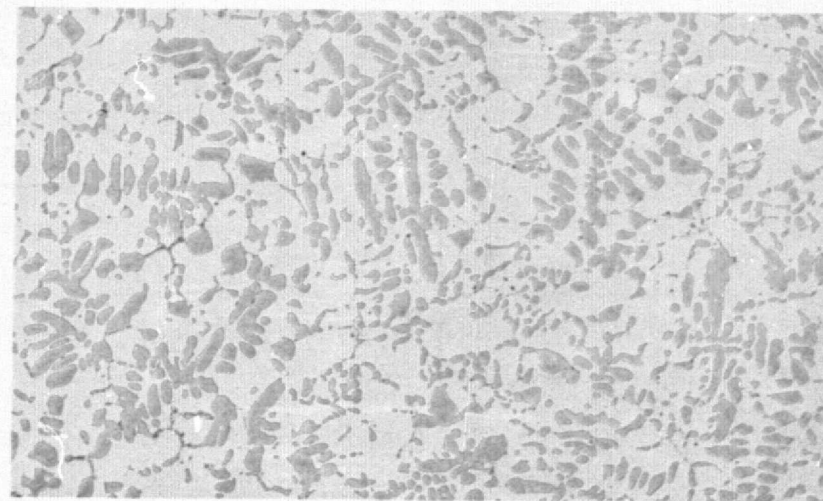
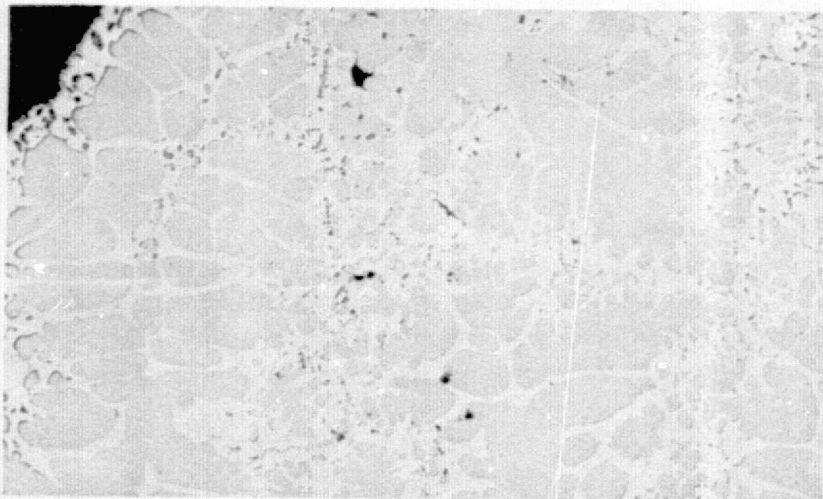
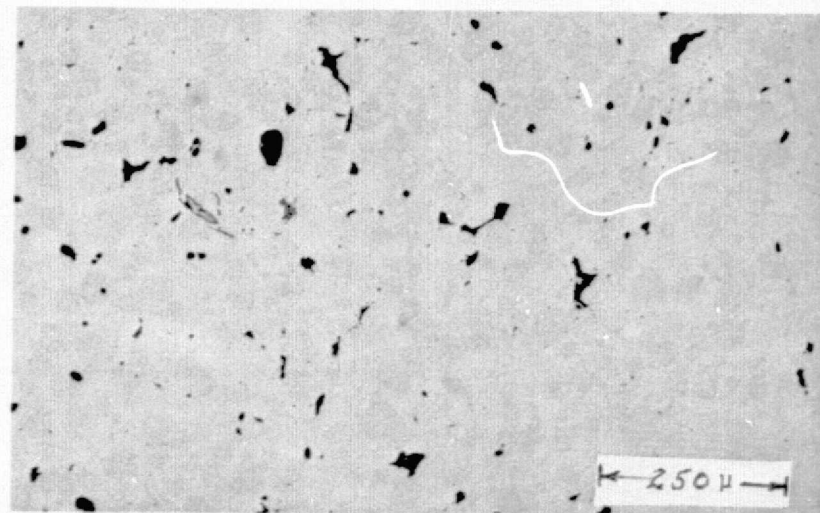
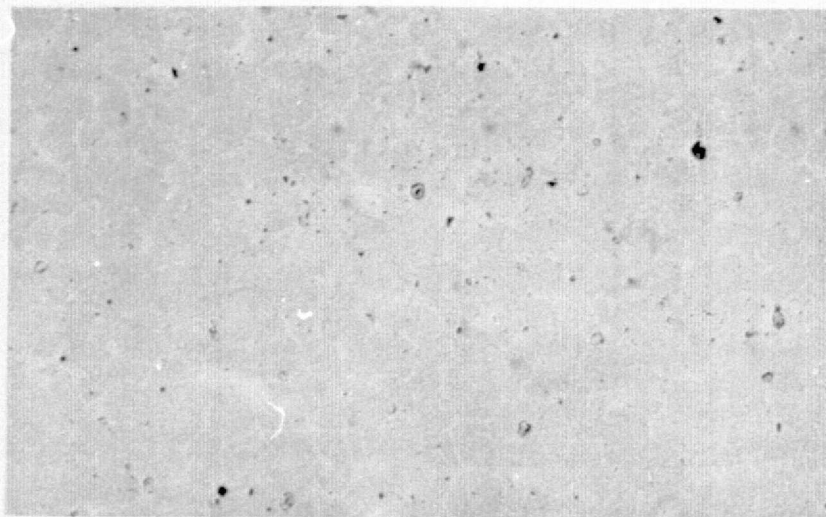


Figure 16 Modulus of Elasticity of NiCrAlY



1316C (2400F)



1288C (2350F)

100X

Figure 17 Melting Point Determination of Hot Pressed Compacts from NiCrAlY Powders from Lot Nos. 6091 and 6408. Held for Fifteen Minutes in Hydrogen Atmosphere

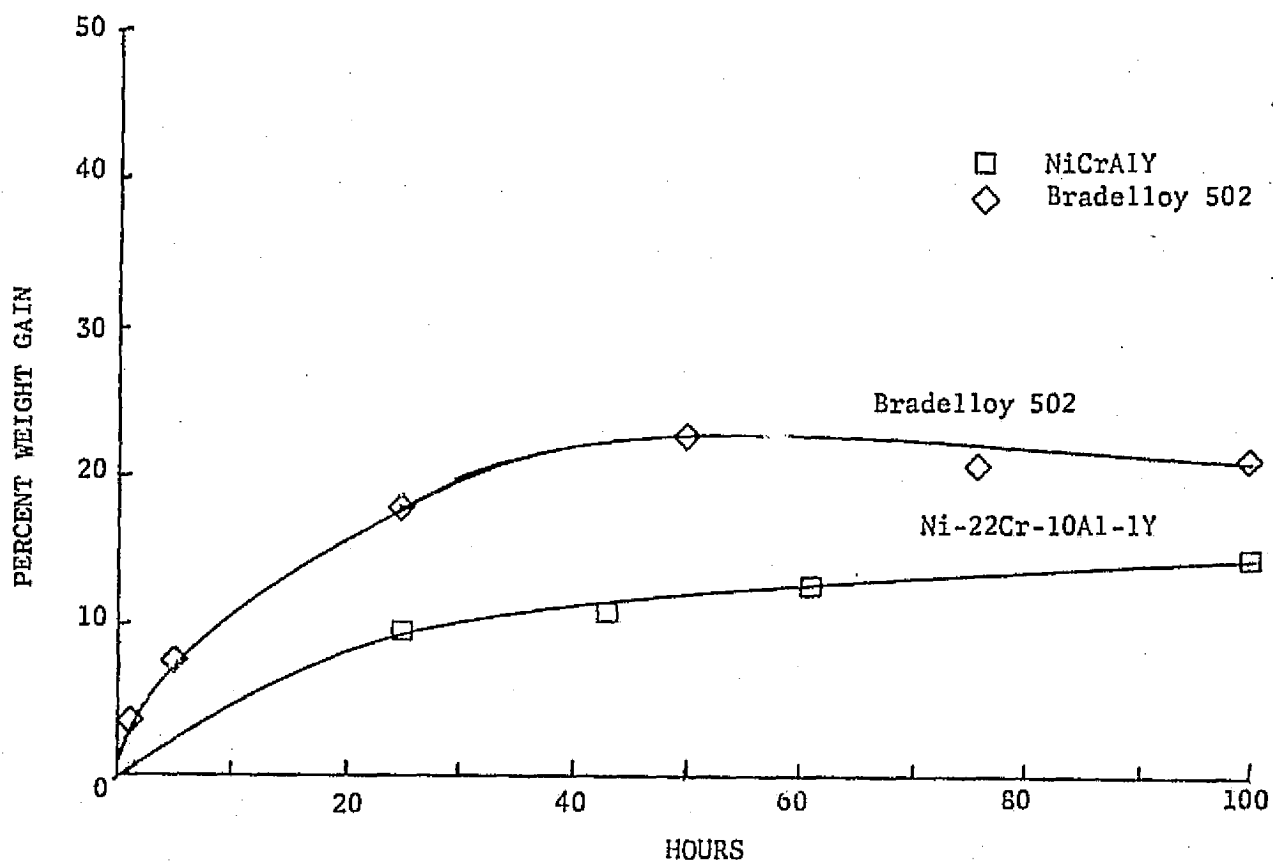
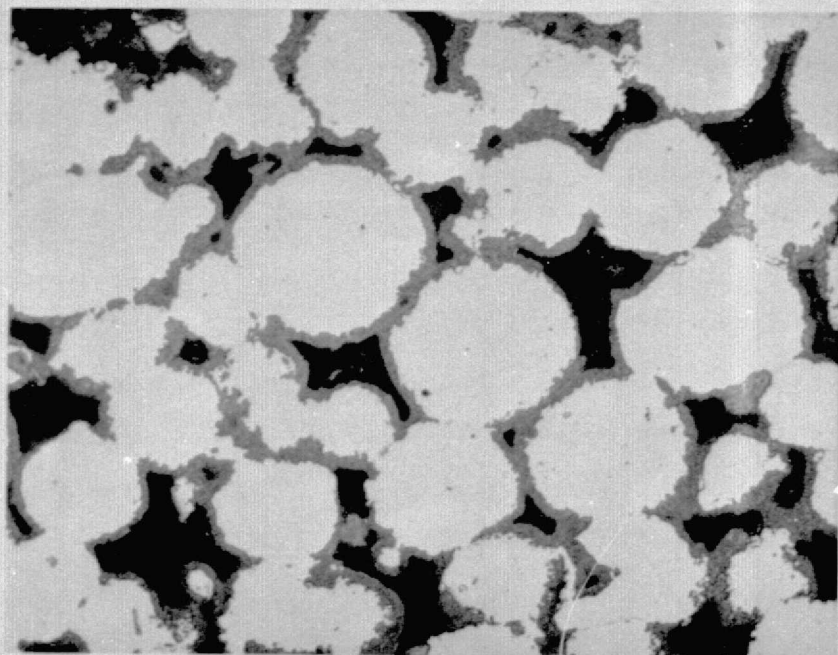
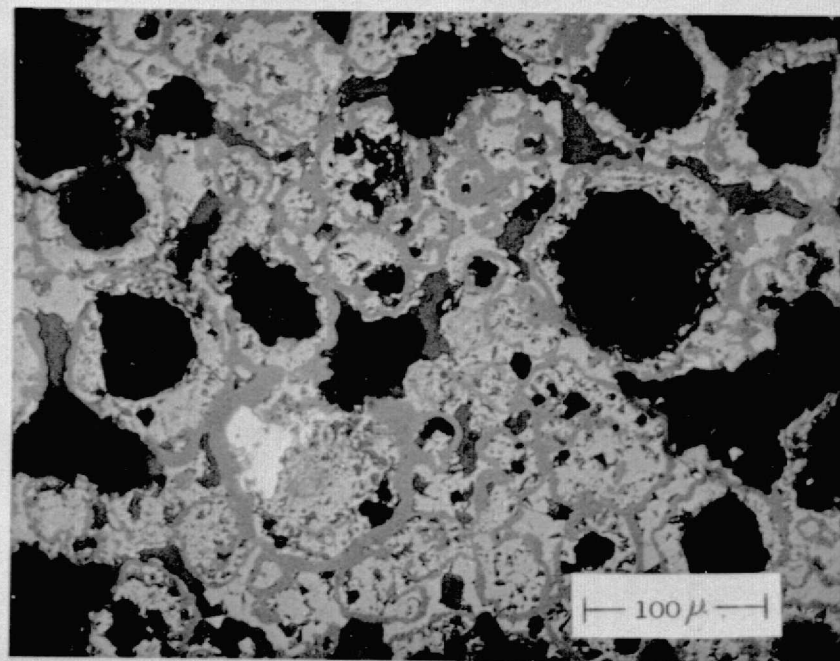


Figure 18 1316C (2400F) Low Velocity Oxidation Test



NiCrAlY - 80 HOURS



BRADELLOY - 22 HOURS

Figure 19 Typical Microstructure of NiCrAlY and Bradelloy After Mach 0.8 High Velocity Oxidation Test at 1204C (2200F) for 80 Hours and 33 Hours, Respectively (250X)

The erodent was injected in the gas stream through a water cooled nozzle; the flow rate of the erodent was controlled by a Plasmadyne powder feeder. Testing was initiated at 1204C (2200F) using 1000 grams per hour of 50 μ m Al₂O₃ erodent at a blast pressure of 138kPa (20 psi). Because of the high exposure temperature, weight gain due to oxidation exceeded the weight loss due to erosion. After 20 hours the exposure temperature was reduced to 982C (1800F) and the blast pressure maintained at 138kPa (20 psi) for a period of five hours. The blast pressure was then increased to 207kPa (30 psi) for a 25 hour period and to 276kPa (40 psi) for a 25 hours period. The test results are shown graphically in Figure 20. With the reduction in test temperature to 982C (1800F) losses due to erosion exceeded the weight gains due to oxidation. Under the latter conditions, the Bradelloy 502 was the least erosion resistant with the Bradelloy 500 second, and the effect was visible. NiCrAlY showed little erosion loss. Total depth of erosion at the end of the test is also indicated in Figure 20 for each material.

Ballistic impact tests were run at 1 ft/lb and 5 ft/lb on NiCrAlY, Bradelloy 500 and Bradelloy 502 compacts in the as-processed condition and after an exposure of 100 hours at 1204C (2200F), using an air rifle and a 0.175 inch diameter, 0.3576 gram steel pellet. There was no evidence of spalling or cracking in either condition for any of the materials.

Cohesive strength measurements were made on Bradelloy 500 and NiCrAlY at room temperature and 816C (1500F). Compacts, 0.25" x 1.0" diameter were brazed to pull-rods for conducting these tests. Results were:

<u>Material</u>	<u>Cohesive Strength, psi</u>	
	<u>Room Temp.</u>	<u>816C (1500F)</u>
Bradelloy 500	3,640	1,220
NiCrAlY	15,300	18,800

The bond strength of NiCrAlY to the backing material was greater than the cohesive strength of the NiCrAlY itself, as evidenced by the fact that all tensile failures occurred in the NiCrAlY and not at the braze interfaces.

DESIGN ANALYSIS

Finite element analyses for temperature and thermal stress were conducted for the CF6 stage 1 high pressure turbine shroud filled with NiCrAlY. The objective of this analysis was to predict the effect on shroud temperatures and life due to the substitution of NiCrAlY for Bradelloy as a shroud filler material. Four cases were analyzed using material properties for as-processed Bradelloy, oxidized Bradelloy, as-processed NiCrAlY and oxidized NiCrAlY. The condition analyzed was for maximum peak hot day take-off conditions. Calculated temperatures are shown in Figures 21 - 24. Maximum calculated temperatures were in the forward edge for the Rene' 77 casting and at the forward quarter point in the filler. Due to higher conductivity, the NiCrAlY yielded lower surface temperatures and lower radial gradients than Bradelloy. Bulk temperatures were unchanged. Upon oxidation both fillers showed an increase in surface temperature and in radial gradient, with Bradelloy showing the largest changes.

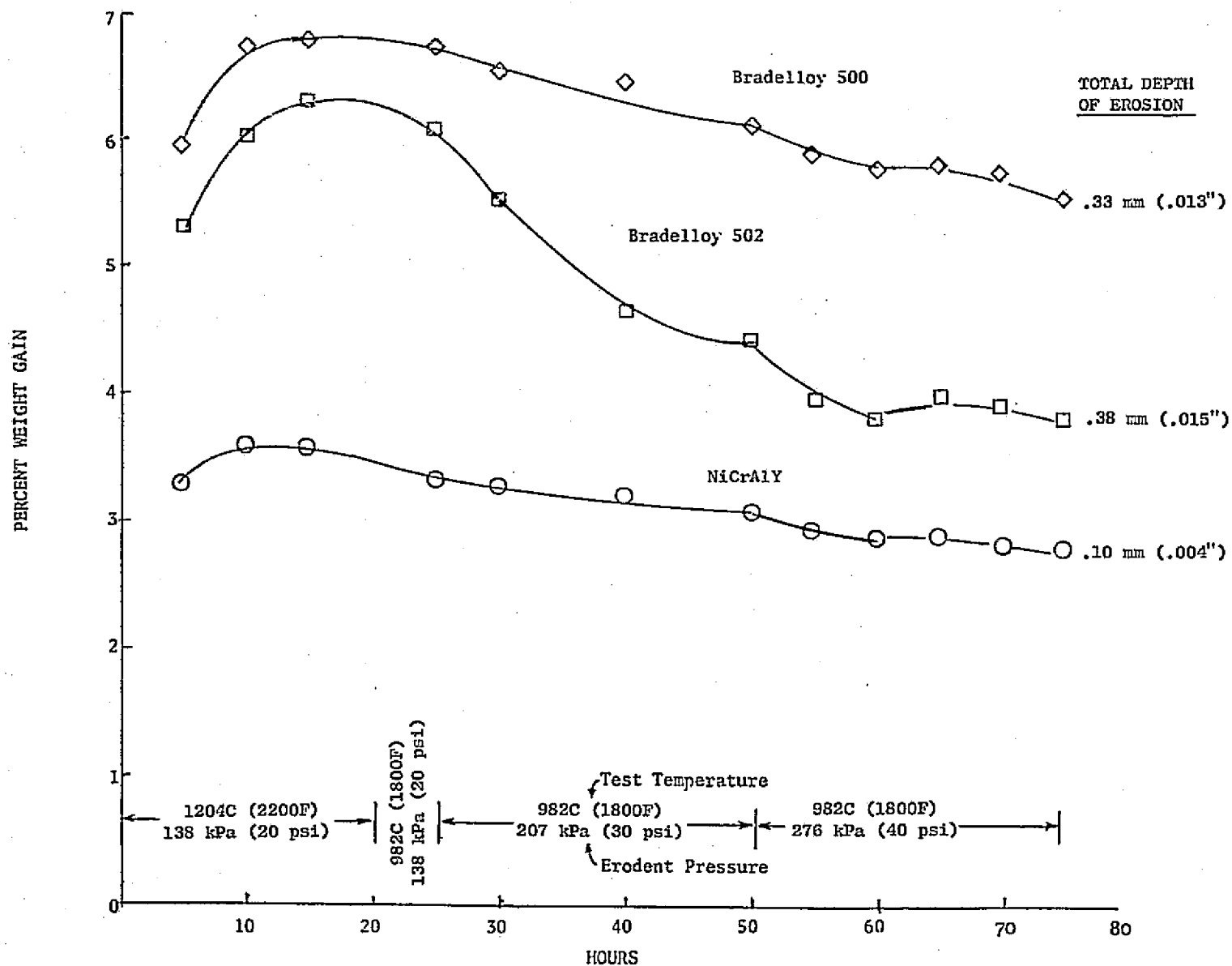
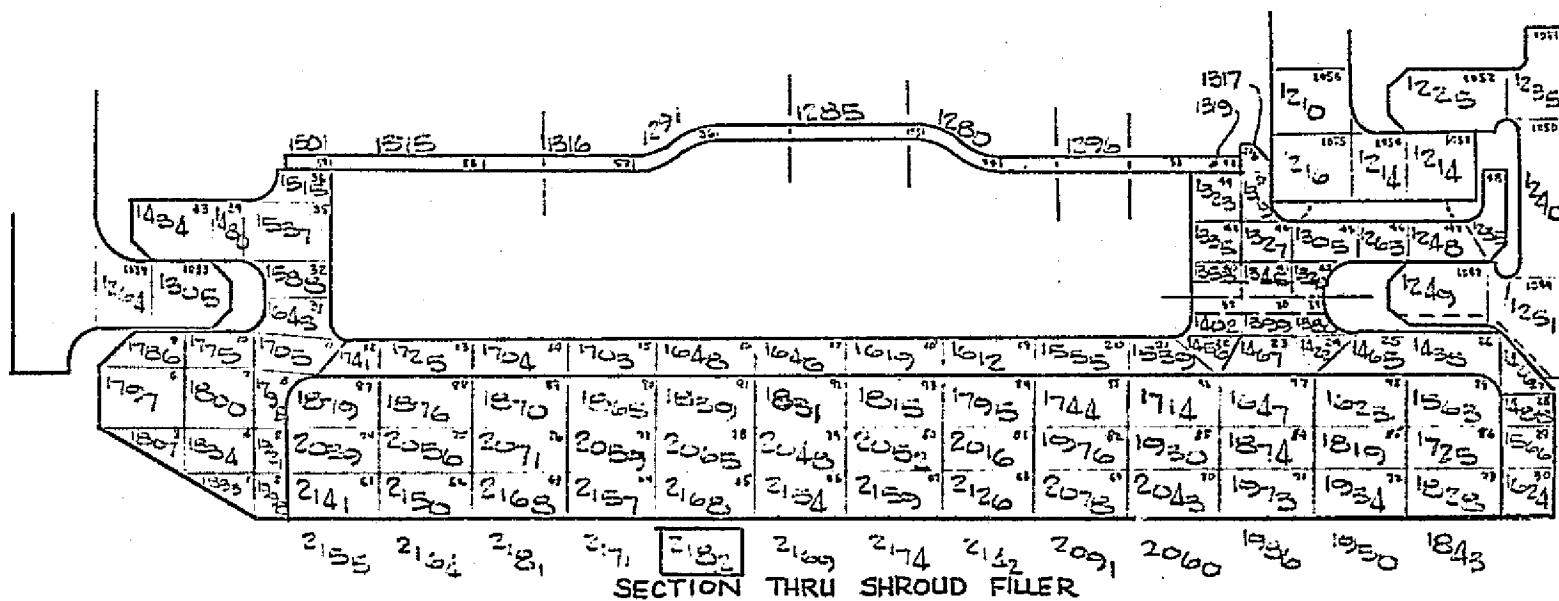


Figure 20 Hot Partical Erosion Test



REPRODUCIBILITY OF THE
ORIGINAL PAGE IS POOR

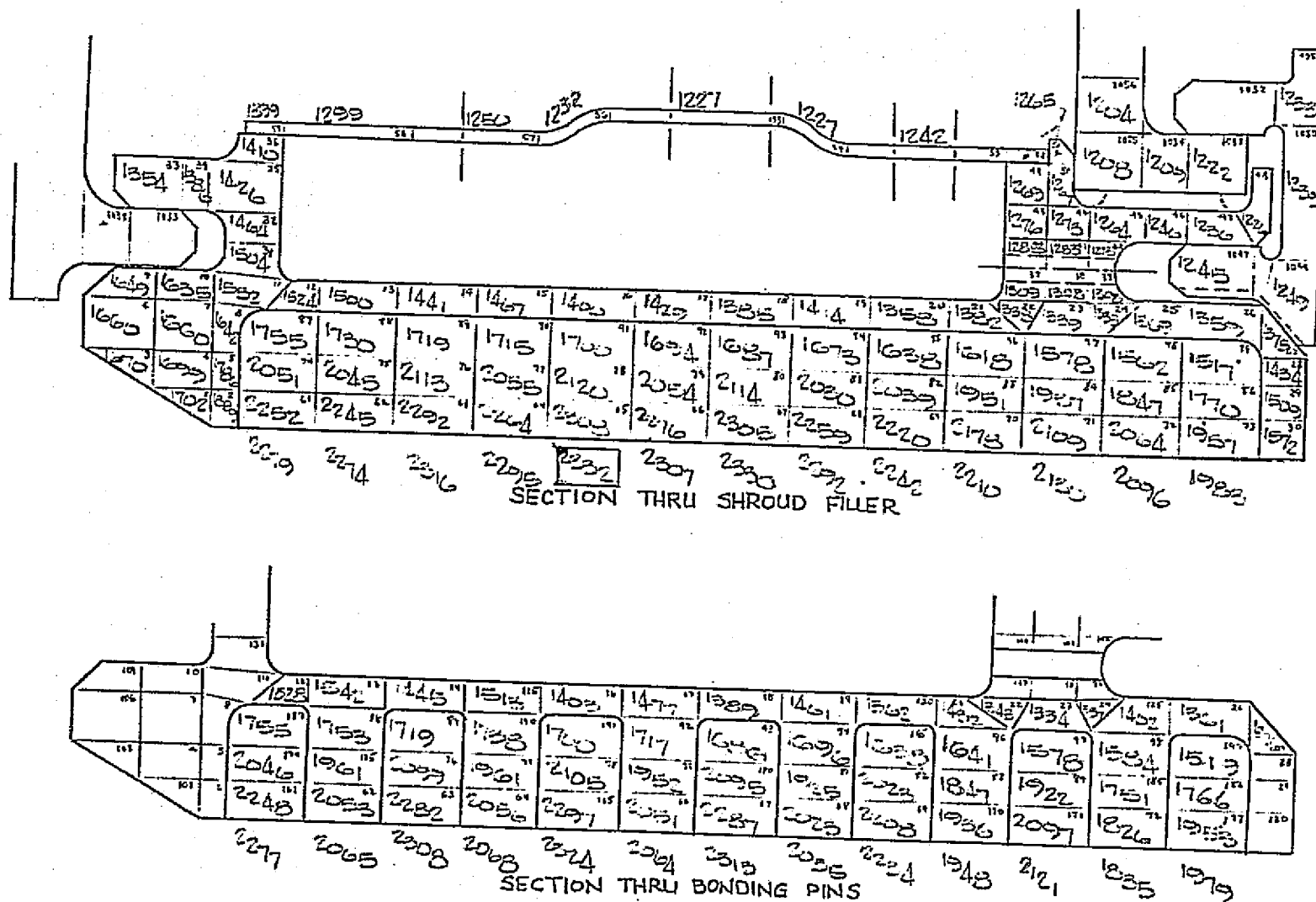


Figure 22 Typical HPT Shroud Cooling Study, Bradelloy Oxidized, Temperature, °F

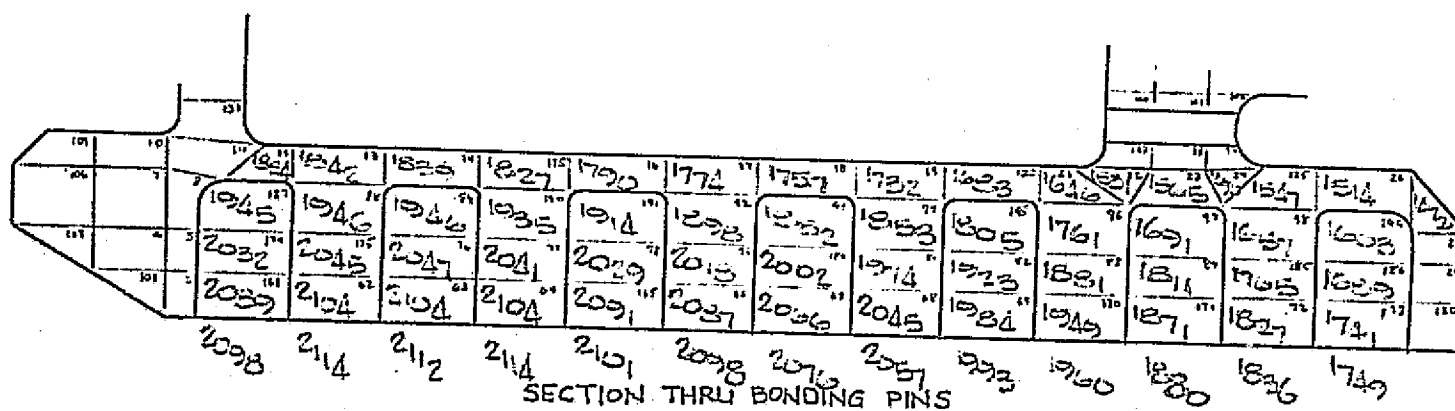
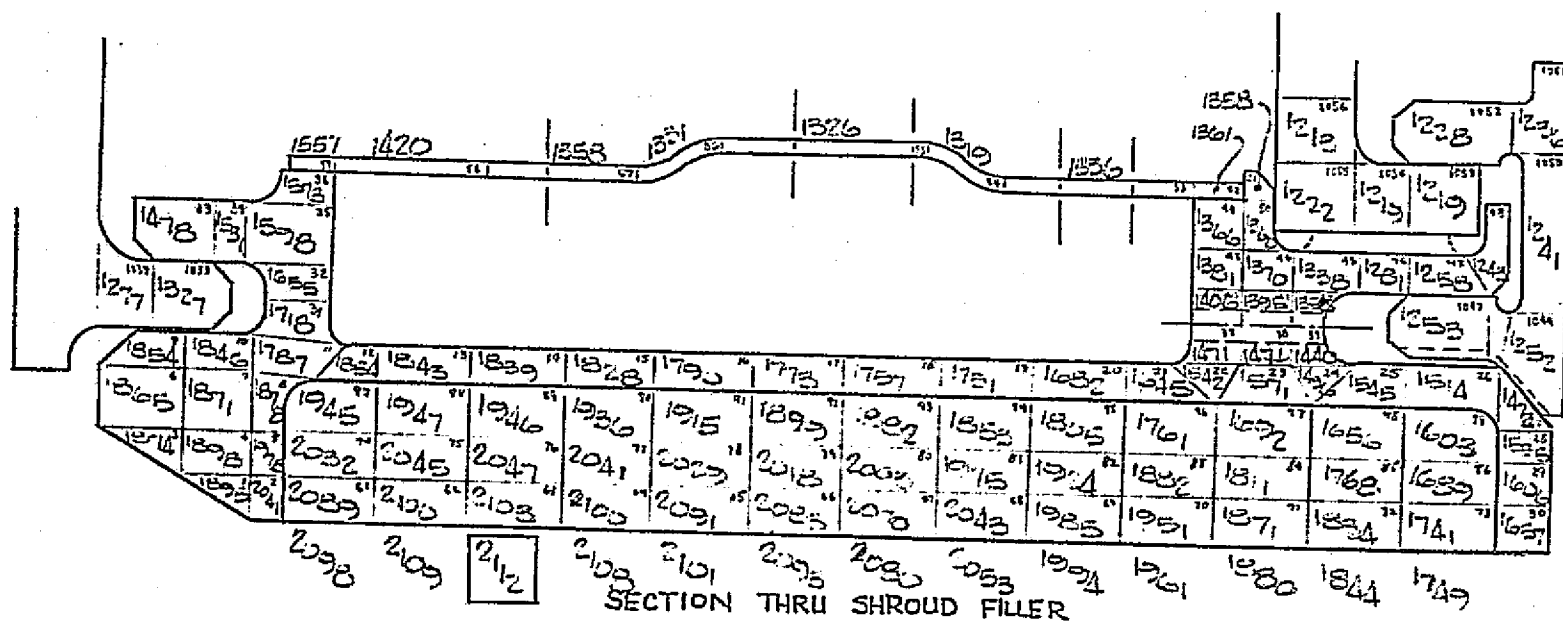
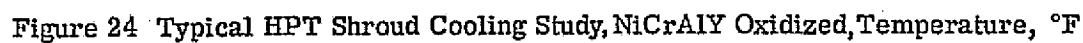


Figure 23 Typical HPT Shroud Cooling Study, NiCrAlY As-Processed, Temperature, °F



The following procedure was used to calculate thermal stresses. The initial radius of curvature is known for the neutral axis of any given section. The average temperature and ΔT across the section are obtained from the temperature analysis. The unconstrained radius of curvature with the temperature distribution is

$$R_u = \frac{1}{\frac{1}{\bar{R} [1 + \alpha (\bar{T} - 70)]} - \frac{t}{\alpha \Delta T}}$$

where

$\bar{R} \triangleq$ initial radius of curvature of neutral axis

$\bar{T} \triangleq$ bulk temperature of section

$\Delta T \triangleq$ temperature change across the section

$t \triangleq$ thickness of section

$\alpha \triangleq$ coefficient of thermal expansion of shroud

The radius of curvature as constrained by the shroud support is

$$R_c = \bar{R} [1 + \alpha_s (T_s - 70)]$$

where

$T_s \triangleq$ shroud support bulk temperature

$\alpha_s \triangleq$ coefficient of thermal expansion of shroud support

From flexure theory

$$M = \int_{R_1}^{R_2} \frac{EI}{R^2} dR$$

$$= EI \left(\frac{1}{R_1} - \frac{1}{R_2} \right)$$

and

$$S_b = \frac{Mc}{I}$$

where

$M \triangleq$ bending moment

$E \triangleq$ modulus

$I \triangleq$ moment of inertia about the neutral axis

$c \triangleq$ distance from the neutral axis

$S_b \triangleq$ bending stress

Substituting for M

$$S_b = Ec \left(\frac{1}{R_1} - \frac{1}{R_2} \right)$$

Thermal stress in the shroud in the given section is then

$$S_b = Ec \left(\frac{1}{R_u} - \frac{1}{R_c} \right)$$

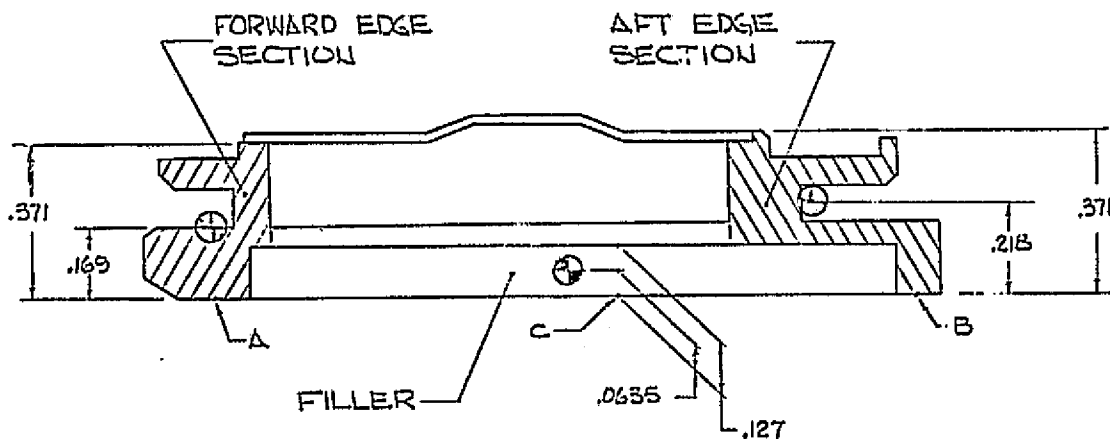
Since I drops out of the equation, the only section property required is the location of the neutral axis. This analysis was done at three locations, the forward edge, the aft edge, and the location of maximum ΔT across the filler material. These locations and the results of the analysis are shown in Figure 25. The calculated thermal stresses in the casting, based on the temperatures shown, are in terms of stress ratio as based on present Bradelloy shown, are in terms of stress ratio as based on present Bradelloy shroud stresses. In engine service, Bradelloy oxidizes 100% but NiCrAlY only oxidizes at the surface. Therefore, comparisons should be made between as-processed NiCrAlY and oxidized Bradelloy.

Based on the analyses, the following was concluded:

- a) Substitution of NiCrAlY for Bradelloy in CF6-50 HPT Stage shrouds should have no significant effect on segment casting life.
- b) The higher thermal conductivity of NiCrAlY would produce a lower shroud surface temperature and lower thermal gradients than Bradelloy. Thus, oxidation life should increase, thermal stress should be less, and distortions from volume expansion of the filler and from stresses should be less.

	Forward Edge		Aft Edge		Filler	
	ΔT T_{EUX}	σ_A T_{SFC}	ΔT T_{EUX}	σ_B T_{SFC}	ΔT T_{EUX}	σ_C T_{SFC}
BRADELLO AS PROCESSED	519 1690	1.01 2000	323 1333	0.82 1624	514 1893	0.10 2132
BRADELLO OXIDIZED	514 1563	1.00 1890	325 1333	0.82 1572	511 1837	0.19 2332
NiCrAlY AS PROCESSED	503 1755	0.98 2040	312 1424	0.79 1660	269 1827	0.05 2112
NiCrAlY OXIDIZED	510 1727	1.00 2040	317 1423	0.80 1645	335 232	0.27 2140

ALL STRESSES NORMALIZED TO OXIDIZED BRADELLO
FORWARD EDGE STRESS, ALL TEMPERATURES IN °F.



STRESS ANALYSIS MODEL

Figure 25 Temperature and Stress Summary

SHROUD COMPONENT RIG TEST

Oxidation-thermal shock tests were conducted on NiCrAlY and Bradelloy 500* filled CF6 turbine shrouds using a test rig specially designed to simulate the high temperatures, thermal gradients and rates of temperature change seen in engine service. The shrouds were tested for 150 cycles under the following conditions:

Shroud face temperature	1302C (2375F)
Shroud shell backing temperature	815C (1500F)
Time at temperature per cycle	5 minutes
Cooling cycle - a maximum of 1 minute to 136C (275F) face temperature	
Heating cycle - a maximum in 1-1/2 minutes to test temperature, 1302C	

Close up of the shroud surfaces after testing are shown in Figure 26. The Bradelloy shroud exhibited heavy oxidation and spalling of the filler; by comparison the NiCrAlY shroud exhibited little filler distress, confirming the design analysis predictions. Both shrouds exhibited some thermal cracking of the aft wall of the shroud casting similar to that seen in engine run parts.

FABRICATION

A 1974 in-house program on MCrAlY shrouds developed the basic procedure used to fabricate the NiCrAlY shrouds for the initial engine test. That procedure used an intermediate nickel-base braze alloy, Ni-20Cr-10Si, (GE81) between the filler material and the CF6 cast peg, Rene' 77 shroud shell. The NiCrAlY filler was applied as a slip of the powder and a liquid binder (Marex) by trowelling into the braze-coated shroud cavity. Subsequently, the filler in the shroud segment was vacuum hot pressed at 1093C (2000F) for 45 minutes with a hot press ram load of 18 tons (1000 psi). A quasi-fluid medium (refractory powder) was used to transmit the press load to the specimens.

The first engine test shrouds (discussed later) exhibited filler erosion in the corners and near the sidewalls of the shrouds which was identified as being due to lower-than-desired filler density (<70%) in these areas. In general, the areas away from the corners and sidewalls had the desired density and showed little, if any, erosion.

This led to extensive studies to improve the filler density in the corners. These studies involved four major approaches:

1. Improvement of green density by use of a different slip medium.
2. Modification of the press cycle by prolonging time at temperature.

*Bradelloy 500 rather than 502 was used since, during the course of this program, the 500 version replaced 502 in the CF6 design.

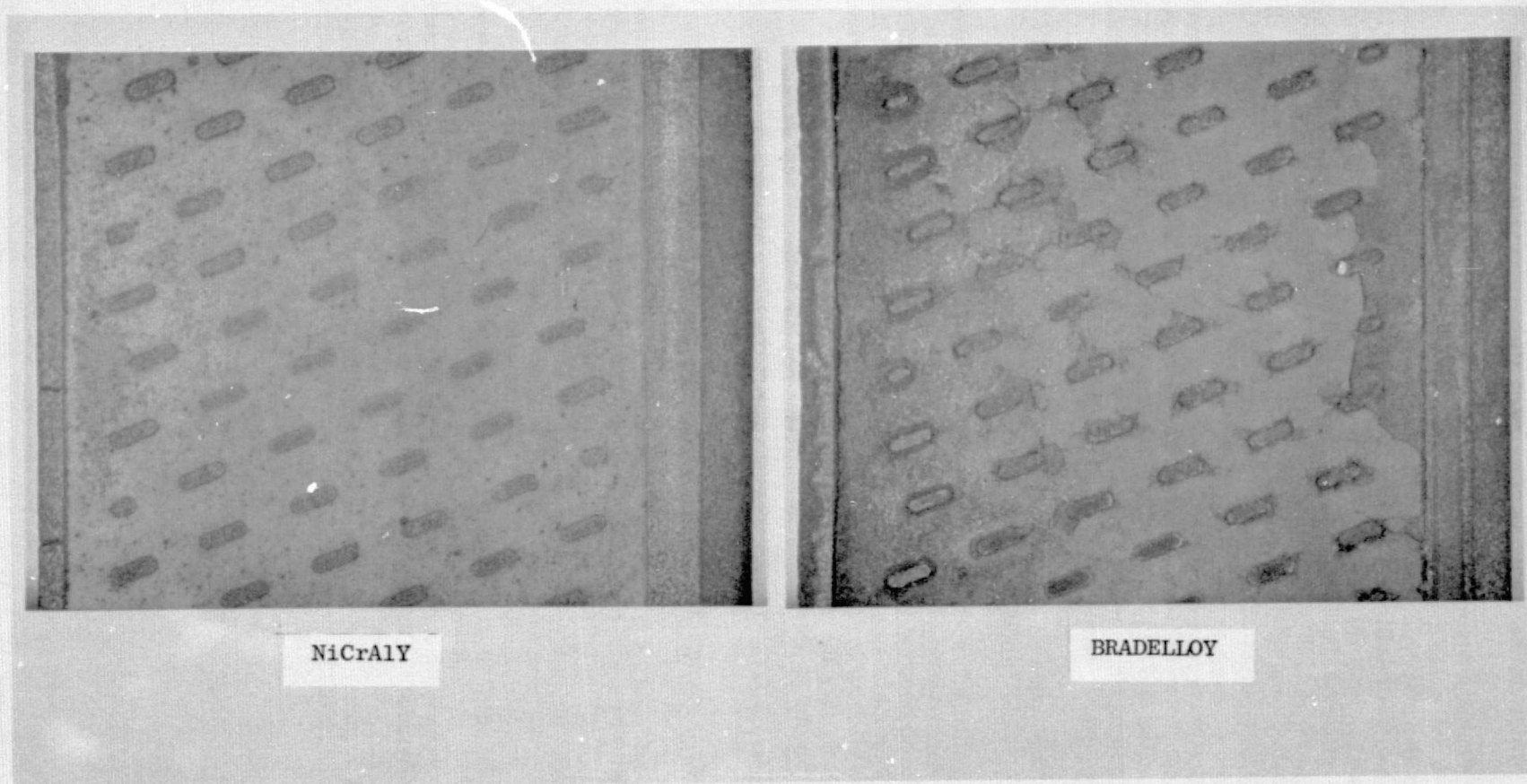


Figure 26 Close Up of NiCrAlY and Braedelloy Shroud Surfaces After 150 Cycles in Shroud Thermal Shock Test - (2.3X)

3. Modification of the shroud cavity to ease trowelling in the slip.
4. Tooling modifications which allowed improved compaction in the corners.

Aspects of each of the above approaches were incorporated in a modified procedure that resulted in the achievement of sufficient density in all parts of the filler. The modified procedure incorporated (1) removal of four pegs from one end of the shroud cavity prior to filling, (2) use of acetone as the slip medium, (3) use of a more rugged hot press tool and (4) increased press cycle (105 minutes at 1093C (2000F)). The variation in filler density could be controlled to a 70-85% range. Figure 27 compares the filler densities of the original and the improved procedures.

In addition, the quality control procedures were modified to include cold particle erosion tests in the corners and center areas (five individual tests per shroud) of the fabricated shrouds to confirm that the desired result was achieved. Figure 28 compares erosion tested shrouds processed by the original and improved procedures. The dark stripes on the shroud surfaces represent areas that were masked during all five erosion tests.

The improved hot press and quality control procedures were used to produce NiCrAlY shrouds for the second and third engine tests.

Autoclaving was also evaluated as an alternative to hot pressing. These efforts were only partially successful. Compaction of the filler was achieved; however, good bonding of particles was not achieved because of the inability to satisfactorily degas the can containing the shroud prior to hot isostatic pressing (HIP). Figure 29 compares the compacted filler for vacuum hot pressing and autoclaving. The poor particle-to-particle bonds experienced with autoclaving were probably the result of surface oxidation of the particles due to residual gases in the can during the HIP cycle.

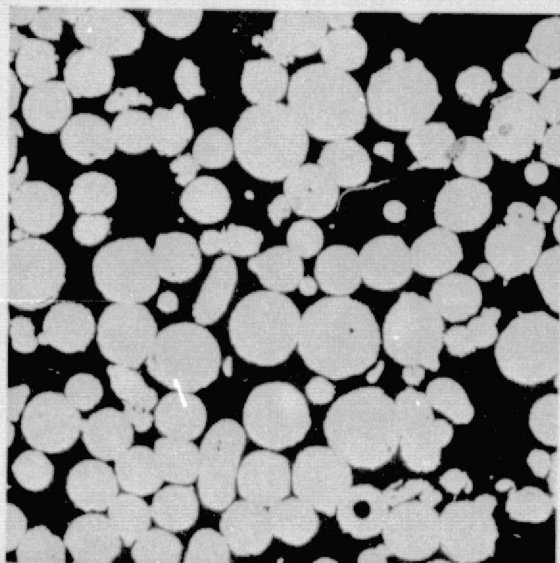
FABRICATION SCALE-UP

The original procedure for vacuum hot pressing NiCrAlY into one CF6 shroud in each vacuum hot press run, while not cost effective, was an expedient processing method capable of providing test materials for NiCrAlY property determination and NiCrAlY-filled shrouds for engine test. This was a temporary expedient which resulted in only a one-shroud yield per shift. Upon verification of the superiority of NiCrAlY over Bradelloy 500 and 502, and with an increasing demand for NiCrAlY-filled shrouds for engine testing, a more effective pilot process was needed. A program was begun which had as its goal a limited cost reduction of NiCrAlY to ~ 2.5 times (or less) that of Bradelloy through greater production capacity. The goal of producing at least six shrouds per press run was desired.

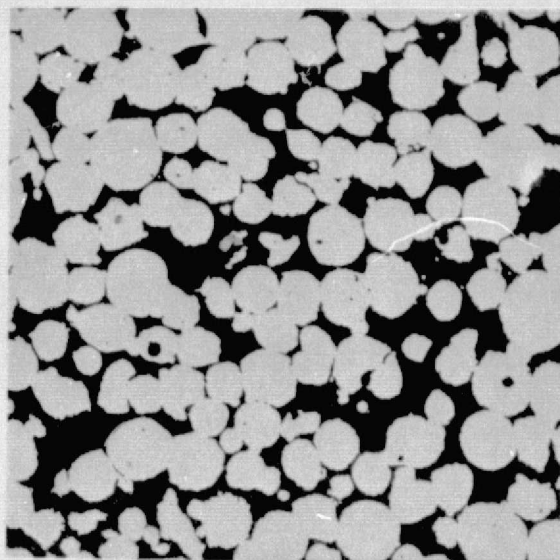
Two vacuum hot presses and two air hot presses were found to be available. Each facility was of sufficient size that six or more shrouds could be made in a single run. Examination of equipment complexities indicated that the air hot press would be the most flexible provided that satisfactory shrouds could be made with the use of an inert gas cover. Therefore, an argon-shrouded press box capable of pressing two CF6 size shroud segments was constructed*.

*All tooling was furnished to this program by General Electric Co.

Corner

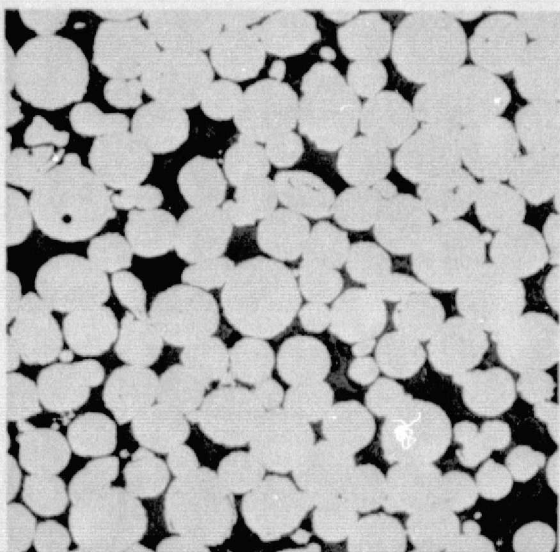


60 - 65%

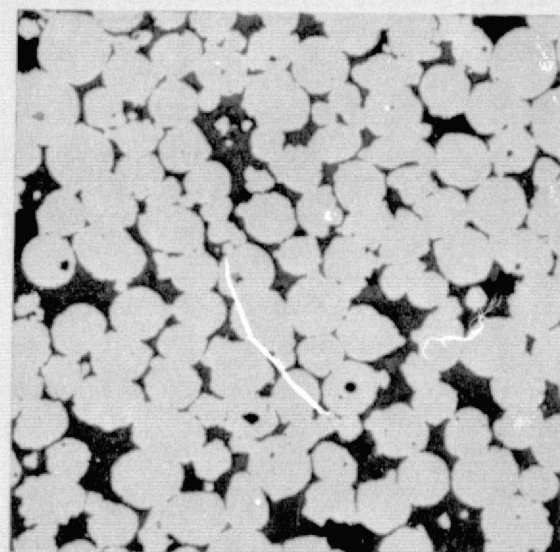


70 - 75%

Center



76 - 80%



75 - 85%

Figure 27 Comparison of Filler Densities of NiCrAlY Shrouds - 100X

Left: Original Hot Press Procedure
Right: Improved Hot Press Procedure

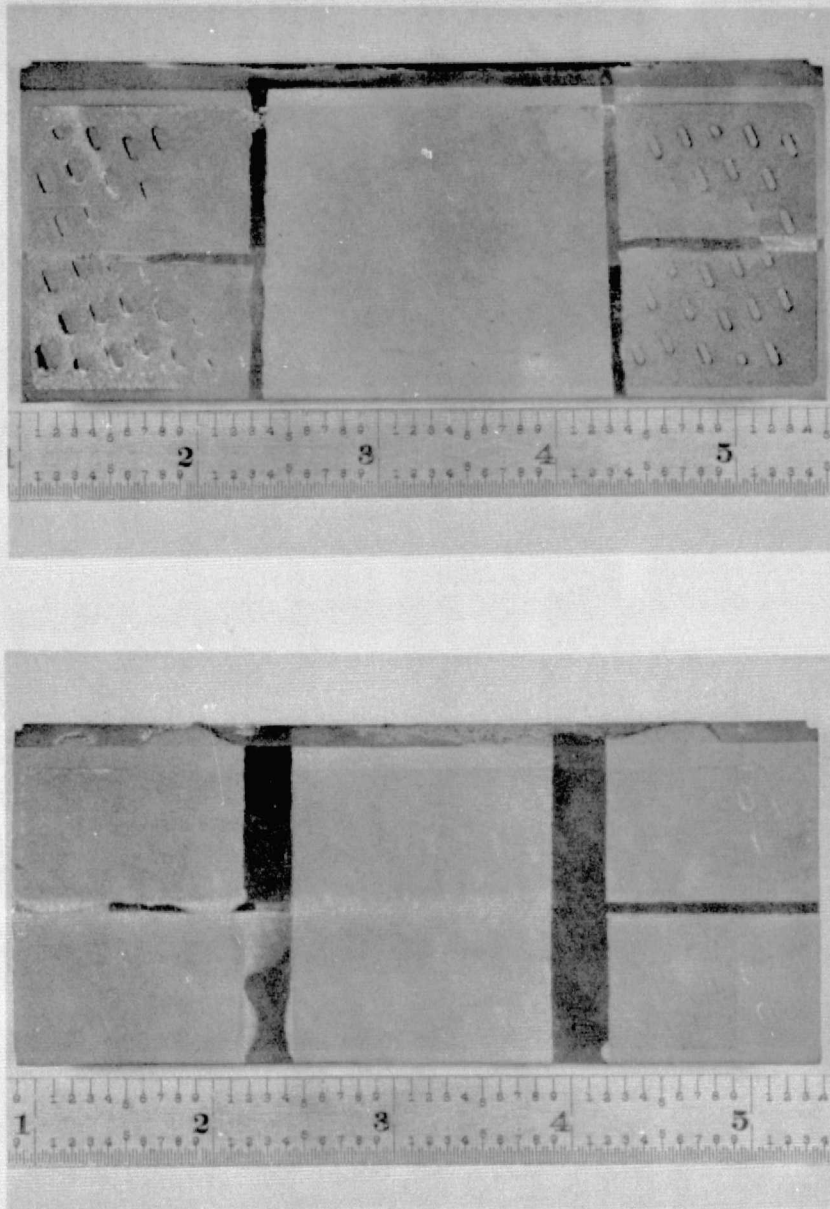


Figure 28 Comparison of Erosion Tested NiCrAlY Shrouds

Top: Original Hot Press Procedure - Note Erosion
in Corners

Bottom: Improved Hot Press Procedure

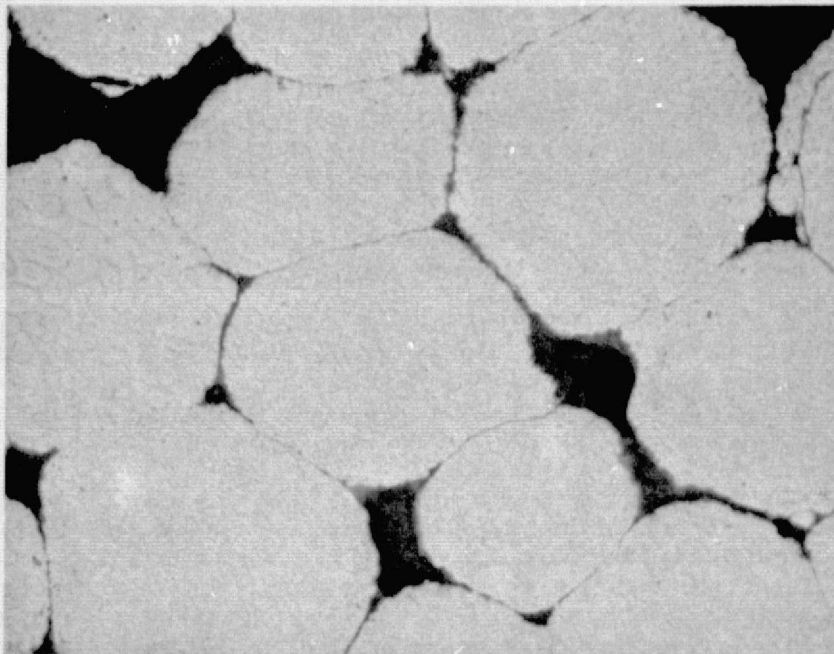
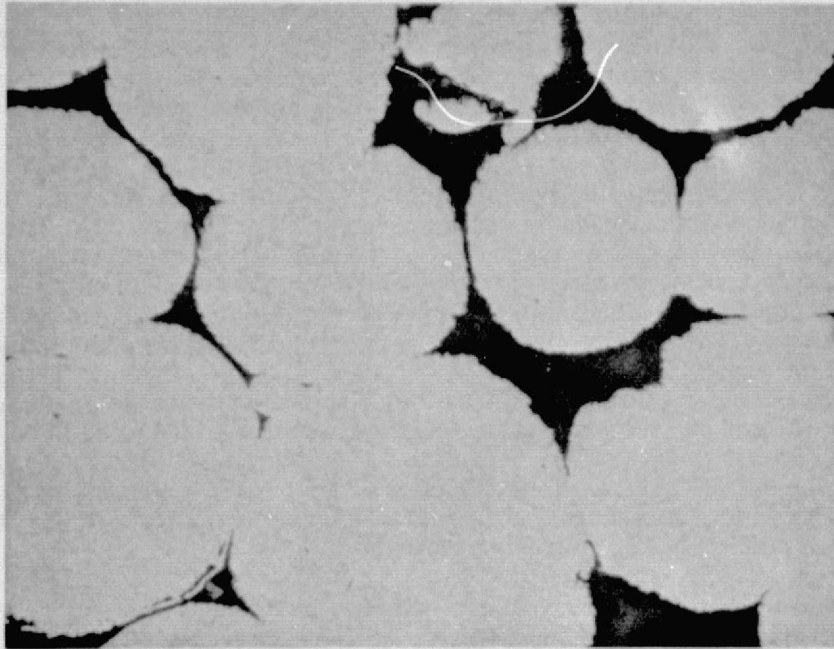


Figure 29 Comparison of Bonding of NiCrAlY Particles - 500X

Top: Vacuum Hot Pressed - Note Good Diffusion
Bonding of Particles

Bottom: Autoclave - Note Poor Diffusion Bonding of
Particles and Interface Line

Preliminary experiments were run to determine whether the argon-shrouded press box could produce the desired compaction of the NiCrAlY powder and satisfactory interparticle bonding. In these experiments, two shroud segments and one quality control specimen were fabricated in the press box (Figure 30).

Examination of the hot-pressed shroud and quality specimen showed a satisfactory metallographic comparison against vacuum hot pressed NiCrAlY (Figure 31). Erosion tests run on the shroud also showed results equivalent to vacuum hot pressed shroud materials. Therefore, an argon hot press method was selected for the scale-up effort. This approach offered the advantages of mechanical simplicity compared to the vacuum hot press and more rapid cycling since, conceptually, the retort could be removed from the platens while still warm and another press box inserted without fully cooling the platens. The rapid cycling technique was not required for this program since the capacity of the press facility was not being fully utilized and the production rates were not required to be high.

As a result of the successful two piece pressing experiments, a press box capable of simultaneously pressing four shroud segments was constructed (Figure 32), and this box was used for the majority of the parametric studies.

Later, after the density of shroud segments pressed in the four segment press box had been shown to be satisfactory, a six segment press box was constructed (Figure 33). All the press boxes had the same basic components, an inner pressure container and an argon-containment retort.

Shroud segment preparation prior to hot pressing in any of the various press boxes consisted of grit-blast cleaning, braze coating, NiCrAlY filling and contamination shielding against the pressing medium powder. Shroud segments representing each step in the sequence are shown in Figure 34. Grit blasting with 150 mesh glass beads removed surface contamination of the shroud segment cavity prior to brazing. The cleaned segment was then spray coated with a clear lacquer which remained tacky and retained the braze powder which was subsequently distributed over all surfaces. The shroud was then heated (in vacuum) slightly above the braze solidus allowing the braze to wet the surface.

A form which controlled powder filling thickness was then placed around the perimeter, and NiCrAlY powder was added and settled by tapping. A cellulose nitrate binder was added to the powder so that the formed shape would be maintained when the form was removed. Prior to pressing, the form was removed and a thin stainless steel shield was added to prevent contamination of the NiCrAlY by the alumina pressing sand.

Before the filled shroud segments were positioned in the press box, a 0.75 inch layer of sand was placed in the bottom of the box. The shroud segments were then placed in the box, and 2.25 inches of sand were added to the box to cover the segments. Finally, the pressing ram, which consisted of several thick Hastelloy X plates, was placed over the sand. A cross-section of the assembly, including the sand seal used to maintain positive argon pressure in the press box, is shown schematically in Figure 35. Prior to heating, air was purged from the press box with argon which was introduced through the top of the press box. Argon flow was maintained throughout the pressing cycle and after pressure removal until the temperature was reduced to 260C (500F).

NOTE: Figures 36, 37, and 38 to be forwarded under separate cover.

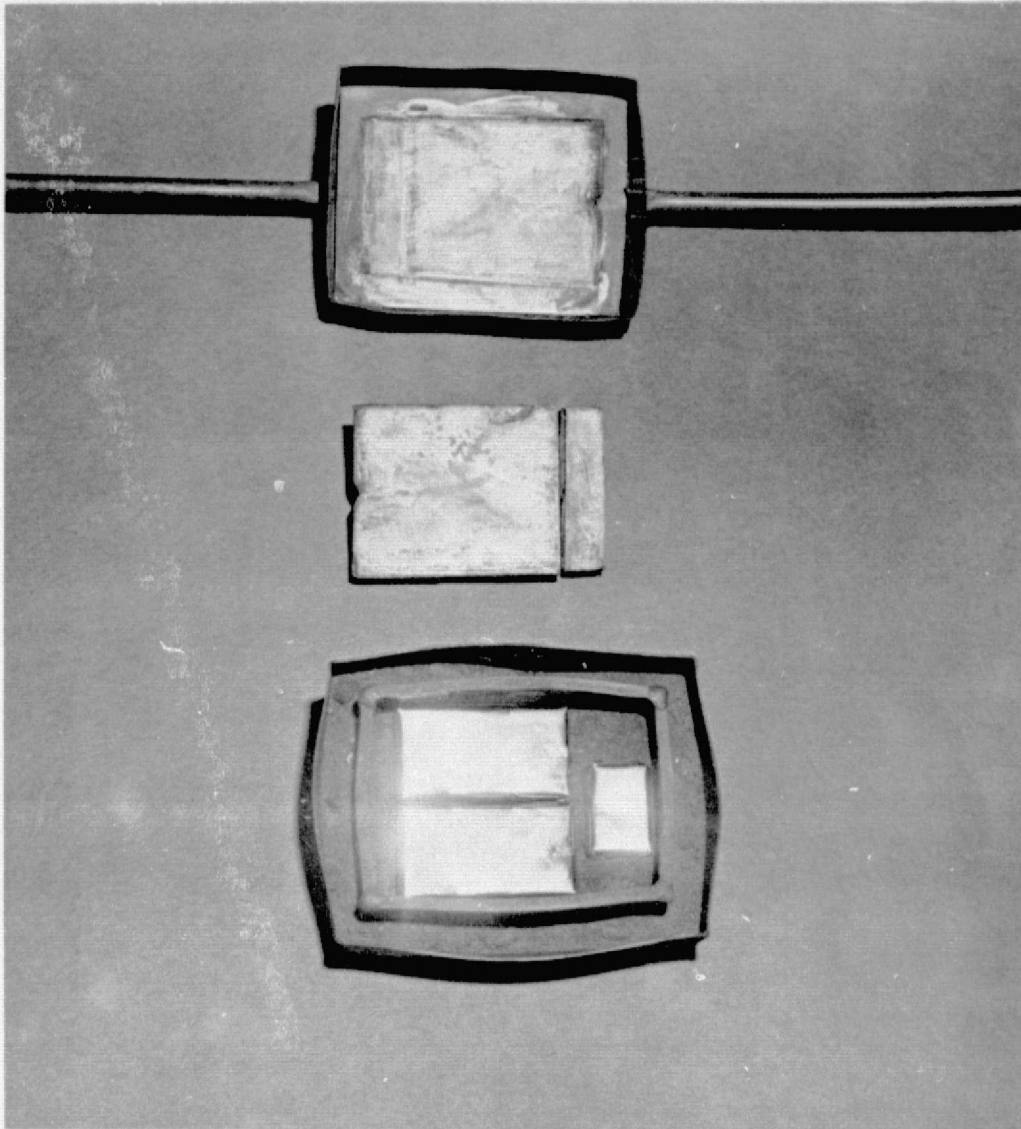
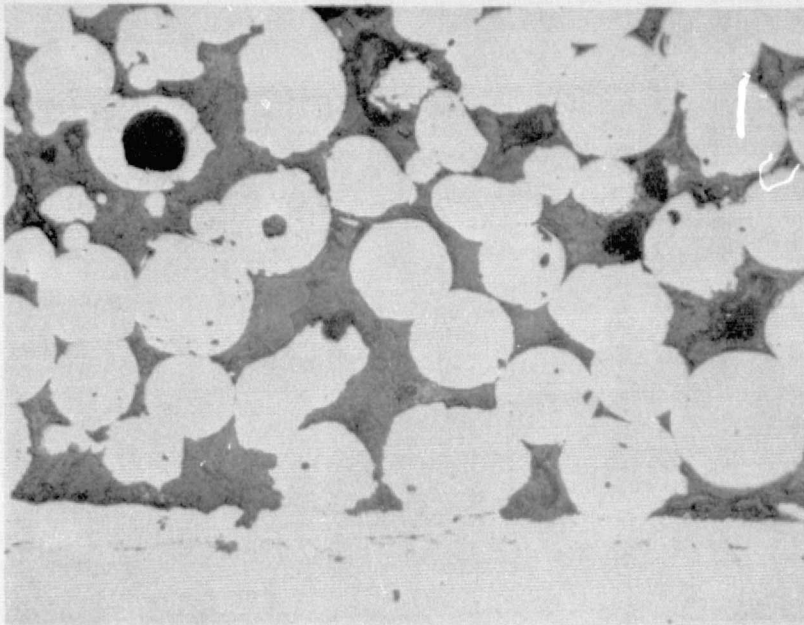
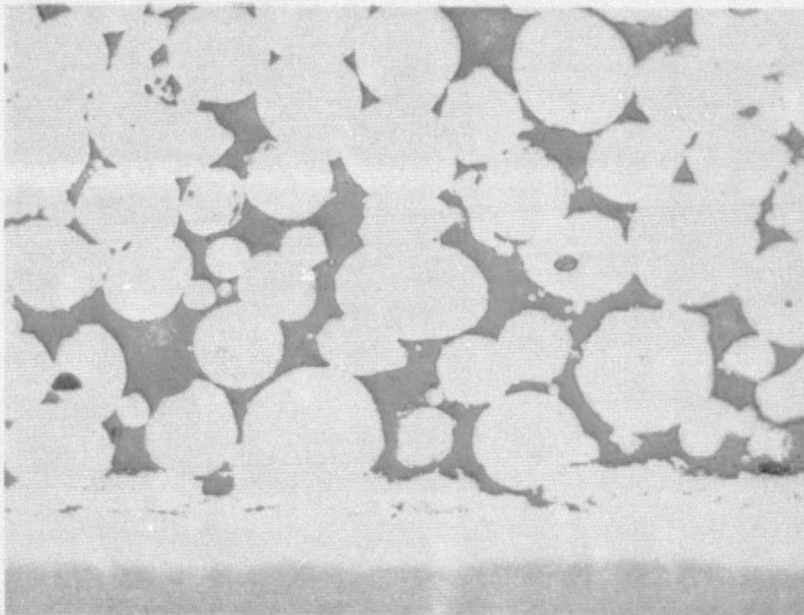


Figure 30 Disassembled Two Segment Argon Retort Showing Two Shroud Segments and QC Sample in Place



VACUUM HOT
PRESSED
NiCrAlY



ARGON HOT
PRESSED
NiCrAlY

Figure 31 Microstructures of Vacuum Hot Pressed (Top) and Argon Hot Pressed (Bottom) NiCrAlY Showing the Uniformity of Density and Inter-Particle Bonding for Both Pressing Techniques

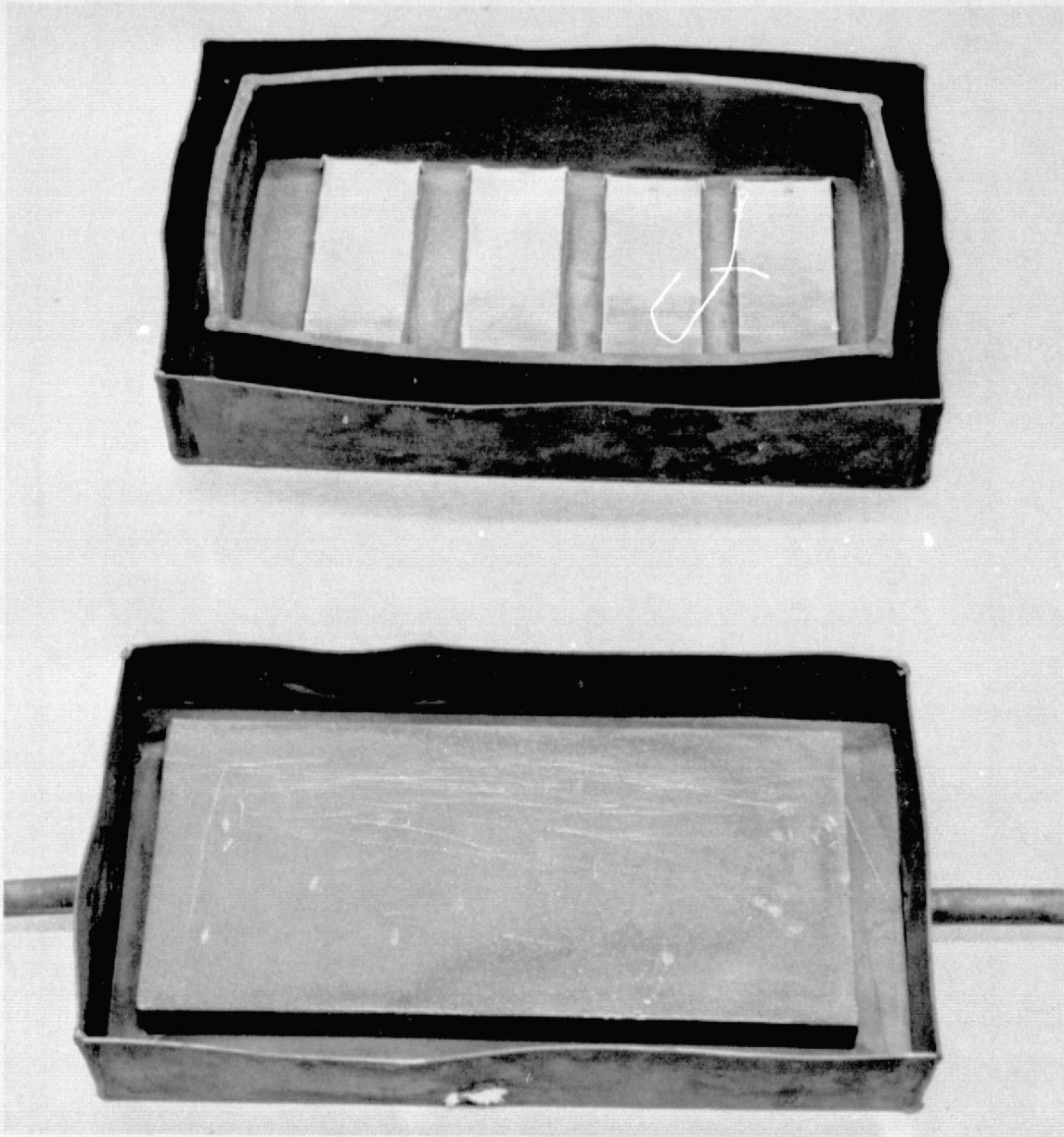


Figure 32 Disassembled Four Segment Argon Press Box with Shroud Segments in Place



Figure 33 Six Segment Press Box with Unfilled Shroud Segments in Place

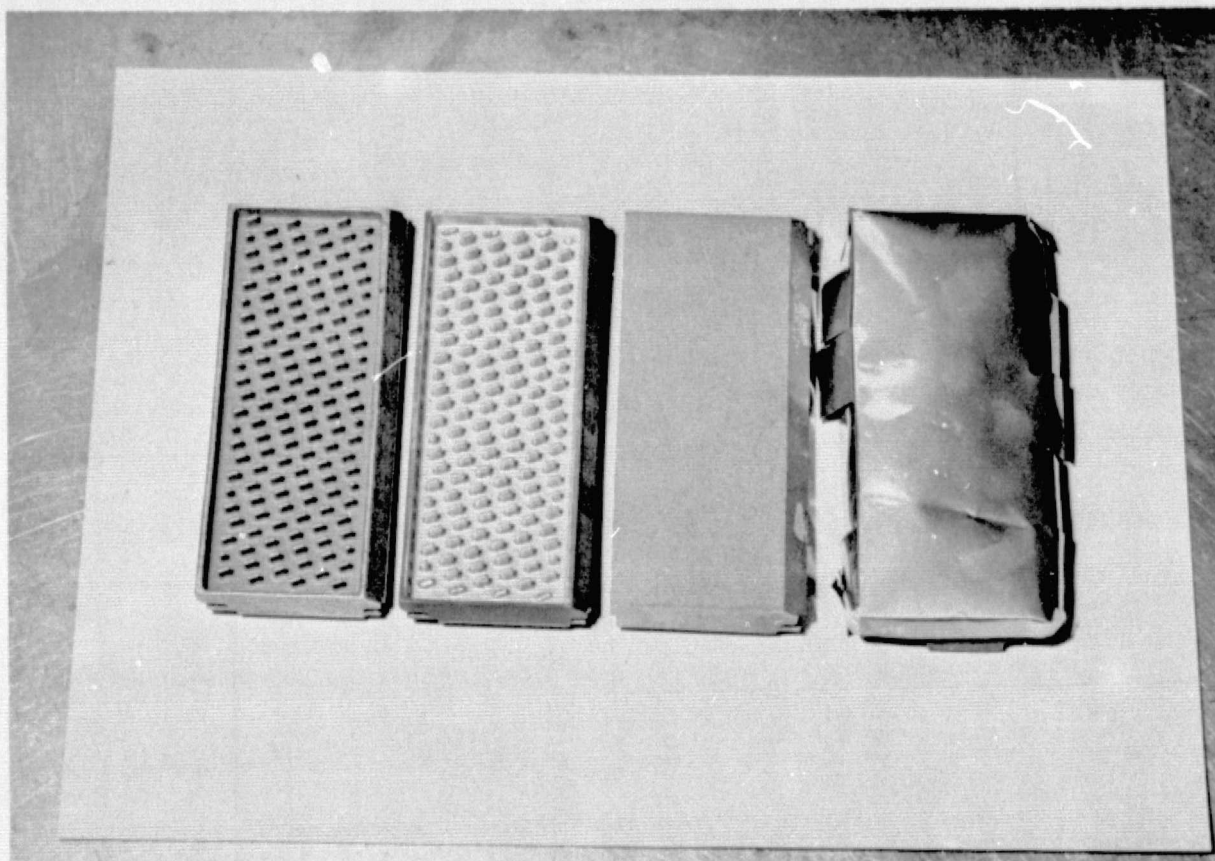


Figure 34 Shroud Segments in Various Stages of Preparation:
Left to Right, Grit Blasted Cavity, Braze Coated
Cavity, NiCrAlY Filled Cavity, Shielded Segment
Ready for Pressing Operation

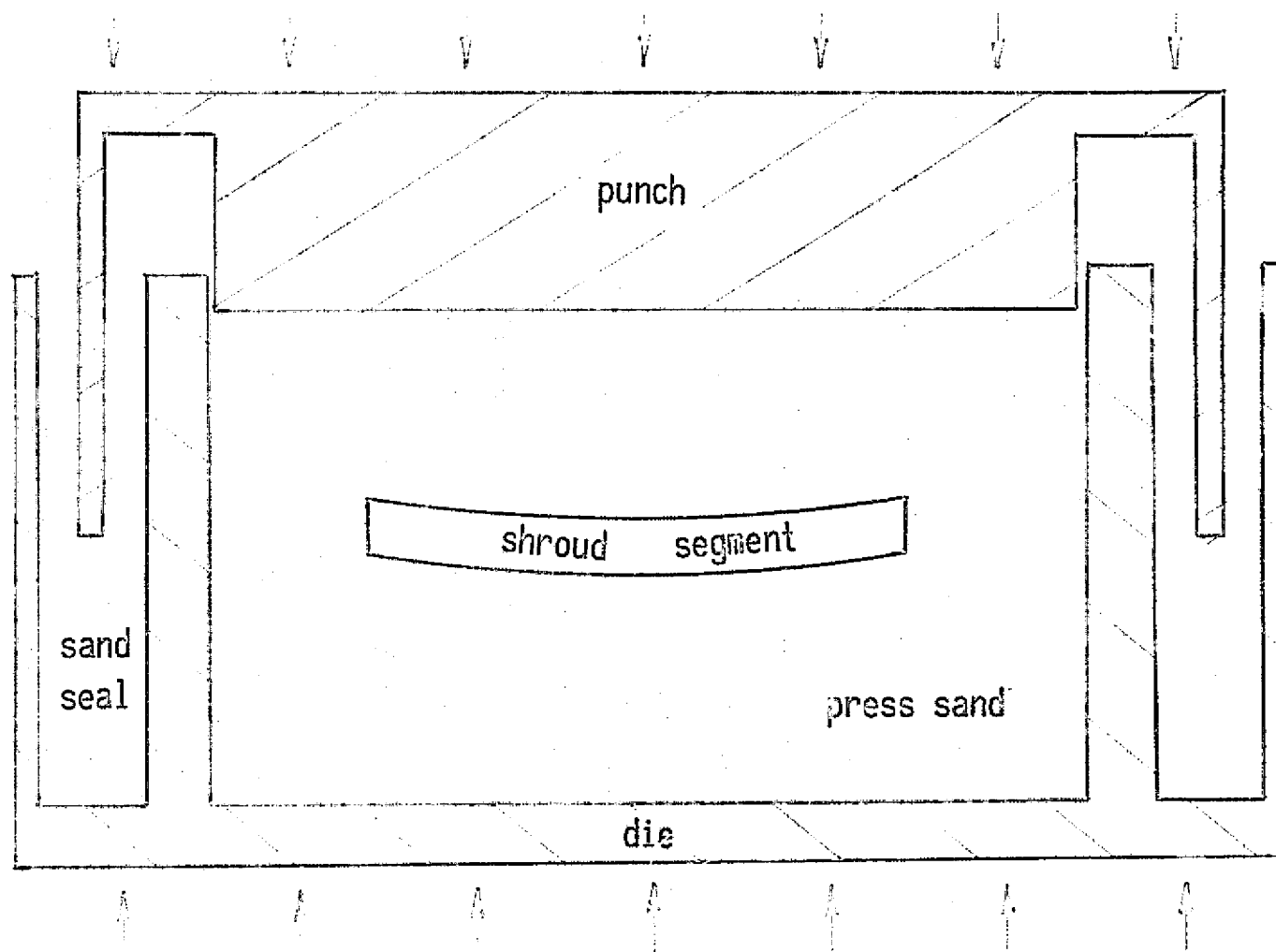


Figure 35 Schematic Cross-Section of Argon Press with Shroud Segments in Place

Hot pressing was carried out in the argon flushed retort mounted in the air press with suitable insulative shielding so that temperature uniformity in the box can be attained. Hot pressing was carried out in the 1038-1093C (1900-2000F) range with pressures varied as a function of component geometry and pressing sand.

The reproducibility of properties was assessed from three successive batch operations using six shroud segments, all operated under the same conditions at 1066C (1950F). The variation in shroud filler density was measured at 36 locations on the fabricated segments and were all within the 70-85% density range, with batch variations of less than 2%.

With process reproducibility demonstrated, a fourth batch was made to verify total shroud segment quality control. Criteria used for judging quality were erosion resistance, braze bonding efficiency and particle to particle bonding.

Erosion resistance was measured at each of the corners of the six shroud segments using the standard two minute erosion test (750 gms. or 50 μ m Al₂O₃ particles impinged on sample for two minutes at a 90° angle with 60 psi air pressure). The mass of material eroded per unit of surface area is shown in Table VII. In all cases the maximum allowable weight loss of 0.200 gm/in² was not exceeded.

During the braze coating operation, and prior to filling, 99% braze coverage of the casting area was obtained. Braze bonding of the bulk of the NiCrAlY particles in contact with the shroud casting was achieved, a factor important to filler retention during engine operation. An example of the desired braze bond structure is shown in Figure 39. More than 50 bonds per inch were achieved. Figure 39 also shows the degree of interparticle bonding required to give NiCrAlY its 15,000 psi cohesive strength.

In summary the six-shroud argon hot press method of fabrication is technically equivalent to the previously used vacuum hot press method. It has been demonstrated that the new process is acceptable in terms of product quality and reproducibility.

COST FACTORS

The principal driving forces for increasing the production rate of NiCrAlY shroud segments were two-fold: to increase the fabrication capacity of a pressing facility, and to reduce the cost of the individual shroud segments. An examination was made of the various operations required to fabricate a filled NiCrAlY shroud relative to an initial cost reduction and initial scale-up within the context of using hot pressing as the developed technique. The original technique used a small vacuum hot press capable of holding one shroud segment and a QC piece only.

A comparison was made of the facilities available for hot pressing from 6 to 10 shrouds per batch. Both vacuum hot presses (VHP) and argon retort hot presses were available with sufficient capacity. Capitalization costs of the two types of equipment are dramatically different. A new argon retort hot press cost about \$30,000, with the associated instrumentation; a new vacuum hot press with a similar capacity was estimated to cost about \$150,000.

TABLE VII

EROSION TEST WEIGHT LOSS DATA

<u>Shroud Segment</u>	Erosion (gm/in ²)			
	<u>Corner 1</u>	<u>Corner 2</u>	<u>Corner 3</u>	<u>Corner 4</u>
1	0.163	0.125	0.119	0.192
2	0.168	0.154	0.120	0.170
3	0.173	0.177	0.128	0.179
4	0.161	0.174	0.117	0.169
5	0.170	0.137	0.107	0.168
6	0.180	0.131	0.122	0.169

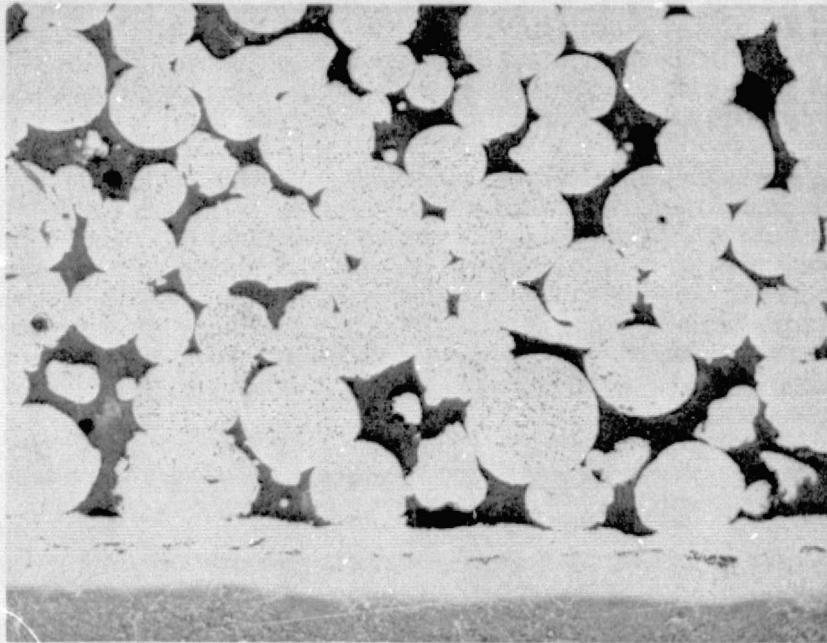


Figure 39 Microstructure of NiCrAlY Filler at the Braze Interface Showing Typical Braze Structure and Interparticle Bonding. (200X)

The maintainability requirements were estimated to be nearly the same: The ceramic platens (about \$3,000) for the argon retort hot press require replacement every few months; the heating elements in the vacuum hot press would last for a longer period, but the replacement cost would be substantially greater (\$10,000 for elements for the single shroud press). Maintenance of conventional hot presses or vacuum hot presses shows that the added complexity of the vacuum feed throughs and bellows in the VHP would result in slightly higher maintenance costs.

Tooling cost for both the argon retort hot press and the vacuum hot press were nearly identical. Modifications of design to accommodate the argon cover gas necessitated a slightly more complex design, which added about \$500 to the initial model tooling cost over the cost for a comparable VHP box. In the course of the work on both presses, it was found that each of the press boxes degraded by creep. Oxidation was not a factor. It was estimated that the refurbishment costs of the press boxes were about the same comparing the vacuum and argon methods when amortized over the actual number of shrouds pressed. Thus, tooling costs are equivalent for the two methods.

A comparison was made of the labor expended to prepare, fill, press, and check the quality of shrouds made one at a time in the vacuum hot press, and for multiple parts in the argon hot press. Table VIII shows the relative times required for this sequence. The data show that a multiple part press run in argon could be made with more than double the labor efficiency of the single piece vacuum hot press method. The resultant cost per shroud in terms of labor was 19.5 man hours for the single shroud vacuum hot press, and 7.8 man hours per shroud for the six piece argon hot press, a significant improvement. If a given shop quotes at a \$10 per hour labor + overhead rate, a savings of \$117 per shroud segment looks realistic.

The new material costs for filling shroud segments are about the same for both methods, being about \$20 per shroud.

In summary, the cost analysis comparing the one-per-shift laboratory operation to a six per batch pilot operation revealed that the argon retort hot press method with six segment batches achieves a reduction in costs equivalent to the difference in labor, assuming all equipment costs are already amortized. That difference is 11 man hours per shroud segment. If the labor cost is assumed to be \$10 per hour including shop overhead, the cost reduction would amount to \$117 per shroud segment.

ENGINE TESTS

During the course of this activity, NASA suggested that Genaseal be considered as a name for the NiCrAlY shroud. The name was adapted, and will be used hereafter to designate this particular component.

The initial CF6 factory engine test of four hot pressed Genaseal shrouds produced localized erosion of the filler along the trailing edge and sidewalls and particularly in the corner regions after 501 factory engine cycles. The Bradelloy shrouds with similar engine time did not exhibit any filler loss due to erosion, but did show surface oxidation, filler growth, and local charring typical of severe CF6 test engine experience. As mentioned previously, metallographic examination of the shrouds revealed the filler loss due to erosion to be associated with lower than desired filler density, and modifications in fabrication procedures were adopted to produce the desired filler density distribution.

TABLE VIII

LABOR COSTS FOR FABRICATING NiCrAlY SHROUDS

<u>Operation</u>	<u>Vacuum Hot Press Single Shroud (Man Hours)</u>	<u>Argon Hot Press Six Shrouds (Man Hours)</u>
Segment Preparation		
Remove Corner Pegs	0.08	0.5
Clean Shroud Casting	0.08	0.5
Apply Braze Powder	0.25	1.5
Braze Coat	0.33	2.0
Inspect	0.17	1.0
Segment Filling		
Fill	0.75	4.5
Load Retort	0.25	1
Fill and Load QC Sample	0.75	0.75
Hot Pressing		
Purge Retort	0.17	0.25
Load Press	2.0	1.0
Apply Pressure	6.0	7.0
Unload Press	2.0	1
Unload Retort	0.17	1.5
Prepare Retort for Next Run	0.42	0.17
Quality Evaluation		
Grind Surface	2.6	15.6
Erosion Test	1.0	6.0
Metallography	2.5	2.5
Total Batch Labor Hours	19.5	46.8
Labor Hours per Shroud	19.5	7.8

Micro examination of the first engine test shrouds also confirmed Genaseal's superior oxidation resistance over Bradelloy. The NiCrAlY particles near the surface exhibited only a thin oxide film even in the hottest areas of the shrouds and little, if any, swelling above the shroud pegs (Figure 40, bottom). Similar areas of the Bradelloy shrouds exhibited a substantial layer of completely oxidized filler and swelling above the shroud pegs (Figure 40, top).

One shroud each of Bradelloy and Genaseal exhibited an area of blade tip rub. In the case of Genaseal, the filler at the surface compacted and smeared (Figure 41, top), indicating a degree of compliance under the rub. The Bradelloy, being more oxidized, showed no evidence of being able to absorb the rub (Figure 41, bottom). SEM EDAX analyses of the two rub surfaces indicated no transfer of blade material in the case of Genaseal, but definite blade metal pick up (scabbing) on the Bradelloy surface.

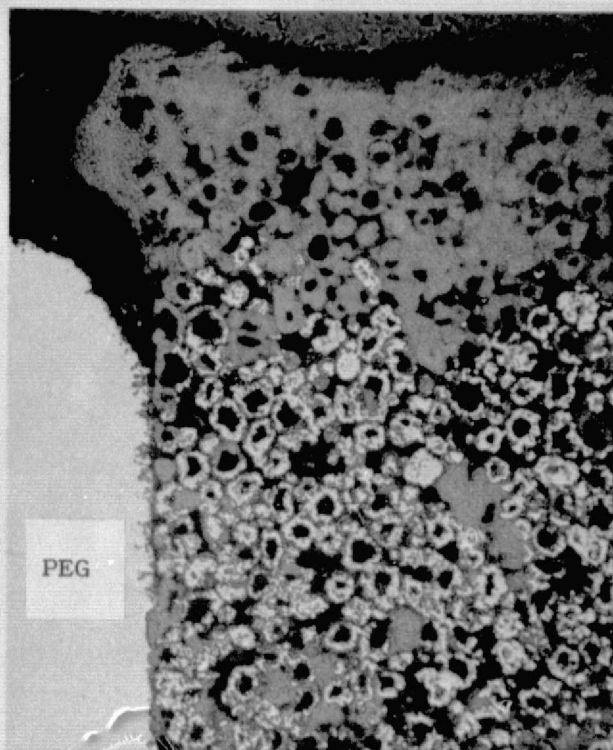
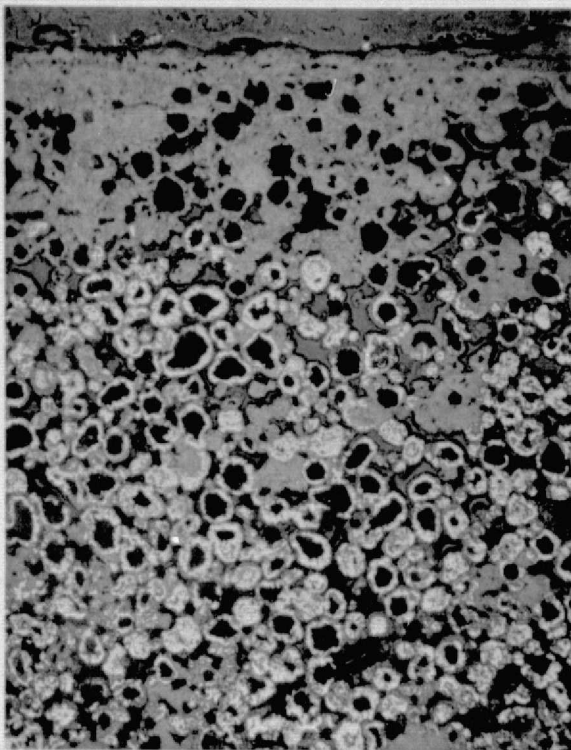
Using the modified fabrication procedures described earlier, 18 Genaseal shrouds were produced for the second and third CF6 engine tests. Six shrouds were installed in CF6-50 engine 455-508/12 and 12 shrouds were installed in CF6-50 engine 455-504. Both engines were run for 1000 cycles (250 hours). The cycle test schedule is shown in Figure 42.

None of the Genaseal shrouds exhibited the filler erosion problem seen in the first engine test, demonstrating the effectiveness of the modified fabrication techniques. Figure 43 shows some of the shrouds in engine 455-508/12's turbine stator during engine teardown after completion of the 1000 "C" cycle testing. The close-up insert in Figure 43 demonstrates the significantly lower amount of swelling or oxide volume growth of the Genaseal filler compared to Bradelloy for the cast peg shrouds. Other shrouds seen in the photo represent various versions of repaired Bradelloy shrouds with replacement of the cast pegs with honeycomb. Figure 44 similarly shows some of the shrouds in engine 455-504/11's turbine stator support during engine teardown. Note the loss of filler at the trailing edge of the film cooled Bradelloy shrouds. In both engines, the Genaseal shrouds were cooled from the back by the standard CF6-50 air impingement method.

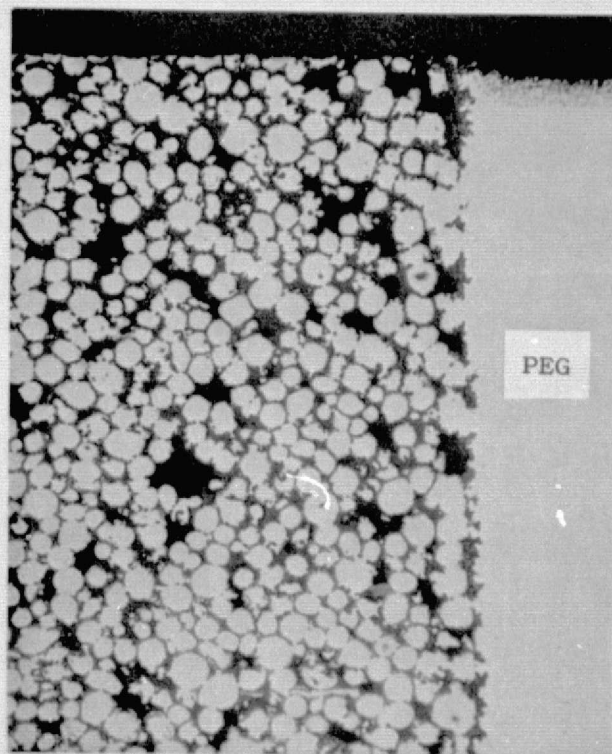
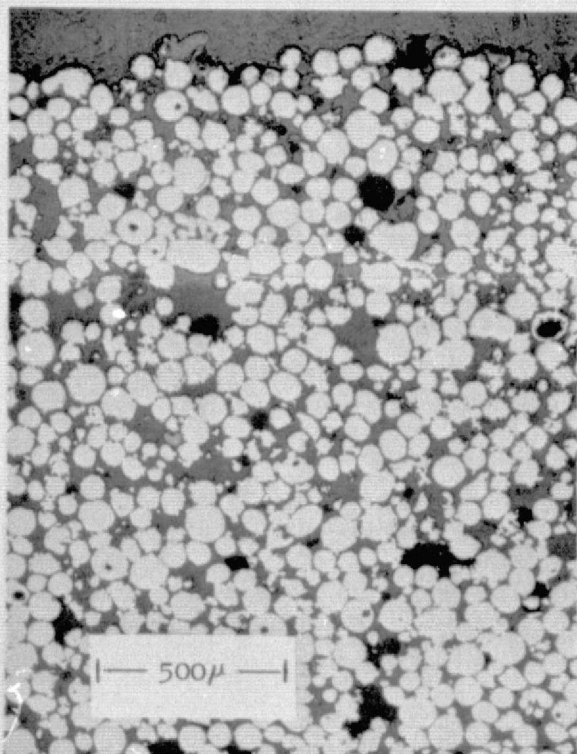
Micro examination of the engine test shrouds again confirmed Genaseal's superior oxidation resistance over Bradelloy. The NiCrAlY particles near the surface exhibited only a thin oxide film even in the hottest areas of the shrouds and little, if any, swelling above the shroud pegs (Figure 45, right). Similar areas of the Bradelloy shrouds exhibited a substantial oxidation of the filler and swelling above the shroud pegs (Figure 45, left).

A Genaseal shroud from engine 455-504/11 exhibited one area of blade tip rub (Figure 46, left). As was the case of Genaseal in the first engine test, the filler at the surface compacted and smeared (Figure 46, right) indicating a good degree of compliance under the rub. In contrast to finding no evidence of blade metal transfer in the case of the first engine test, SEM EDAX analysis of the rub surface of the -504/11 shroud showed evidence of blade metal transfer to the shroud.

The second and third engine tests also showed the benefits of Genaseal's higher conductivity relative to Bradelloy. Less thermal fatigue cracking at the segment edges and aft edge of the shroud segment castings appeared on the Genaseal shrouds than on the Bradelloy shrouds. Also, judging from the relative amounts of distress, the 150F cooler gas path surface temperature predicted by finite element analysis for Genaseal filled segments seemed credible.



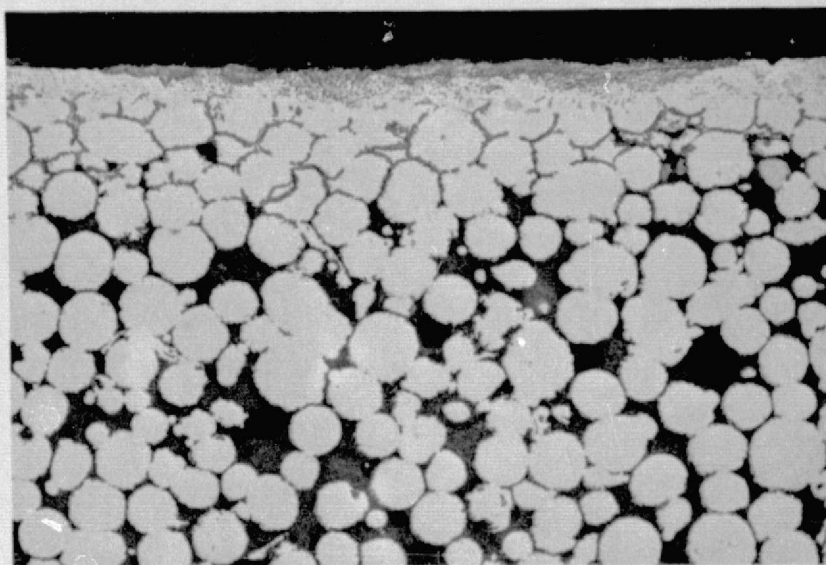
BRADELLOY



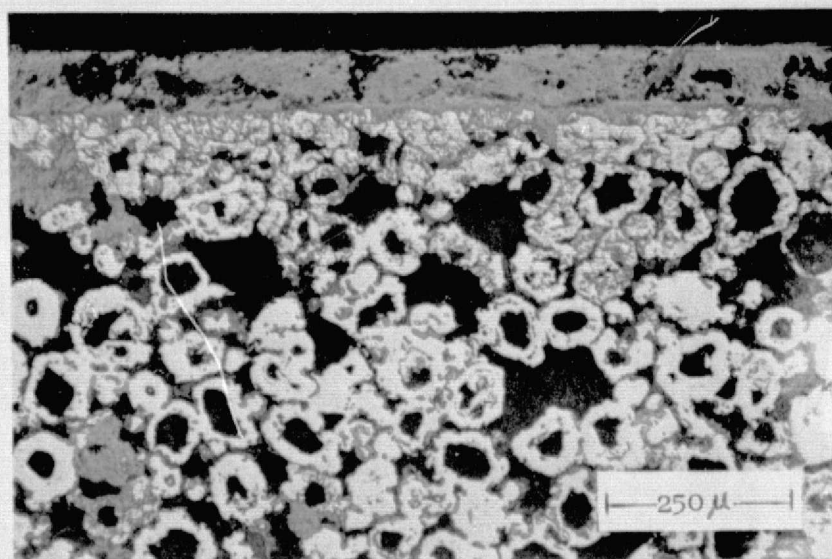
GENASEAL

Figure 40 Microstructure of Bradelloy and Genaseal Engine Test Shrouds in Hot Area of Shrouds - (50X)

Left - General Surface
Right - Next to Cast Peg



NiCrAlY



BRADELLOY

Figure 41 Structure of Blade Rub Areas on NiCrAlY and Bradelloy Engine Test Shrouds - (100X)

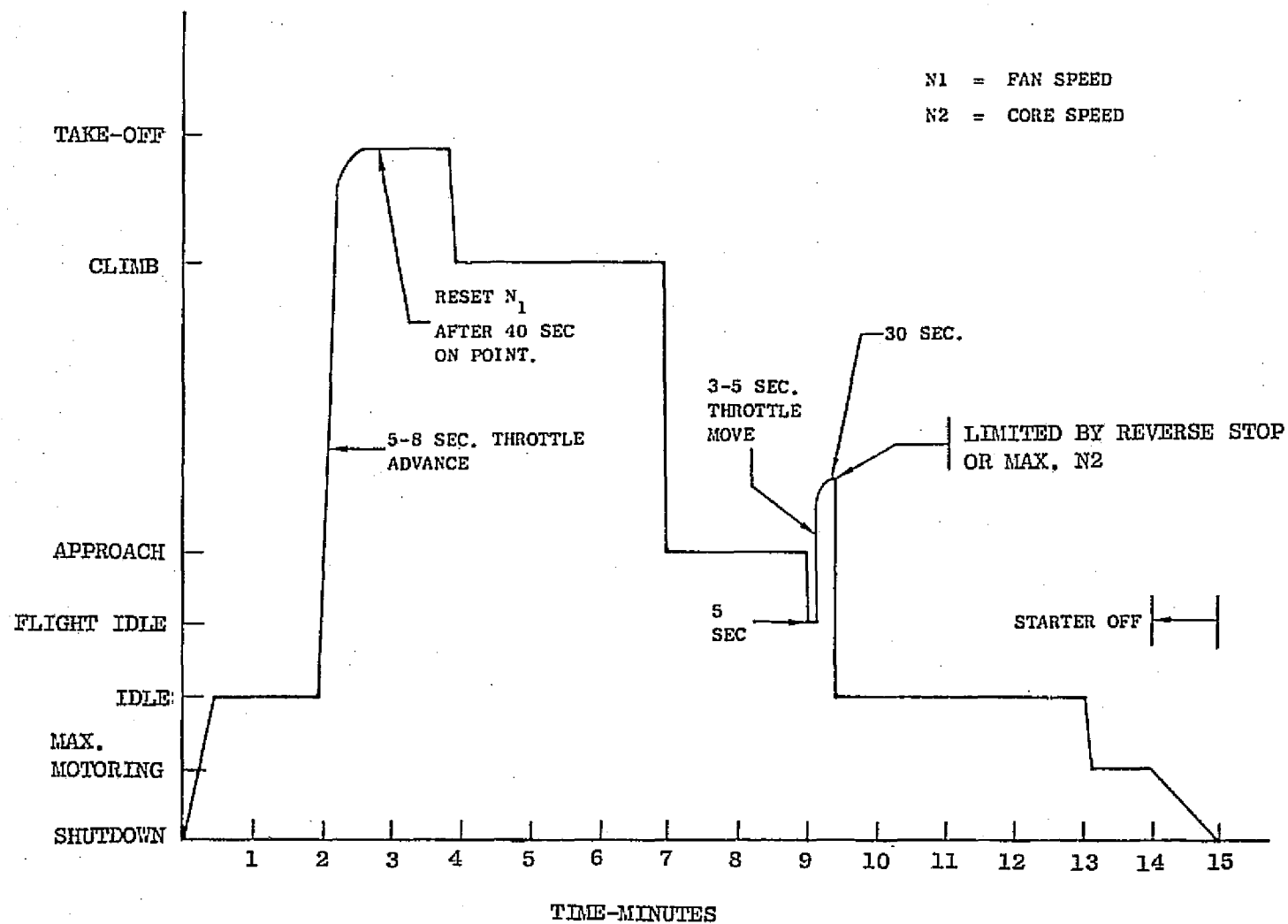


Figure 42 Engine Test Cycle

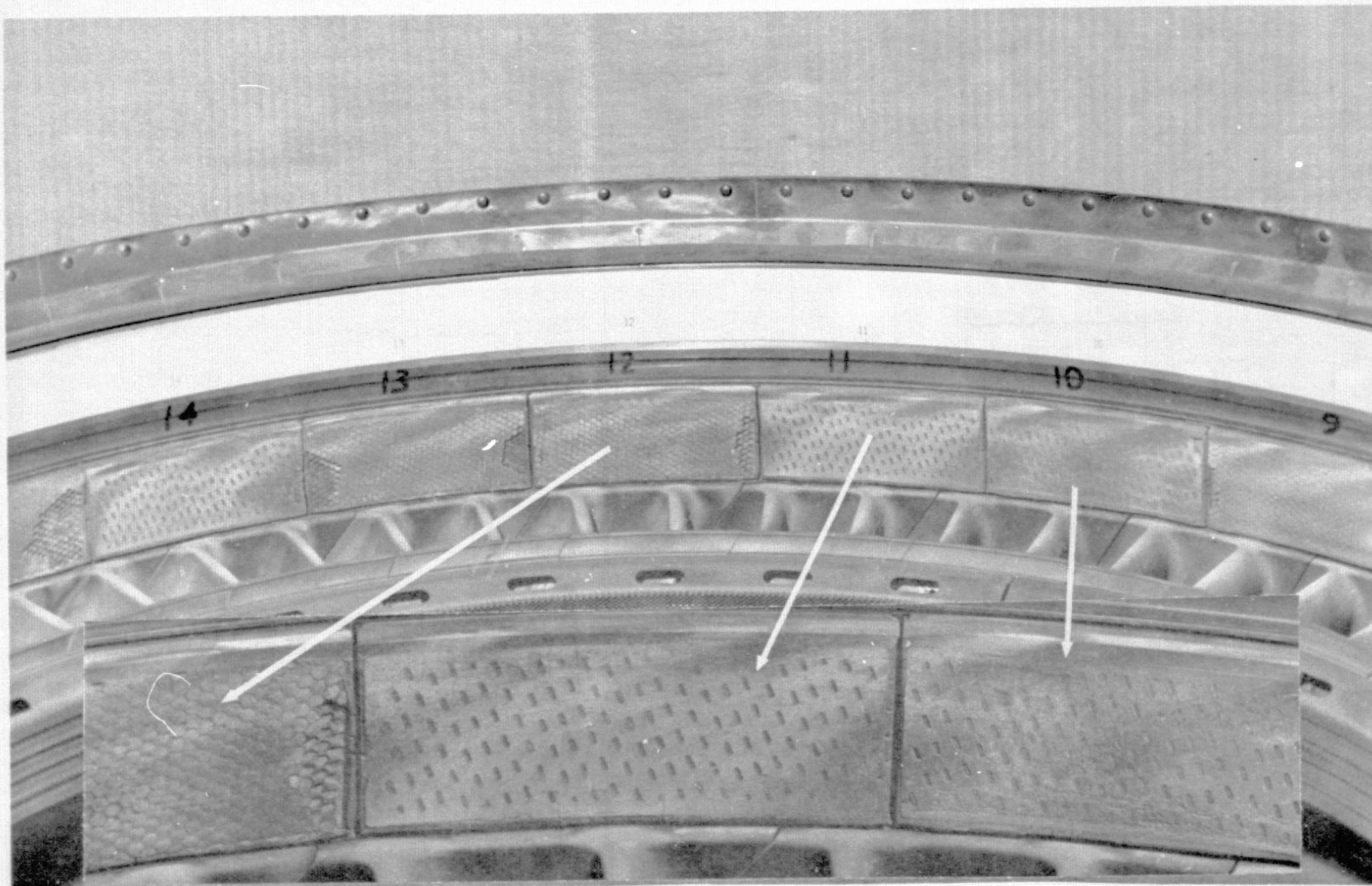


Figure 43 Genaseal and Bradelloy Shrouds After 1000 "C" Cycles Testing in CF6-50C Engine 455-508/12. Genaseal Numbers 11 and 14; Bradelloy Number 10, and Repaired Bradelloy Numbers 9, 12 and 13

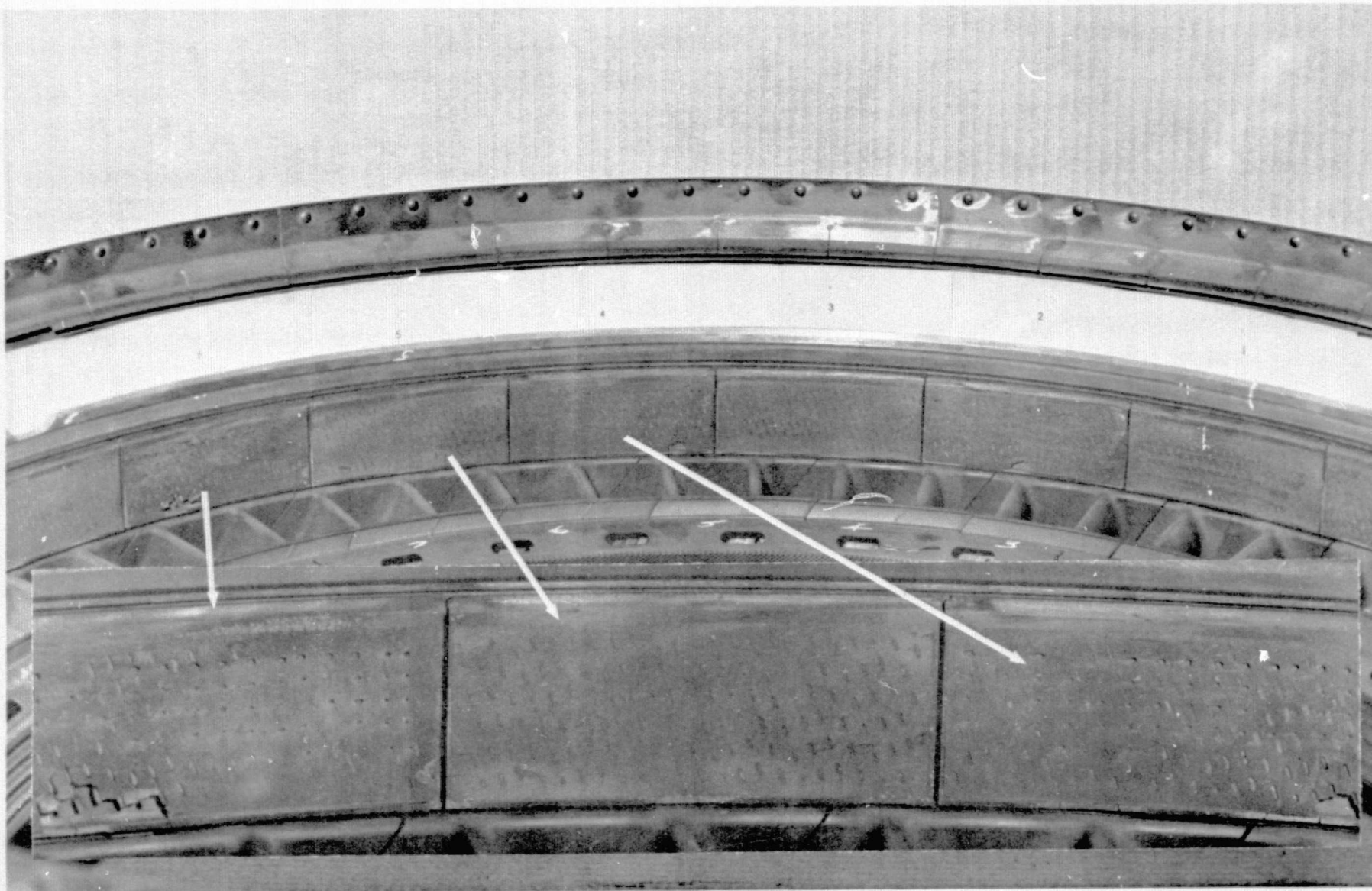


Figure 44 Genaseal and Film-Cooled Bradelloy Shrouds After 1000 "C" Cycles Testing in CF6-50L Engine 455-504/11. Genaseal Numbers 1, 3 and 5, Filmcooled; Bradelloy Numbers 2, 4 and 6

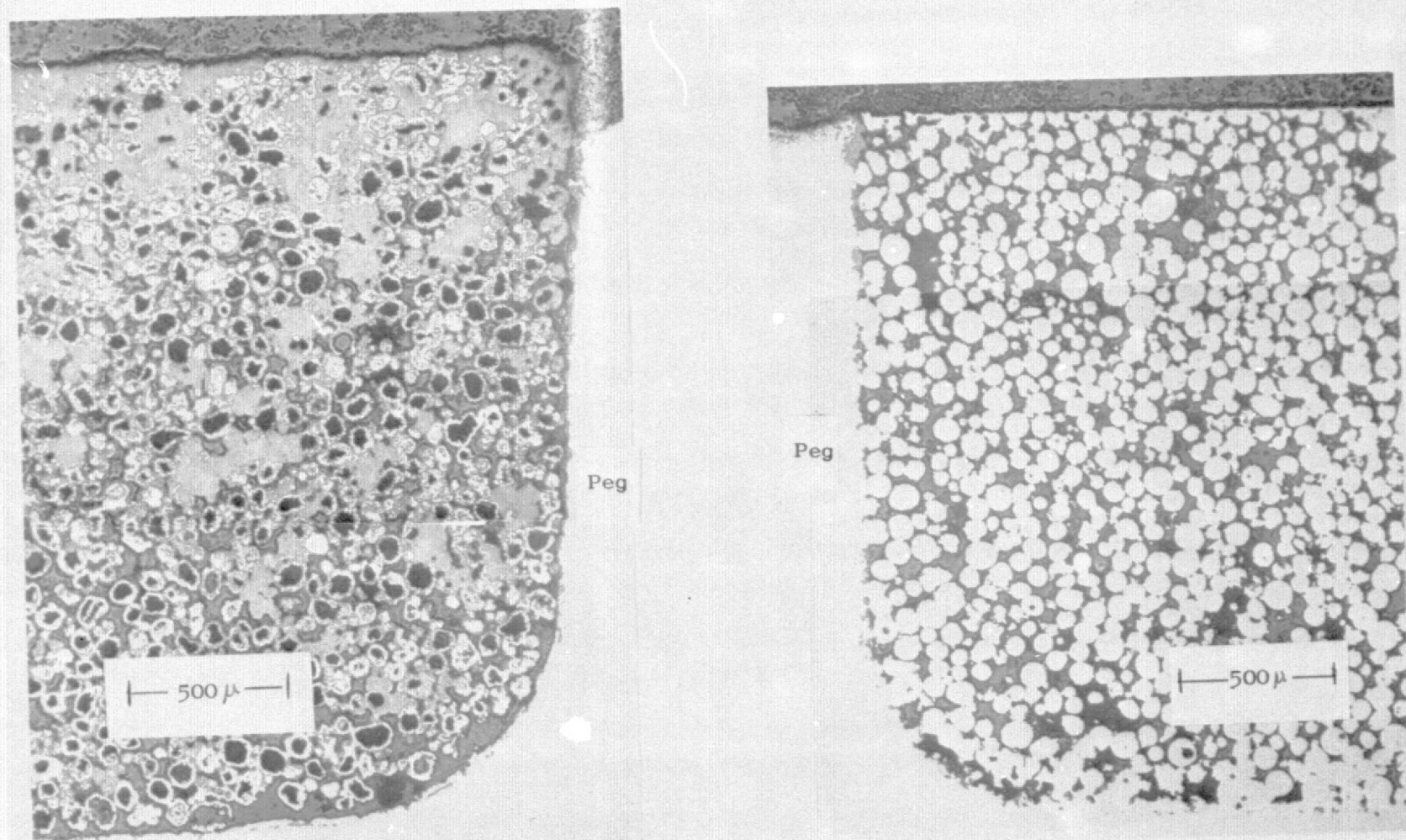


Figure 4b Typical Microstructure of Bradelloy (Left) and Genaseal (Right)
Engine Test Shrouds (50X)

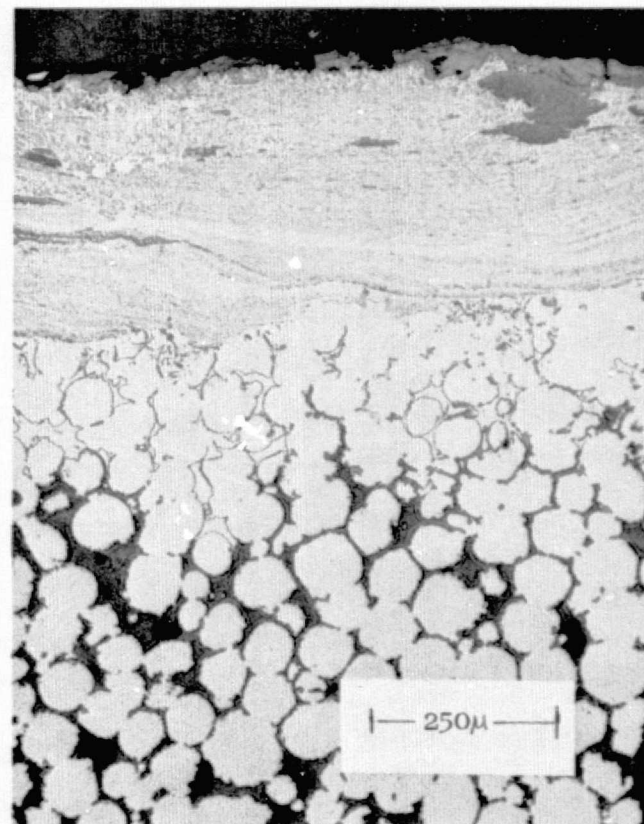
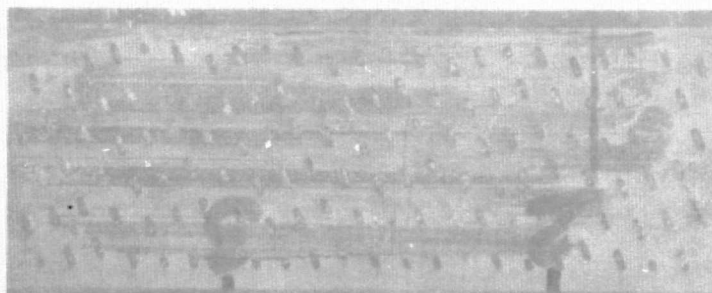


Figure 46 Blade Rub on Genaseal Shroud. Left - Surface of Shroud (1X).
Right - Microstructure Through Rub Area (100X)

CONCLUSIONS

1. On the basis of rig and engine test results, a 70-85% dense shroud filler material having good oxidation resistance provided an improvement over Bradelloy filled turbine shrouds. That filler material is an alloy of Ni-22Cr-10Al-1Y.
2. Property advantages include better oxidation resistance, reduced spalling from thermal cycles, reduced filler growth and distortion, and improved thermal conductivity that allows easier cooling of the gas path surface.
3. The shrouds can be filled by a hot press method that provides adequate control of filler properties.
4. A multiple batch method, an initial scale-up attempt, reduced fabrication cost by the equivalent of 11.7 man hours per shroud segment (CF6-50).